

CHARACTERISTICS OF REACTIVE POWDER CONCRETE PRODUCED WITH
LOCALLY SOURCED UNREFINED METAKAOLIN AND GEAR INNER WIRE

BY

ABDULLAHI GETSO IBRAHIM

DEPARTMENT OF BUILDING
FACULTY OF ENVIRONMENTAL DESIGN
AHMADU BELLO UNIVERSITY, ZARIA-NIGERIA

MAY, 2021

CHARACTERISTICS OF REACTIVE POWDER CONCRETE PRODUCED WITH
LOCALLY SOURCED UNREFINED METAKAOLIN AND GEAR INNER WIRE

BY

Abdullahi Getso IBRAHIM
(P13EVBD9002)

A PhD THESIS SUBMITTED TO THE SCHOOL OF POSTGRADUATE STUDIES,
AHMADU BELLO UNIVERSITY, ZARIA-NIGERIA
IN PARTIAL FULLFILMENT FOR THE AWARD OF DOCTOR OF PHILOSOPHY
CONSTRUCTION TECHNOLOGY,

DEPARTMENT OF BUILDING
FACULTY OF ENVIRONMENTAL DESIGN
AHMADU BELLO UNIVERSITY, ZARIA

MAY, 2021

Declaration page

I declare that the work in this thesis entitled “**Characteristics of Reactive Powder Concrete Produced with Locally Sourced Unrefined Metakaolin and Gear Inner Wire**” has been performed by me in the Department of Building, Faculty of Environmental Design, Ahmadu Bello University, Zaria. The information derived from the literature has been duly acknowledged in the text and a list of references provided. No part of this thesis was previously presented for another degree or diploma at this or any other Institution.

Abdullahi Getso Ibrahim
(P13EVBD9002)

Signature

Date

Certification page

This is to satisfy that this thesis entitled “**CHARACTERISTICS OF REACTIVE POWDER CONCRETE PRODUCED WITH LOCALLY SOURCED UNREFINED METAKAOLIN AND GEAR INNER WIRE**” by Abdullahi Getso IBRAHIM meets the regulations governing the award of the degree of Doctor of Philosophy (PhD) in construction technology of the Ahmadu Bello University, and is approved for its contribution to knowledge and literary presentation.

Prof. Muhammad M. Garba
Chairman, Supervisory Committee

Signature

Date

Prof. O.G. Okoli
Member, Supervisory Committee

Signature

Date

Prof. I.K. Zubairu
Member, Supervisory Committee

Signature

Date

Dr. D. Dahiru
Member, Supervisory Committee

Signature

Date

Dr. D. Dahiru
Head of Department

Signature

Date

Prof. S. Abdullahi
Dean, School of Postgraduate Studies

Signature

Date

Dedication

This work is dedicated to my late Mother, Father, Uncles and Aunties. May Allah continue to shower His mercy on you!

Acknowledgement

All praise is due to the almighty Allah (SWA). We praise Him and seek His forgiveness. We seek His assistance from the evil of our own souls and from the weakness of our own deeds. May the peace and blessings of Allah be upon the seal of the prophets and the leader of the luminary worshippers, his family, his companions and those who follow in piety up to the day of reckoning. I would like to express my sincere gratitude to my supervisory team: Prof. M.M. Garba, Prof. O.G. Okoli, Prof. I.K. Zubairu and Dr. D. Dahiru for their un-ending guidance and mentoring. I really appreciate their suggestions, objective and constructive criticisms throughout the study. I also wish to express my appreciation and thanks to Dr. Jamilu Usman for his continued guidance, advice and invaluable insight throughout this research. My appreciation goes to Prof. Ikemufuna Mbamali, Prof. Kabir Bala, Prof. I.H. Mshelgaru, Dr. A.D. AbdulAzeez, Dr. A.M. Stanley, Dr. S. Muhammad, Dr. D. AbdulSalam, Dr. D.W. Dadu, Dr. Sulaiman Aliyu Shika, Dr. A.M. Ibrahim, Mal. M.S. Saleh, Dr. I.M. Khalil, Dr. M. Mamman, Dr. B.M. Manzuma, M.Z. Muhammad, Dr. M. Dodo, Dr. M.M. Sa'ad, Dr. Mu'awiya Abubakar, Dr. Sanusi Gambo, Muhammad Mustafa Ibrahim and all other staff whose names could not be mentioned here for their advice and encouragement. Special thanks go to the staff of the concrete technology laboratory: Mal. Abdulazeez Abdullahi, Mal. Harisu Ado, Alh Audi, and Mal Sa'idu for their supports during the experiment. So also, Engr. Ejembi Williams and Ebel Onivehu of the concrete technology laboratory, Department of Civil Engineering, A.B.U. Zaria. I am also indebted to all my family members especially Colonel Ahmed Ibrahim Getso and Dr. Kabiru Ibrahim Getso for their support and encouragement.

Finally, special thanks to my lovely wife (Firdausi Ibrahim Abdullahi) for her words of encouragement who always says "*you just have to do it, it requires sacrifice*" and my

children (Abdallah Assiddiq & Ibrahim Khalil) for their prayers, unconditional patient and continued support throughout the research period. Thank you all for being there for me.

Abstract

With the soaring need to use innovative and sustainable materials in the construction industry, a new concrete known as Reactive Powder Concrete (RPC) is currently a material of significant interest globally. The concrete has cement, silica fume, fine sand, quartz sand and fibre as its ingredients. However, silica fume and fibre are relatively expensive in Nigeria due to their non-availability. This research evaluated the properties of RPC produced with unrefined Metakaolin (MK) as substitute to silica fume and Gear Inner Wire (GIW) as fibre. Reactive powder concrete specimens produced with up to 30% MK by weight of cement, and a constant GIW content of 0.25% by weight of concrete were subjected to compressive strength (50mmx50mmx50mm), tensile strength (100mmx50mm) and flexural strength (50mmx50mmx160mm) tests (at 27°C) at 7, 14, 28, 90 and 180 days of curing. Residual compressive strength, ultrasonic pulse velocities of the RPC samples after heating to temperature of 200 °C, 400 °C, 600 °C and 800°C for 2 hours were also assessed. In addition, X-ray diffraction, Fourier transform infrared spectroscopy and scanning electron microscopy analysis were undertaken to examine the microstructure of the specimens. Similarly, RPC produced with 20% silica fume as control was tested. Mathematical models were developed using DataFit software. Results showed that unrefined MK of up to 20% by weight of cement can be used to produce RPC with 72.5 N/mm² compressive strength and 0.25% GIW by weight of concrete can be used to produce RPC with tensile strength and flexural strength of 7.1 N/mm² and 22.3 N/mm² respectively. Reactive powder concrete with 20% MK performed better than other samples (10% MK & 30% MK) in terms of residual strength, absorption and ultrasonic pulse velocity (UPV) when exposed to elevated temperatures. It was found that at higher temperature of 800°C, all RPC specimens experienced drastic reduction in strength but 20% MK and 30% MK

showed relatively better strength retention capacity as substantiated by the XRD results compared to the 20% SF and 10% MK specimens. It was recommended that unrefined metakaolin and gear inner wires can be used in the production of RPC. Models developed can be used to predict the compressive strength, flexural strength and water absorption capacity of RPC produced with unrefined MK and GIW.

Table of Contents

Declaration page	iii
Certification page.....	iv
Dedication	v
Acknowledgement	vi
Abstract	viii
Table of Contents.....	x
List of Tables	xvi
List of Figures	xvii
List of Plates.....	xix
Appendices.....	xx
CHAPTER ONE	1
1.0 INTRODUCTION.....	1
1.1 General Background.....	1
1.2 Statement of the Research Problem	5
1.3 Justification for the Study	6
1.4 Significance of the Study	7
1.5 Theoretical Framework.....	7
1.6 Aim and Objectives.....	9
1.6.1 Aim.....	9
1.6.2 Objectives.....	9
1.7 Scope and Limitations	10
1.7.1 Scope.....	10
1.7.2 Limitations	10
CHAPTER TWO	11
2.0 LITERATURE REVIEW.....	11
2.1 An overview of Advances in Concrete Technology.....	11
2.1.1 Normal strength concrete	13
2.1.2 High strength concrete	15
2.1.3 High performance concrete.....	16
2.1.3.1 <i>Benefits of using HPC</i>	20

2.1.3.2 Applications of HPC	21
2.2 Reactive Powder Concrete	21
2.2.1 Composition of reactive powder concrete	22
2.2.1.1 Cement	22
2.2.1.2 Silica fume	23
2.2.1.3 Fine sand.....	23
2.2.1.4 Quartz sand	24
2.2.1.5 Admixtures	25
2.2.1.6 Fibres in RPC.....	27
2.2.2 Properties of reactive powder concrete.....	31
2.2.2.1 Fresh properties	31
2.2.2.2 Hardened properties of RPC.....	32
2.2.3 Types of RPC	37
2.2.4 Application of reactive powder concrete	37
2.3 General Overview on the Use of Pozzolanas in RPC	38
2.3.1 Silica fume	38
2.3.1.1 Production of silica fume	39
2.3.1.2 Properties of silica fume	39
2.3.1.3 Reaction mechanism of SF	42
2.3.1.4 Application of SF in RPC.....	43
2.3.1.5 Influence of SF on the properties of RPC	44
2.3.1.6 Challenges of using SF	45
2.3.2 Fly ash.....	45
2.3.2.1 Production of Fly ash.....	46
2.3.2.2 Properties of Fly ash.....	47
2.3.2.3 Reaction mechanism of FA	48
2.3.2.4 Influence of FA on the properties of RPC.....	49
2.3.2.5 Challenges of using fly ash	51
2.3.3 Ground granulated blast furnace slag.....	51
2.3.3.1 Production of GGBFS.....	51
2.3.3.2 Properties of GGBFS.....	52

2.3.3.3	<i>Reaction mechanism of GGBFS</i>	53
2.3.3.4	<i>Influence of GGBFS on the properties of RPC</i>	54
2.3.3.5	<i>Challenges of using GGBFS</i>	56
2.3.4	Rice husk ash	56
2.3.4.1	<i>Production of rice husk ash</i>	56
2.3.4.2	<i>Properties of RHA</i>	57
2.3.4.3	<i>Reaction mechanism of RHA</i>	57
2.3.4.4	<i>Influence of RHA on the properties of RPC</i>	58
2.3.4.5	<i>Challenges of using RHA</i>	59
2.3.5	Metakaolin	59
2.3.5.1	<i>Production of metakaolin</i>	60
2.3.5.2	<i>Properties of MK</i>	61
2.3.5.3	<i>Reaction mechanism of MK</i>	63
2.3.5.4	<i>Influence of MK on the properties of RPC</i>	63
2.3.5.5	<i>Challenges of using MK</i>	63
2.4	Performance of RPC at Elevated Temperatures	64
2.5	Model Development	67
2.6	DataFit Software	73
2.7	Summary of Literature Review	74
3.0	MATERIALS AND METHODS	78
3.1	Preamble	78
3.2	Materials	78
3.2.1	Binders (cement, silica fume and metakaolin).....	78
3.2.2	Fine aggregates	79
3.2.3	Chemical admixture	79
3.2.4	Fibre	80
3.2.5	Water.....	82
3.3	Preparation of Binder	82
3.3.1	Production of MK	82
3.4	Characterization of Materials	84
3.4.1	Physical properties	84

3.4.1.1 <i>Specific gravity and loss on ignition</i>	84
3.4.1.2 <i>Particle size distribution</i>	85
3.4.1.3 <i>Specific surface area</i>	85
3.4.2 <i>Chemical compositions</i>	85
3.4.3 <i>Mineralogical compositions of MK and sand</i>	86
3.4.3.1 <i>X-Ray diffraction (XRD) of kaolin, MK and sand</i>	86
3.4.4 <i>Pozzolanic activity</i>	86
3.4.5 <i>Characterization of fine aggregate</i>	87
3.5 Mix Proportion	88
3.6 Specimens Preparation	88
3.6.1 <i>Mixing</i>	88
3.6.2 <i>Specimens casting and curing</i>	90
3.7 Fresh Property of RPC	90
3.8 Hardened Properties of RPC	91
3.8.1 <i>Compressive strength</i>	91
3.8.2 <i>Tensile strength</i>	92
3.8.3 <i>Flexural strength</i>	93
3.9 Water Absorption Capacity	94
3.10 Sorptivity Test	95
3.11 Elevated Temperature	96
3.11.1 <i>Ultrasonic pulse velocity</i>	97
3.11.2 <i>Microstructure analysis of RPC</i>	98
3.12 Development of Models	99
3.12.1 <i>Processes of models' development using DataFit software</i>	99
3.13.2 <i>Assumption on the use of the models</i>	100
3.14 Data Analysis	101
3.14.1 <i>Correlation analysis</i>	101
3.14.2 <i>Probability (P-value)</i>	101
CHAPTER FOUR	102
4.0 RESULTS, ANALYSIS AND DISCUSSIONS	102
4.1 Preamble	102

4.2 Characterization of the Constituent Materials of RPC	102
4.2.1 Chemical compositions and physical properties of RPC constituents	102
4.2.2 Mineral composition of kaolin, calcined kaolin and fine sand	104
4.3 Mix Proportion of RPC	106
4.3 Flowability of RPC	107
4.4 Hardened Properties of RPC	108
4.4.1 Compressive strength unrefined RPC	108
4.4.2 Tensile strength of unrefined RPC	111
4.4.3 Flexural strength	114
4.5 Performance of the RPC Exposed to Elevated Temperature	116
4.5.1 Physical observation	116
4.5.2 Residual and normalized compressive strengths	117
4.5.2.1 <i>Unfibred RPC</i>	118
4.5.2.2 <i>Fibred RPC</i>	120
4.5.3 Ultrasonic pulse velocity (UPV) of RPC exposed to elevated temperatures	122
4.5.3.1 <i>Unfibred RPC</i>	122
4.5.3.2 <i>Fibred RPC</i>	123
4.5.4 Water absorption capacity (%) of RPC exposed to elevated temperatures	124
4.5.5 Relationship between ultrasonic pulse velocity and residual strength of RPC	126
4.5.6 Relationship between ultrasonic pulse velocity and water absorption of RPC	127
4.5.7 Sorptivity of RPC exposed to elevated temperatures	128
4.5.7.1 <i>Sorptivity of RPC at ambient temperatures</i>	129
4.5.7.2 <i>Sorptivity of RPC samples at 200°C</i>	131
4.5.7.3 <i>Sorptivity of RPC samples at 400°C</i>	133
4.5.7.4 <i>Sorptivity of RPC samples at 600°C</i>	135
4.5.7.5 <i>Sorptivity of RPC samples at 800°C</i>	136
4.6 Microstructure Analysis of RPC	138
4.6.1 X-Ray diffraction (XRD) analysis	138
4.6.2 Fourier transforms infrared spectroscopy (FTIR) results	141
4.6.2.1 <i>FTIR result at 27°C</i>	141
4.6.2.2 <i>FTIR results at 200°C</i>	144

4.6.2.3 RFTIR results at 800°C	147
4.6.3 Scanning electron microscopy (SEM) analysis	150
4.6.3.1 SEM of RPC specimens exposed to 27°C	150
4.6.3.3 SEM of RPC exposed to 800°C	152
4.7 Models Development for the Optimised RPC Samples	153
4.7.1 Model development for the prediction of compressive strength of RPC with.....	153
4.7.1.1 Validation of compressive strength model	154
4.7.1.2 Model development for the prediction of flexural strength of RPC with	155
4.7.1.3 Validation of flexural strength model	156
4.7.1.4 Model development for the prediction of water absorption capacity of RPC	157
4.7.1.5 Validation of water absorption capacity model	158
4.7.2 Limitations of the models	159
CHAPTER FIVE.....	160
5.0 SUMMARY, CONCLUSIONS AND RECOMMENDATIONS	160
5.1 Summary	160
5.2 Conclusions	161
5.3 Recommendations	162
5.4 Recommendations for Further Study	163
5.5 Contribution to Knowledge.....	163
REFERENCES.....	165
APPENDICES	178

List of Tables

Table 2.1: Strength classification of concrete	14
Table 2.2: Materials used in high performance concrete	18
Table 2.3: Selected properties of high-performance concrete	19
Table 2 4: Characteristics of quartz	25
Table 2.5: Summary of the hardened properties of RPC	36
Table 2.7: Physical properties of SF	41
Table 2.8: Chemical properties of SF	41
Table 2.9: Chemical composition and classification of FA	46
Table 2.10: Chemical composition of fly ash	48
Table 2.11: Typical chemical composition of GGBF reported by different researchers	53
Table 2.12: Physical properties of RHA	57
Table 2.13: Chemical composition of RHA.....	57
Table 2.14: Physical properties of metakaolin.....	61
Table 2.15: Typical chemical composition of MK	62
Table 2.16: Changes in concrete during heating.....	66
Table 2.17: Results of researchers across the Globe using different pozzolans	77
Table 3.1: Properties of gear inner wire (GIW) as fiber	80
Table 3.2: Coordinates of kaolin site	83
Table 3.3: Range of value of SP used	89
Table 4.1: Oxide compositions and physical properties of RPC constituents	103
Table 4.2: Mix proportion of RPC	106
Table 4.2: Summary of FTIR results at 27°C.....	143
Table 4.3: Summary of FTIR results at 200°C.....	146
Table 4.4: Summary of FTIR results at 800°C.....	149
Table 4.5: Experimental versus predicted compressive strength of RPC	155
Table 4.6: Experimental versus predicted flexural strength of RPC.....	157
Table 4.7: Experimental versus predicted absorption of RPC	159

List of Figures

Figure 4.1: X-Ray diffraction result of metakaolin.....	104
Figure 4.2: XRD of fine sand.....	105
Figure 4.3: Effect of MK content on the compressive strength of unfibred RPC.....	108
Figure 4.4: Effect of MK content on the compressive strength of fibred RPC.....	108
Figure 4.5: Effect of MK content on the tensile strength of unfibred RPC	111
Figure 4.6: Effect of MK content on the tensile strength of fibred RPC	112
Figure 4.7: Effect of MK content on the flexural strength of unfibred RPC	114
Figure 4.8: Effect of MK content on the flexural strength of fibred RPC	114
Figure 4.9: Residual strengths of unfibred RPC exposed to elevated temperatures	118
Figure 4.10: Normalized compressive strength results of unfibred RPC exposed to elevated temperature.....	118
Figure 4.11: Residual compressive strength of fibred RPC exposed to elevated temperatures	120
Figure 4.12: Normalized compressive strength of fibred RPC exposed to elevated temperatures	120
Figure 4.13: Ultrasonic pulse velocity results of unfibred RPC	122
Figure 4.14: Ultrasonic pulse velocity results of fibred RPC	123
Figure 4.15: Water absorption of unfibred RPC exposed to different elevated temperature	124
Figure 4.16: Water absorption of fibred RPC exposed to different elevated temperature..	125
Figure 4.17: Relationship between UPV and residual compressive strength of unfibred RPC	126
Figure 4.18: Relationship between UPV and residual compressive strength of fibred RPC	126
Figure 4.19: Relationship between UPV and water absorption of unfibred RPC.....	127
Figure 4.20: Relationship between UPV and water absorption of fibred RPC.....	128
Figure 4.21: Sorptivity of unfibred specimens exposed to ambient temperature	129
Figure 4.22: Sorptivity of fibred specimens exposed to ambient temperature	129
Figure 4.23: Sorptivity of unfibred specimens exposed to 200°C	131
Figure 4.24: Sorptivity of fibred specimens exposed to 200°C	131
Figure 4.25: Sorptivity of unfibred specimens exposed to 400°C	133

Figure 4.26: Sorptivity of fibred specimens exposed to 400°C	133
Figure 4.27: Sorptivity of unfibred specimens exposed to 600°C	135
Figure 4.28: Sorptivity of fibred specimens exposed to 600°C	135
Figure 4.29: Sorptivity of unfibred specimens exposed to 800°C	136
Figure 4.30: Sorptivity of fibred specimens exposed to 800°C	137
Figure 4.31 XRD patterns of RPC specimens at 27°C.....	138
Figure 4.32 XRD patterns of RPC specimens at 200°C.....	139
Figure 4.33 XRD patterns of RPC specimens at 800°C.....	140
Figure 4.34: FTIR result of 20% SF	141
Figure 4.35: FTIR result of 20% MK	142
Figure 4.36: FTIR result of 10% MK	142
Figure 4.37 FTIR result of 20% SF\	144
Figure 4.38: FTIR result of 10% MK	144
Figure 4.39: FTIR result of 20% MK	145
Figure 4.40: FTIR result of 30% MK	145
Figure 4.41: FTIR result of 20% SF	147
Figure 4.42: FTIR result of 10% MK	148
Figure 4.43: FTIR result of 20% MK	148
Figure 4.44: FTIR result of 30% MK	149
Figure 4.46: Scanning electronic microscopy (SEM) of RPC specimens at 200°C	151
Figure 4.47: Scanning electronic microscopy (SEM) of RPC specimens at 800°C	152
Figure 4.48: Model plot for compressive strength.....	154
Figure 4.49: Model plot for flexural strength	156
Figure 4.50: Model plot for water absorption capacity.....	158

List of Plates

Plate I: Container of Conplast SP 430	79
Plate II: A sample pack of the GIW	81
Plate III: Sample of GIW	81
Plate IV: Tensor meter	81
Plate V: Digital weighing balance	82
Plate VI: Coordinates of kaolin site in Getso town.....	83
Plate VII: Furnance with kaolinite to be calcined.....	84
Plate VIII: X-Ray fluorescence (Niton XL3t).....	86
Plate IX: Mortar Mixer	89
Plate X: Sample of RPC after casting	90
Plate XI: Measuring the Flowability of the RPC	91
Plate XII: RPC samples under compressive strength test.....	92
Plate XIII: RPC samples under tensile strength test	93
Plate XIV: RPC samples under flexural strength test.....	94
Plate XV: Samples subjected to Sorptivity test	96
Plate XVI: UPV instrument	97
Plate XVII: Display of number of independent variables.....	100
Plate XVIII: Display of Interface.....	100
Plate XIX: Flowability of RPC	107
Plate XX: Control @ 27 °C.....	116
Plate XXI: Sample exposed to elevated temperatures	116

Appendices

Appendix A: Trials test	178
Appendix B: Hardened properties of RPC.....	179
Appendix C: Relationships results.....	180
Appendix D: Residual strength of RPC specimens	184
Appendix E: Absorption Capacity of RPC exposed to different elevated temperature	186
Appendix F: Ultrasonic Pulse Velocity of RPC exposed to different elevated temperature	187
Appendix G: Sorptivity of RPC specimens	188
Appendix H: Model development.....	193

CHAPTER ONE

1.0 INTRODUCTION

1.1 General Background

Many research works have been undertaken over the years aimed at achieving high mechanical performance of concrete with cementitious matrix materials (Chana, Luo & Sunb 2000; Aitcin, 2003; Momtazi, Ranjbar, Balalaei & Nemati, 2007; Maroliya & Modhere 2010; Patil, Gupta & Deshpande, 2013; Shan, Rijuldas & Aiswarya , 2016). Such efforts led to the development of an ultra-high strength and ductile concrete called Reactive Powder Concrete (RPC) that was first made by Richard and Cheyrezy in 1995. It was produced by the application of a certain number of basic principles relating to the composition, mixing and treatment of the concrete.

Reactive powder concrete was developed through microstructure enhancement techniques for cementitious materials which include eliminating coarse aggregates, reducing the water-to-binder ratio and incorporating steel micro-fibres (Yazici, Yardimci, Aydin & Karabulut, 2009). There are a lot of researches carried out across the globe which indicate that RPC is a future concrete material because of its high mechanical properties.

Reactive powder concrete could have a compressive strength of between 170 N/mm^2 to 200 N/mm^2 and flexural strength of between 20 N/mm^2 to 60 N/mm^2 (Richard & Cheyrezy 1995) by using silica fume as the pozzolan. A compressive strength of 80 N/mm^2 , tensile strength of 10 N/mm^2 and flexural strength of 20 N/mm^2 was achieved using local materials (quartz powder, silica fume, sand, cement, super plasticizer and steel fibers) available in Pakistan (Qureshi, Tasaddiq, Ali & Sultan, 2017). Thus, RPC exhibits varied compressive strength when cured under different conditions.

The basic mechanical properties of RPC were examined under different curing conditions and the results indicated that the compressive strength at 28 days varied between 170 N/mm² to 202 N/mm² for heat treated specimens; up to 400 N/mm² for autoclaving and between 130 N/mm² and 150 N/mm² for non-heat-treated specimens (Cwirza, Penttala & Vornanen 2008; Maroliya, 2012; Yazici, *et al.*, 2009; Tam *et al.*, 2010; Yazici, Yardimci, Yigiter, Aydin & Turkel 2010).

The use of cement in conventional RPC is high and silica fume (SF) content is up to 25% (by weight of cement). Some of the shortcomings of SF are high cost, increase heat of hydration which causes shrinkage problems (Peng, Kang, Huang, Liu & Chen 2015) and non-availability in some countries like Nigeria. Moreover, steel fibre used in the production of RPC is also not available in Nigeria (Ibrahim, Garba, Usman & Gambo 2018). The non-availability of these two major materials of RPC production is a hindrance to the Nigerian construction industry because of importation cost and the execution of projects at acceptable prices to their clients.

The use of other mineral admixtures in the production of the RPC has proved to be a feasible solution to the problems of SF (Rougeau & Borys, 2004; Yazici *et al.*, 2009; Yazici *et al.*, 2010; Agharde & Bhalchandra, 2015; Kushartomo, Bali & Sulaiman 2015). When fly ash was used to replace SF in the production of RPC, compressive strength of between 62.9 N/mm² to 324 N/mm² and a flexural strength of 8.8 N/mm² to 32 N/mm² were obtained (Yazıcı, Yigiter, Karabulut & Baradan 2008; Yazici *et al.* 2009; Demiss, Oyawa & Shitote 2018). A compressive strength of 128 N/mm² to 250 N/mm² and a flexural strength of between 25.6 N/mm² to 32 N/mm² were obtained with ground granulated blast furnace slag (Yazici *et al.* 2009; Peng, Hu & Ding 2010). Also, Asteray, Oyawa and Shitote (2017)

observed that for 28 curing day's compressive strength of 57.3 N/mm^2 was achieved when rice husk ash was used to replace the SF in the production of the RPC.

The use of alternative materials as fibre in the production of mortar and concrete in areas where conventional fibres are not available and they have proved to be so effective. Some researchers like Foti (2013) studied concrete specimens reinforced with fibers made from waste polyethylene terephthalate (PET) bottles. Jalal (2012) used waste steel fibre recovered from milling and machining in concrete production and the results indicate improvement of the fragile matrix, mostly in terms of toughness, energy absorption and post-cracking behavior. Studies on the influence of adding waste materials like lathe waste, soft drink bottle caps, empty waste tins, waste steel powder from workshop at a dosage of 1% of total weight of concrete as fibres was undertaken by Murali *et al.*, (2012). These materials were deformed into rectangular strips of 3 mm width and 10 mm length. Results show that a concrete block incorporated with steel powder had increased in compressive strength of 41.25% and tensile strength of 40.81%. Concrete made with soft drink bottle caps exhibited an increase in flexural strength of 25.88%.

The effect of polyethylene terephthalate (PET) as fibre using different volumes (0%, 0.5%, 1.0% and 1.5%) in mortar production were investigated by Pereira de Oliveira & Castro-Gomes (2011). Outcomes of the research show that the incorporation of PET fibres significantly improved the flexural strength and toughness of mortars and, a 1.5% was regarded as good for desired workability. More recently, Ibrahim, Garba, Usman and Gambo (2018), used waste gear inner wire (WGIW) as fibre in mortar production. Results show that the fibred mortar sample had higher compressive and tensile strengths at 28 days

by 30.9% and 20% respectively than the unfibred one. The research concludes that WGIW at 2% volume fraction could be used as fibre in mortar production.

Thus, for RPC to be produced in Nigeria there is the need to find similar, available and alternative material to SF and steel fibre in terms of performance. This way, the cost of producing the concrete could be reduced by cutting down importation cost of materials. Metakolin has been found to perform similar to SF on the properties of concrete and is used in the same manner (ACI 232.1R-2000). Another advantage of using MK is that it improves tensile strength and bond strength (Vipat & Kulkarni 2016). The use of up to 8% MK enhances tensile strength (Haroon, Ashad, Vikas & Alvin 2017) of concrete; but 10% has been reported by Badogiannis (2005) to be more favourable.

There is an estimated reserve of about two billion metric tons of kaolin deposit scattered in different parts of Nigeria (Foraminifera Market Research, 2016; Raw Material Research and Development Council, 2019). Some percentage (15%) of the SF has been partially replaced with commercial MK in the production of RPC, which indicates savings (Smith, Gururaj & Siddesh 2015). In normal concrete, unrefined metakaolin has been shown to improve the strength and durability properties of concrete similar to the refined one (Badogiannis & Tsivilis 2009). Therefore, further savings could be realized if the refined metakaolin is replaced with the unrefined one in the production of RPC. Nigeria's large deposits of kaolinitic clay may be used to produce the unrefined metakaolin.

This research, therefore, focused on the production of RPC from Gear Inner Wire (GIW) and locally sourced unrefined metakaolin obtained from the abundant kaolinitic clay deposits in Nigeria as SF is expensive and also not readily available in the country.

1.2

Statement of the Research Problem

The continued need for high strength concrete for high rise buildings, slimmer section of concrete members, changing design patterns, long span bridges and nuclear power stations are significantly increasing in developing countries. High strength concretes (over 100 N/mm²) are needed and much higher shall be required in the future (Maroliya 2012; Anjan, Asha and Narayana 2013). High performance concrete has achieved its maximum compressive strength in its existing form of microstructure, but at such a level of strength, the coarse aggregate becomes the main source of weakness in the concrete (Smith, Gururaj & Siddesh, 2015). In addition, the high contents of cement in high strength concrete, contribute to shrinkage and thermal cracking that impairs the durability of the concrete. The exclusion of coarse aggregates and the inclusion of pozzalanic material (silica fume) to produce RPC address the short comings of high-performance concrete (Richard & Cheyrezy, 1995). Reactive powder concrete is a material of choice for some special structures where high performance is of paramount importance. However, SF and fibre, which are the major ingredients of RPC are not available in Nigeria and there are limited resources and significant cost constraints (Nguyen, Guang, Klaas & Oguzhan 2011). For such concrete (RPC) production in Nigeria, similar, available and alternative material to SF and steel fibre in terms of performance need to be investigated. Metakaolin and SF have similar performance on the properties of concrete and are use in the same manner (ACI 232.1R-2000). Metakaolin improves tensile strength and bond strength of concrete (Badogiannis, 2005; Vipat & Kulkarni, 2016; Haroon, Ashad, Vikas & Alvin, 2017). There are large deposits of kaolinitic clay from which MK is obtained across Nigeria (Ibrahim, Okoli, & Dahiru 2016). Savings was reported by Smith *et al.*, (2015) when 15% SF was partially replaced with refined MK in the production of RPC. On the other hand, unrefined

metakaolin improved the strength and durability properties of concrete similar to the refined one (Badogiannis & Tsivilis 2009). Further savings could be realized if the refined MK and SF content are completely replaced with unrefined MK in the production of RPC by eliminating refining and beneficiating processes associated with refined MK. This research, therefore, focused on the production of RPC from Gear Inner Wire (GIW) and unrefined metakaolin. Efforts towards development of RPC using locally sourced materials will have far-reaching advantage in view of the fear that there is no need for the use of coarse aggregates which, many experts predicted that, in future, it would not be available in large quantity for heavy construction work.

1.3 Justification for the Study

There are large deposits of kaolinitic clay from which metakaolin is obtained across Nigeria (Ibrahim, Okoli & Dahiru 2015; Foraminifera Market Research, 2016; Raw Material Research and Development Council, 2019). Some percentage of up to 15% of the silica fume has been partially replaced with commercial metakaolin, which indicated savings (Smith *et al.*, 2015). In normal concrete, unrefined metakaolin has been shown to improve the strength and durability properties of concrete similar to the refined one (Badogiannis & Tsivilis 2009). More recently, Ibrahim *et al.* (2018) used waste gear inner wire as fibre (WGIW) in mortar production. Results showed that the fibred mortar sample has higher compressive and tensile strengths at 56 days by 19% and 21.1% respectively than the unfibred one and concluded that WGIW at 2% volume fraction could be used as fibre in mortar production. Therefore, further savings can be realized if the unrefined MK and GIW are used to replace refined MK and steel fibre in the production of the RPC. Nigeria's large deposits of kaolinitic clay served as sources of the material for unrefined metakaolin. The

results of the research showed that the use of unrefined MK and GIW in the production of RPC could serve as alternative to SF and steel fibre which will reduce cost of producing the RPC, create employment opportunities and bring economic benefits to the government in addition to producing concrete structures with slimmer sections that are cheap, strong and durable.

1.4 Significance of the Study

Result of this study will lead to the production of RPC from locally sourced materials. Also, experts have noted that the exploitation and application of coarse aggregates in concrete in Nigeria is unsustainable. If this research is successfully carried out and positive results are obtained, the use of unrefined metakaolin and gear inner wire (GIW) in the production of RPC could serve as alternative to SF and fibre, reduce cost of producing the RPC, enhance economic activities of the local communities thereby creating employment opportunities, and bring economic benefits to the government in addition to producing RPC structures with slimmer sections that are cheap, strong and durable.

1.5 Theoretical Framework

There are many researches works that have been carried out over the years aimed at achieving high mechanical performance with cementitious matrix materials (Chana *et al.*, 2000; Aitcin, 2003; Momtazi *et al.*, 2007; Maroliya & Modhere 2010; Patil *et al.*, 2013; Shan *et al.*, 2016). High strength and workable concretes with 28-day compressive strengths higher than 80 N/mm² are currently possible owing to the use of super plasticizer which leads to very low water-cement ratios (less than 0.3) and the use of supplementary cementitious materials with ultrafine particles. The ultrafine particles fill the voids between the cement particles thereby reducing water requirements and facilitate pozzalanic effect

(De Larrard, 1989). However, the concept of high packing density has recently been discovered as a key to obtaining ultra-high performance cementitious materials in which Solid Suspension Model was used and with 0.14 water/binder ratios, 236 N/mm² compressive strength was obtained (De Larrard & Sedran, 1993). Such development of an ultra-high strength and ductile concrete designated Reactive Powder Concrete (RPC) was made possible by the application of a certain number of basic principles relating to the composition, mixing and post-set heat curing of the concrete (Richard & Cheyrezy, 1995).

Reactive powder concrete is a new generation concrete that was developed through microstructure enhancement techniques for cementitious materials which include eliminating coarse aggregates, reducing the water-to-binder ratio, lowering calcium oxide (CaO) to silicon oxide (SiO₂) ratio by introducing the silica components and incorporating of steel micro-fibres (Yazici *et al.*, 2009). The term ‘reactive powder concrete’ reflect the fact that all powder components in RPC chemically react after casting: cement by conventional hydration, pozzolanic materials through pozzalanic reaction with the calcium hydroxide (CH) liberated from cement, quartz sand by providing dissolve silica for the formation of further calcium silicate hydrates (C-S-H) gel, crush quartz to alter the calcium oxide (CaO) to silicon oxide (SiO₂) ratio and favour the formation of tobermorite and xonotlite when RPC is subjected to heat treatment or setting pressure (Tam *et al.*, 2010). But the use of cement in RPC is high and silica fume content is often over 25% (by weight of cement) which, not only increases the production costs, but also has negative effects on the strength and durability of concrete due to thermal cracks resulting from increase heat of hydration which cause shrinkage problems (Peng *et al.*, 2015). It was shown that replacing the cement with other mineral admixtures other than silica fume seems to be a feasible

solution to the problems (Rougeau & Borys, 2004; Yazici *et al.*, 2009; Yazici *et al.*, 2010; Agharde & Bhalchandra, 2015; Kushartomo *et al.*, 2015). Ultrafine particles other than silica fume such as fly ash, limestone micro-filler, blast furnace slag and metakaolin can be used in the production of ultra-high-performance concrete (Rougeau & Borys, 2004, Yazici *et al.*, 2009, Yazici *et al.*, 2010). This research is focused on the production of RPC from locally sourced unrefined MK and GIW as alternatives to SF and steel fibre.

1.6 Aim and Objectives

1.6.1 Aim

The research aimed at assessing the properties of reactive powder concrete made with locally sourced unrefined MK and GIW with a view to establishing the suitability of Nigerian kaolin for the production of ultra-high-performance concrete.

1.6.2 Objectives

The aim of this study was achieved through the following objectives:

- I. To characterize the properties of OPC, MK, quartz sand and normal sand to be used in the production of RPC
- II. To determine an appropriate mix ratio for the production of the RPC
- III. To determine the fresh and hardened properties of the RPC produced with unrefined MK
- IV. To evaluate the properties of the RPC exposed to elevated temperatures
- V. To examine the microstructure of the RPC exposed to elevated temperatures
- VI. To develop mathematical models for predicting properties of RPC

1.7

Scope and Limitations

1.7.1 Scope

The research was confined to the evaluation of the following properties: flowability, compressive strength, tensile strength and flexural strength (measured at 7, 14, 28, 90 and 180 days of curing), also durability test such as sorptivity, absorption and elevated temperatures (27-800°C) of the RPC produced with unrefined MK and GIW. Micro-structure analysis of the RPC specimens exposed to elevated temperatures was also carried out using XRD, FTIR and SEM. The MK used was obtained locally from the kaolinite deposit called *Farar Kasa* in Getso town, Gwarzo LGA, Kano State.

1.7.2 Limitations

However, due to some constraints such as lack of state of the earth heat treatment equipment, heat treatment could not be done on the RPC specimens. Other properties of RPC such as shrinkage and exposure to chemically aggressive environment were also not assessed.

CHAPTER TWO

2.0

LITERATURE REVIEW

2.1

An overview of Advances in Concrete Technology

Concrete is the most widely used construction material, second to water as the most utilized material on the planet (Gambhir 2006, Mehta & Mantero 2007). It is made by mixing cementitious materials, aggregates, water and sometimes admixtures in the required proportions.

Normal strength concrete (NSC) was first made in the early 1900's. It is still a material of choice due to its versatility, low cost and excellent resistance to water (Mehta, 1999), but it has some shortcomings. Hardened Portland cement concrete is heterogenous and porous in nature (Buitelaar, 2004). This is the reason why the concrete becomes affected when exposed to aggressive media, resulting to durability problems. Since strength was used as the only index of determining the quality of concrete at that time, a high strength concrete was developed.

The use of High Strength Concrete (HSC) has its application where durability of concrete is affected by factors such as abrasion, aggressive environment and so on (Mehrotra, 2009). American Concrete Institute (ACI363-1984) defined HSC as a concrete having special attributes such as high workability, good strength (41 N/mm^2 or greater) and high durability. Mehrotra, (2009) stated that HSC should have strength of between 75 and 100 N/mm^2 at 28 days with improved impermeability and durability over the NSC. This opinion seems to be more appropriate considering the new innovations, improved technology and materials in concrete production. The HSC is however, associated with some challenges such as brittleness, low tensile strength and strain capacities (Mehrotra, 2009). Because of

these problems, a High-Performance Concrete (HPC) was developed in the 1950s (Aıtcin, 2003).

Mehrotra (2009) and Gambhir (2006) defined HPC as follows:

A concrete in which certain characteristics are developed for a particular application and environment so that it will give excellent performance in the structure in which it will be placed, in the environment in which it will be exposed, and with the load to which it will be subjected during its design life.

High performance concrete is made up by the addition of pozzolanic materials with low water-binder ratio (between 0.30-0.40), high strength of up to 120 N/mm² which is more durable than normal concrete and its capillary and pore networks are somewhat disconnected due to the development of self-desiccation (Chan *et al.*, 2000; Agharde & Bhalchandra, 2015). The continuous search for high performance concrete for construction in advanced civil engineering and building structures such as long span bridges, skyscrapers, nuclear stations, etc. has led to the discovery of Ultra-High-performance concrete (UHPC) also known as Reactive Powder Concrete (RPC) with better properties than the HPC.

Reactive powder concrete is a special cement-based material with excellent properties than the HPC that could solve the shortcomings of concrete today (Al-hassani, Khalil & Danha, 2014). It was first produced by Richard and Cheyrezy (1995) in Bouygues laboratory, France. It was made possible by optimizing the packing density of the concrete with precise gradation of all the mix particles (cement, sand, quarts, pozzolans, superplasticizer and steel fiber). RPC has a high strength of up to 800 N/mm², high ductility (about 250 times that of conventional concrete) and high flexural strength (30 -60 N/mm²) (Maroliya, 2012, Sujatha & Basnathi, 2014).

2.1.1 Normal strength concrete

Development in concrete technology has been ongoing since 1900s. With each successive development and corresponding strength increase, the definition of strength was revised. Chan, Peng and Chan (1996) described concrete with strength between 28-47 N/mm² as NSC. Historically, concrete with 25 N/mm² was considered HSC in the middle of the 20th century (Wu, Sofi & Mendis 2010). In the 1980s, 50 N/mm² concrete was considered HSC. Moreover, there is no exact point of separation between NSC and HSC (ACI363-84). Thus, HSC is defined as that concrete which has compressive strength from 41 N/mm² and above. This value was adopted by ACI 363 in 1984, but is not yet hard and fast, because ACI recognizes that the definition of high strength varies on a geographical basis. Another classification of concrete was given in Table 2.1 by Prof. Francis Young of the University of Illinois (Farny & Panarese 1994):

Table 2.1: Strength classification of concrete

	Conventional concrete	High strength concrete	Very high strength concrete	Ultra-high strength concrete
Strength, MPa	< 50 (7250)	50-100 (7250-14,500)	100-150 (14,500-21,750)	> 150 (21,750)
Water-cement ratio	> 0.45	0.45-0.30	0.30-0.25	< 0.25
Chemical admixtures	Not necessary	WRA/HRWR	HRWR	HRWR
Mineral admixtures	Not necessary	Fly ash	Silica fume	Silica fume
Permeability coefficient (cm/s)	> 10^{-10}	10^{-11}	10^{-12}	< 10^{-13}
Freeze-thaw protection	Needs air entrainment	Needs air entrainment	Needs air entrainment	No freezable water

Source: Farny and Panarese (1994)

So, because ACI is one of the world leading research institutes, their definition has been considered in this research to be more appropriate. Therefore, it can be said that any concrete with strength below 41 N/mm² can be regarded as NSC.

2.1.2 High strength concrete

High strength concrete (HSC) is a concrete that has improved properties more over NSC particularly strength. The ACI defined it as a concrete with designed 28 days strength of 41 N/mm² and above. HSC is a concrete with compressive strength of 70 N/mm² or above (Kosmatka & Wilson 2012). Nayak and Jain (2012) describe HSC as a concrete of strength between 65 and 100 N/mm². However, looking at the lowest and highest figure stated above, it can be concluded that any concrete with strength between 41 and 100 N/mm² can be regarded as HSC. Kosmatka and Wilson (2012) were of the view that the production of HSC does not require special materials; only the designer should know the factors affecting compressive strength and vary them for better results. Moreover, many were of the opinion that the use of HSC depends economically on the availability of high-quality materials for use in the concrete (Nayak & Jain 2012, Mehrotra, 2009). It can be argued that factors affecting compressive strength could be materials (source and method of processing the material) or the way they are used in concrete production. Therefore, HSC depends greatly on the optimization of the concrete and its constituent materials. When producing HSC, the designer should optimize the following according to Mehrotra, (2009):

- a. Cementitious paste: the water-cement ratio of the paste should be adequate to give the required consistency and workability without segregation.

- b. Aggregates: the fine and coarse aggregates should have the required grading as specified by the relevant standard taking into consideration the optimum cement content.
- c. Paste Aggregates Bond: the bond between paste and aggregates is a weak one; attention should be paid to improve its contribution to the overall concrete strength. Attention should also be paid to materials, mix design, handling, placing, compaction and finishing.

The use of HSC has advantages in the precast and prestressed construction which include the rapid output of component and reduction in damage during transportation and handling. It allows the use of thinner concrete sections, longer beams spans which results in overall dead load reduction of the structure (Mehrotra, 2009). The permeability is low, HSC may be used in aggressive environment like the marine environment, etc. However, HSC is believed to be a concrete with limited application such as construction of columns in high rise buildings or off-shore platforms which are critical components of the structure exposed to aggressive environment (Nayak & Jain 2012).

Conclusively, HSC is characterized by superior strength, high stiffness and better durability compared to NSC. On the other hand, high brittleness, low tensile strength and strain capacities were identified as the shortcoming of HSC (Mehrotra, 2009).

2.1.3 High performance concrete

Advancement in concrete technology including the use of improved materials led to the use of HSC for modern infrastructure development. However, the use of concrete has been extended to aggressive environment and strength or high strength alone is no longer the index used in determining the performance of concrete. Performance or high performance is defined as the ability and efficiency of a concrete to perform its designed purpose for and or

above the specified period of time with little or no maintenance (Mehrotra, 2009). A performance enhance concrete or HPC is a specialized concrete designed to obtain some benefits that are not obtainable from NSC (Gambhir, 2006). In addition to this, HPC is a concrete with superior properties than those of NSC and HSC. Any concrete fulfilling certain criteria aimed at overcoming the shortcomings of NSC and HSC may be called HPC. This is a concrete with improved resistance to environmental factors, high strength, reduced construction time without compromising long term serviceability and other requirements. American concrete institute also defined HPC as concrete meeting special combination requirements that cannot always be achieved routinely when using conventional constituents and normal mixing, placing and curing practices. The HPC is characterized by low water-cement ratio (0.2-0.45) (but super plasticizers are used to make the concrete flowable and workable), it has greater durability in mild, moderate or severe environment than other types of concrete (Kosmatka & Wilson 2012). Table 2.2 shows the list of some materials often used in HPC and their selection criteria and Table 2.3 shows some the selected properties of HPC.

Table 2.2: Materials used in high performance concrete

Material	Primary contribution/ desired property
Portland cement	Cementing material
Blended cement	Cementing material/durability/high strength
Fly ash	Cementing material/durability/high strength
Slag cement	Cementing material/durability/high strength
Silica fume	Cementing material/durability/high strength
Metakaolin	Cementing material/durability/high strength
Calcined shale	Cementing material/durability/high strength
Expanded shale, clay, and/or slate	Lightweight
Superplasticizers	Flowability
High-range water reducers	Reduce water to cement ratio
Hydration control admixtures	Control setting
Retarders	Control setting
Accelerators	Accelerate setting
Corrosion inhibitors	Control steel corrosion
Water reducers	Reduce cement and water content
Shrinkage reducers	Reduce shrinkage
ASR inhibitors	Control alkali-silica reactivity
Polymer/latex modifiers	Durability
Optimally graded aggregate	Improve workability and reduce paste demand

Source: Kosmatka and Wilson (2012)

Table 2.3: Selected properties of high-performance concrete

Properties	Test method	Criteria that may be specified
High compressive strength	ASTM C39 (AASHTO T22)	55 to 140 MPa (8000 to 20,000psi) at 28 to 91 days
High-early compressive strength	ASTM C39 (AASHTO T22)	20 to 41 MPa (3000 to 6000psi) at 3 to 18 hours, or 1 to 3 days
High-early tensile strength	ASTM C78 (AASHTO T97)	2 to 4 MPa (300 to 600 psi) at 3 to 12 hours, or 1 to 3 days
Abrasion resistance	ASTM C944	0 less than 2mm depth of wear
Low permeability	ASTM C1202 (AASHTO T277)	500 to 2500 coulombs
Reduced chloride penetration	ASTM C1543 (AASHTO T259 and AASHTO T 260)	Less than 0.07%Cl at 6 months
High resistivity	ASTM G59	
Low absorption	ASTM C642	2% to 5%
Low diffusion coefficient	ASTM C1556	$100 \times 10^{-13} \text{m}^2/\text{s}$
Resistance to chemical attack	Expose concrete to saturated solution in wet/dry environment	No deterioration after 1 year
Resistance to sulfate attack	ASTM C1012	Mild exposure: 0.10% max expansion at 6 months; moderate exposure: 0.10% max expansion at 12 months; severe exposure: 0.10% max expansion at 18 months
High modulus of elasticity	ASTM C469	34 to more than 48 GPa (5 to more than 7 million psi)
High resistance to freezing and thawing damage	ASTM C666, Procedure A(AASHTO T161)	Relative dynamic modulus of elasticity after 300 cycles of 70% to more than 90%
High resistance to deicer scaling	ASTM C672	Visual rating of the surface after 50 cycles of 0 to 3
Low shrinkage	ASTM C157	Less than 800 millionths (microstrain) to less than 400 millionths (microstrain)
Low creep	ASTM C512	70 microstrain/MPa to less than 30 microstrain/MPa (0.52 microstrain/psi to less than 0.21 microstrain/psi)
Increased workability	ASTM C143 (AASHTO T119)	Slump more than 190mm (7.5in)
Increased workability for SCC	ASTM C1611	Slump flow $\leq 600\text{mm}$ (24 in)
Resistance to alkali silica reactivity	ASTM C441	Expansion at 56 days of 0.20% to less than 0.10%
Resistance to delayed ettringite formation	Maximum internal curing temperature (within concrete)	Less than 70 °C (158 °F)

Source: Kosmatka and Wilson (2012)

The life span of HPC is between 75 to 120 years (about 2-times longer than conventional concrete (Mehrotra, 2009). Therefore, according to (Nayak & Jain 2012), for a concrete to be recognized as HPC it must comply with the requirements of impermeability and dimensional stability.

- a. Impermeability: the movement of moisture and harmful chemical ions into concrete can greatly affect the performance of concrete leading to corrosion of steel or expansive reaction within the concrete that affect its service life.
- b. Dimensional or volume stability: this depends on high elastic modulus, low thermal strain, low drying shrinkage and low creep. If these are not taken care of, undesirable stress effects can result in volume changes under restrained conditions. Improved elastic modulus can be achieved through proper selection of materials in concrete proportions. When this is done, the creep and drying shrinkage at 90 days can be reduced to less than 0.04% as against 0.08% common to normal concrete. Volume stability can therefore be achieved by limiting the total volume of the cement paste in concrete and by using coarse aggregate which has high strength and elastic modulus.

2.1.3.1 Benefits of using HPC

The following are some of the benefits according to Mehrotra (2009) that can be derived from using HPC:

- i. Using thinner section (leads to dead load reduction) and reduction in the overall cost of the structure
- ii. Early removal of formwork
- iii. HPC members have greater stiffness and are relatively lighter

- iv. Concrete can be put into service much earlier; for example, an HPC pavement or heavy-duty platform can be opened for use in 4-5 days
- v. Bridge deck made of HPC are more durable and require minimum maintenance
- vi. HPC members have higher axial strength that allow use of smaller columns

2.1.3.2 Applications of HPC

Some of the areas of applications of HPC are as follows:

- i. The common use of HPC is in the construction of high-rise buildings, bridge decks and columns structures, use of reduced column size, increase usable space in high rise buildings with smaller foundations.
- ii. The HPC can be used to satisfy special needs like high compressive strength, high flexural strength, etc. in areas like dams, roads pavements, airport runways, etc.
- iii. It can be used to build long-span bridges components like piers and pier columns abutments, decks, rails, etc. Because of its longer life-span, HPC can cut down significantly maintenance repairs and even replacement needs over the entire life of the bridge.
- iv. The HPC reduces construction time.

2.2 Reactive Powder Concrete

There is growing interest in the emerging of new cementitious materials with better properties than NSC, HSC and HPC. Reactive powder concrete (RPC) has been recognized as a revolutionary material that provides ultra-high strength, excellent ductility and excellent durability (Tam, Tam & Ng, 2010). The RPC is a mixture of very fine powders (cement, sand, quartz powder and silica fume), steel fibers (optional) and super plasticizer

(Song & Liu, 2016). It was first produced in 1995 by Richard and Cherezy in the Bouygues laboratory, France. It is regarded as a promising material for special precast industries members such as those used in industrial and nuclear waste storage facilities (Yazici *et al.*, 2010). RPC is a developing composite material that will allow the concrete industry to optimize material use, generate economic benefits and build structures that are strong, durable and sensitive to the environment (Maroliya, 2010).

2.2.1 Composition of reactive powder concrete

Reactive powder concrete is composed of cement, sand, quartz sand or powder, silica fume, steel fibers (optional) and super plasticizer (Song & Liu, 2016). The use of super plasticizer is at optimal dosage which leads to reduction in water cement ratio while improving the workability of the concrete. Silica fume, as the major ingredient of RPC, is an excellent pozzalanic material that has proven benefits on the properties of concrete (Srivastava, Agarwal & Kumar 2012). Its major influence is that of filler which fill the spaces between the cement particles. Brief description of the constituent materials of RPC is as follows:

2.2.1.1 Cement

Portland cement is hydraulic cement composed primarily of hydraulic calcium silicate. American society for testing and materials (ASTM C150) defined Portland cement as ‘hydraulic cement (cement that not only hardens by reacting with water but also forms a water-resistant product) produced by pulverized clinkers consisting of essentially hydraulic calcium silicates, usually containing one or more of the forms of calcium sulfate as an inter ground addition’. The function of the cement is to bind the constituent materials (sand and stone) together and fill in the voids between them in order to form a compact mass (Gambhir & Jamwal 2014; Mehrotra, 2009). Portland cement sets and hardens by reacting

chemically with water and maintain their stability under water. Hydraulic cements include Portland cement and blended cement. Other types of hydraulic cement include natural cement and slag cement. Cement is also classified into general purpose Portland cement and special purpose cements. They are used in all aspect of construction (Kosmatka & Wilson, 2012).

2.2.1.2 Silica fume

Silica fume is an extremely fine amorphous (non-crystalline) material produced in electric arc-furnaces which is a waste product of silicon and ferrosilicon industry. It is also known as condensed silica fume or micro silica. Details of SF are discussed in section 2.3.1.

2.2.1.3 Fine sand

Aggregate is chemically inert material of selected size, held together by a hardened cement paste, which acts as the binder to the aggregates (Mehrotra, 2009). Aggregates can be natural gravel, crushed rock or an artificially prepared heavy or light weight material which is available in various shapes, sizes and qualities that may range from fine sand to large sand. The aggregates occupy 70-80% of the volume of concrete (Kosmatka & Wilson, 2012; Mehrotra, 2009) which determine the concrete fresh and hardened properties, proportions and even economy of the concrete mixture. A good aggregate must be clean, hard, strong, durable and free from absorbed chemicals, coating of clay and other fine materials in amount that could affect hydration and bond of the cement paste.

Generally, fine aggregates consist of natural sand or crushed stone with particles size smaller than 5 mm. Coarse aggregates consist of gravels, crushed stone or a combination of the two with particles size greater than 5 mm but not greater than 375 mm (Nayak & Jain,

2012). However, concrete like RPC is produced without the use of coarse aggregate. Therefore, fine aggregates of size between 600 and 150 μm are used (Richard & Cheyrezy, 1995). Moreover, the sand offers some advantages in RPC such as very hard material, excellent paste/aggregate interfaces, readily available and low cost.

2.2.1.4 Quartz sand

Quartz sand is also a constituent material of RPC. Quartz is silica in its pure state and seconds the most occurring mineral after feldspar. Its general formula is SiO_2 derived from continuous framework of SiO_4 with each shared between tetrahedral. There are different types of quartz, many of which are semi-precious gemstone and are used in different ways.

Quartz can be used in glass making, abrasive and foundry sand. Quartz sand is used as filler in the manufacture of rubber, paint and putty. It is also used as traction in the railroad and mining industries (Abdullahi, Ibrahim & Buga, 2014). However, the main function of quartz in RPC is to serve as an essential ingredient for heat treated RPC concrete where maximum reactivity is obtained (Richard & Cheyrezy 1995) using smaller particles size. Table 2.4 shows the physical and chemical properties of quartz.

Table 2 4: Characteristics of quartz

Properties	Description
Chemical classification	Silicate
Chemical composition	SiO ₂
Color	Clear, white, gray, purple, yellow, brown, black, pink, green and red
Streak	Colorless (harder than the streak plate)
Luster	Vitreous
Diaphaneity	Transparent to translucent
Cleavage	None-typically break with a conchoidal fracture
Mohs Hardness	7
Specific gravity	2.6 to 2.7
Diagonostic properties	Conchoidal fracture, glassy luster, hardness
Crystal system	Hexagonal

Source: Abdullahi, Ibrahim and Buga, (2014)

Quartz deposits are available in many states in Nigeria ready for quarrying and processing for local and export demands (Abdullahi, Ibrahim & Buga, 2014).

2.2.1.5 Admixtures

Admixtures are materials other than water, cement and aggregates which are added to the concrete during or after mixing to alter one or more of the properties of concrete either at fresh or hardened stage (Gambhir & Jamwal 2014). The use of admixture offers some benefits not attainable by adjusting the proportions of cement and aggregates without affecting any of the concrete properties. Furthermore, admixtures can be chemical or waste

materials used to modify certain properties of concrete. The usually modified properties are rate of hydration or setting time, workability, dispersion and air-entrainment. The admixtures are generally added in small quantity (Gambhir, 2006).

Admixtures are primarily used to reduce cost of concrete construction, modify the performance of hardened concrete, ensure the quality of concrete during mixing, transporting, placing, compacting and curing, and to overcome certain emergencies during concreting operations (Mehrotra, 2009).

Superplasticizer: These are polycarboxylate ether-based admixture which can achieve a high-water reduction of up to 40% with long retention of workability (Nayak & Jain 2012). Polycarboxylate derivatives are the newest generation of high-range water reducers and superplasticizers (Kosmatka & Wilson 2012). Superplasticizer enables the optimization of w/c ratio and workability of a concrete (Gambhir, 2006), i.e., provide enhanced plastic and hardened properties. It is used in self-compacting concrete where proper compaction is impossible due to dense reinforcement, for high strength concrete (like RPC) of above 50 N/mm² where higher fines are required with as low as 0.28 water-binder ratio (Nayak & Jain 2012).

Advantages of using Superplasticizer: The following are some of the advantages of using superplasticizers as stated by Mehrotra (2009) and Gambhir (2006):

- i. Superplasticizers can be used to produce ultra-high strength concrete
- ii. They can be used as retarders in hot weather concrete or where long placing periods is required

- iii. They can be used to avoid segregation of concrete and concrete stiffens in a reasonable period of time
- iv. They can be used for laying large floor areas in a continuous operation with small labour force
- v. They have a workable slump in the range of 75 to 125mm but Gambhir, (2006) stated slump to be ≥ 200 mm
- vi. They can result to a cement saving of between 10-15%
- vii. Speed of concreting is increased
- viii. Finishing surface is of better quality

2.2.1.6 Fibres in RPC

Fibre is discontinuous and 3-dimensionally orientated reinforcement when mixed in concrete. Fibres have been used in ready mixed concrete, precast concrete and shotcrete over three decades. They may be made up of steel, synthetic, glass and natural materials like wood cellulose in different shapes, sizes and thickness (Kosmatka & Wilson 2012).

Difference between fibre and reinforcement: The difference between fibre and reinforcement is described as follows:

1. Fibres are generally distributed throughout the concrete while reinforcement or wire mesh are placed where they are required
2. Fibres are short and closely spaced while reinforcement are continuous
3. Fibres are added to concrete in low volume less than 1% and are effective in reducing plastic shrinkage cracking (Kosmatka & Wilson 2012).

Types of fibres: The different types of fibres are discussed as follows:

Glass fibres: These are used to enhance the crack resistant properties of concrete. Because the alkaline reactivity between glass fibres and cement pastes reduces the strength of the concrete, only alkaline-resistant fibers should be used in the concrete. It is a known fact that glass fibres become brittle during hydration of cement which leads to reduction in strength, toughness and impact resistance with age. Glass fibres can be damaged during mixing; therefore, excessive mixing or handling should be avoided. The main function of the fibre is to improve tensile strength of the concrete, i.e., increase crack resistance.

Synthetic fibres: These are man-made fibres resulting from research and development in the petrochemical and textile industries. Fibres that are used in concrete include acrylic, aramid, carbon, nylon, polyester, polyethylene and polypropylene. The main function of the synthetic fibre is reducing plastic shrinkage and subsidence cracking over steel reinforcement which helps in strengthening concrete after cracks.

Natural fibers: These were used as reinforcement long before the advent of conventional reinforced concrete, e.g., straw for mud bricks, horse hair for mortars, etc. Coconut coir, sisal, bamboo, jute, wood and vegetable fibers were used successfully to make thin sheets for walls and roofs in the early 1960s. They showed good mechanical properties with low durability which is associated with volume changes resulting from variation in moisture content. The natural fibers should conform to ASTM D7357 and ASTM D6942.

Steel fibre: steel fibres are short, discrete lengths of steel with an aspect ratio (ratio of length to diameter) from about 20 to 100 mm and with a variety of cross sections and profiles (Kosmatka & Wilson 2012). The use of steel fibres in concrete provides an

economic approach which minimizes plastic shrinkage cracks, reduces the severity of thermal cracking, improves the thermal cracking, improves the fatigue, impact resistance, increase overall durability and toughness of concrete (Mehrotra, 2009).

The volume of steel fibre normally used is between 0.25 and 2%. More than 2% generally reduce workability and dispersion which will require special mix design or concrete placement techniques. The compressive strength of concrete is slightly affected by the addition of fibres. However, 1.5% by volume of steel fibres can increase the direct tensile strength by up to 40% and the flexural strength of up to 150% in comparison to concrete without steel fibres (Mehrotra, 2009).

Steel fibres have a relatively high modulus of elasticity. Their bond to cement matrix can be enhanced by mechanical anchorage or surface roughness. They are protected from corrosion by the alkaline environment in the cement matrix. Steel fibers are used in airport pavements and run way/taxi overlays, bridge deck, industrial floors, highway pavement. They are also used in precast application for improved impact resistance or toughness. They have also been used to replace conventional reinforcement in utility boxes and septic tanks. Where there is possibility of concrete cracking, steel fibres are used to minimize crack width. They are also used as primary reinforcement or where high abrasion resistance is required or high impact resistance is a possibility.

The advantage of using steel fibres in concrete is to reduce the contraction of concrete due to stresses near the micro cracks by bridging cracks and transferring some of the load across it and fibers near the crack tip resist more loads to their higher modulus of elasticity compared with that of the surrounding concrete (Mehrotra, 2009). Moreover, steel fibres

are not easily damaged during mixing or shortcreting and are chemically compatible with alkaline environment within the cement paste (Kosmatka & Wilson 2012).

Factors influencing fibre performance: The following are some of the factors affecting steel fibre performance:

- i. The shape (straight, hooked, undulated, crimped, twisted, coned)
- ii. The length (12.7 mm to 63.5 mm)
- iii. The diameter (0.4 mm to 1.05 mm)
- iv. The tensile strength (1000 N/mm^2 - 2500 N/mm^2)

However, non-availability of these materials in developing countries like Nigeria is hindering the growth of concrete technology. But there are other ways that such countries can benefit through conversion of waste to wealth. Recently, some researchers like Jalal (2012) used waste steel fibre recovered from milling and machining in concrete production and the results indicated improvement of the fragile matrix, mostly in terms of toughness, energy absorption and post-cracking behavior. Ashish and Rinku (2012) studied the influence of adding lathe machines waste material as fibres at the dosage of 5% to 30% by weight of cement. The results show strength increased up to 20 % of the lathe machines waste was used as steel fibre. But strength decreased when 25 % and 30 % of the lathe machines waste material was used. Strength reduced due to decreasing quantity of cement. On the other hand, adding steel fibre in place of cement did not act as a binding material which affected the bond strength of concrete, hence reducing strength of concrete. Study on the influence of adding waste materials like lathe waste, soft drink bottle caps, empty waste tins, waste steel powder

from workshop at a dosage of 1% of total weight of concrete as fibres was undertaken by Murali *et al.*, (2012). These materials were deformed into rectangular strips of 3 mm width and 10 mm length. Results showed that a concrete block incorporated with steel powder has increase in compressive strength by 41.25% and tensile strength by 40.81%. Concrete made with soft drink bottle caps exhibited an increase in flexural strength by 25.88%. Therefore, this research made use of Waste Gear Inner Wire (GIW) as fibre in the production of RPC.

The use of fibres in RPC: One of the RPC production principles is the achievement of ductile material by the addition of steel fibres. Due to high cement content, RPC becomes brittle in nature. This necessitated the use of fibre in order to reduce the brittle nature of the concrete. By introducing fine steel fibers, RPC can achieve remarkable flexural strength up to 50 N/mm² (Meleka, Bashandy & Arab, 2013). As for the good tenacity, incorporating steel fiber could increase the RPC's fracture energy to 20000–40000 J/m² (Song & Liu 2016). Fibre is an essential ingredient in the production of strong, ductile material known as RPC. It was used by many researchers in the production of this type of concrete (Yazici *et al.* 2009; Maroliya & Modhera, 2010; Maroliya, 2012; Al -Hassani, Khalil, & Danha, 2014)

2.2.2 Properties of reactive powder concrete

The properties of the RPC are highlighted as follows:

2.2.2.1 Fresh properties

At the beginning of the 20th century, the concrete industry deemed it necessary to monitor the workability of concrete to ensure that the concrete can be properly placed and achieve adequate strength (Koehler & Fowler 2003). The workability of fresh concrete influences

micro structural development as well as the ultimate hardened properties of the concrete. Moreover, the main function of any fresh concrete is that it should be consistent in such a way that it is readily consolidated in forms and around reinforcement without excessive bleeding or segregation (Roussel 2007). Therefore, fresh concrete with sufficient workability shall have good hardened properties. The strength of concrete depends upon hydration reaction in which water plays an important role (Tam, Tam & Ng, 2010).

The quantity of water required for chemical combination with cement and occupying gel pores is instrumental for hydration process. Shetty (2015) stated that the theoretical water/cement ratio required is 0.38. Use of water/cement ratio more than this will result in capillary cavities; less than this, will result in incomplete hydration and also lack of space in the system for the development of gel. The use of good water to binder ratio is significant in achieving concrete with required strength. Tam *et al.* (2010) notes that the strength of concrete largely depends on hydration reaction. However, there is different water to binder ratio used by many researchers across the globe to achieve maximum compressive strength. For RPC, the amount of water-binder ratio is lower than the theoretical (0.38). Richard and Cheyrezy (1995) as pioneer researchers of RPC, used water/binder ratio of between 0.15 to 0.19. Subsequent researchers on RPC used between 0.17 to 0.25 (Al-Hassani, Khalil & Danha 2014; Sujatha & Basanthi 2014; Tam *et al.* 2010; Cwirzen *et al.* 2008).

2.2.2.2 *Hardened properties of RPC*

RPC is a developing composite material that will allow the concrete industry to optimize material use, generate economic benefits and build structures that are strong, durable and sensitive to the environment. It was developed by Richard and Cheyrezy (1995) and since then, there have been a lot of researches in this field trying to explain the properties of the

RPC particularly the hardened ones. It was stated that the RPC was made possible by the application of certain number of basic principles relating to the composition, mixing and post-set heat curing of the concrete. It is now possible to produce concrete with strength of between 170 to 200 N/mm² as R200 and between 650 to 810 N/mm² denoted R800. But R800 is obtained with a mixture incorporating steel aggregates. Moreover, R800 has flexural strength of between 30 to 60 N/mm², young modulus of between 50 to 60 N/mm². R800 on the other hand has flexural strength of between 45 to 141 N/mm². RPC is tested in terms of strength, uniaxial compressive stress-strain relation and flexural load deflection relation.

After the discovery of the RPC in 1995, researches have been continued to date. Chang *et al.* (2006) evaluated the performance of RPC used as a retrofitting material. Results showed that the flow of fresh RPC was between 155 to 205%, the average compressive strength was 110.7 N/mm² and 157.9 N/mm² for 7 and 28 days respectively under normal moist curing. Moreover, there was an increase in strength of between 28.7% to 40% when steam cured.

Most of the researches that came after the discovery of RPC achieved the same or similar mechanical properties to those of the pioneer researchers. Another break through is that of using other pozzolanic materials to partially replaced one of the constituent materials of RPC. In 2010, Yazici *et al.* replaced up to 60% Portland cement with ground granulated blast furnace slag (GGBFS) and achieved a compressive strength of over 250 N/mm², after autoclaving (using granite aggregates), 400 N/mm² was achieved with external pressure application during setting and hardening stage (using bauxite aggregate). There was also reduction in cement content; 564 and 376 kg/m³ were used for the two mixes as against 800-1000 kg/m³ for conventional RPC (Yazici *et al.*, 2009). Reduction of cement led to

reduction in heat of hydration. RPC without quartz powder was produced by replacing up to 15% of cement with fly ash and GGBFS (Kumar, Rao & Sabhahit, 2013). The results indicated improvement in compressive strength and modulus of elasticity. More recently, Kushartomo *et al.* (2015) used glass powder of up to 30% of cement by weight to replace quartz in the production of RPC. With 20%, a compressive strength of up to 136 N/mm², average split tensile strength of 17.8 N/mm² and flexural strength of 23.2 N/mm² were achieved.

Reduction of cement content using class-C fly ash up to 60% was targeted under standard curing, autoclave curing and steam curing using bauxite and granite aggregates (Yigiter *et al.* 2012). Test results show that compressive strength of 200 N/mm² was achieved when cured in water. Thermally treated specimens show compressive strength beyond 250 N/mm², when external pressure was applied, a compressive strength of up to 400 N/mm² was achieved. Furthermore, split tensile and flexural strengths greater than 20 N/mm² and 25 N/mm² respectively were achieved. The results obtained by Yigiter *et al.* (2012) and Yazici *et al.* (2010) are in agreement although different materials were used to reduce the cement content in the conventional RPC.

Yazici *et al.* (2009) studied the mechanical properties of RPC containing class-C fly ash and GGBFS under different curing regimes with the results indicate that strength of above 100 N/mm² were possible when cured in water. Moreover, strength of over 234 N/mm² and 250 N/mm² were achieved using steam and autoclave curing respectively. Decreasing cement content led to reduction in heat of hydration and shrinkage which are problems associated with conventional RPC.

Abbas, Soliman and Nehdi (2015) studied a number of UHPC mixtures with varying steel fibres lengths (8 mm, 12 mm and 16 mm) and dosages (1%, 3% and 6%) by volume. Results show an increase in mechanical properties (up to 173 N/mm² of strength) as the fibre dosage increase. UHPC mixtures incorporating short steel fibres exhibited enhanced flexural properties compared to that of mixtures with similar volume of longer steel fibre.

Table 2.5: Summary of hardened properties of RPC

S/No.	Author	Curing method	Hardened properties		
			Compressive Strength (N/mm ²)	Tensile Strength (N/mm ²)	Flexural strength (N/mm ²)
1.	Richard & Cheyrezy (1995)	Water	(170-200) R200	(50-60) R200	(30-60) R200
		Pressure	(650-810) R800	(65-75) R800	(45-141) R800
2.	Cheng <i>et al.</i> (2006)	Water	110.7-157.9		
3.	Yazici <i>et al.</i> (2009)	Water	>100		
		Steam	234		
		Autoclaving	250		
4.	Yazici <i>et al.</i> (2010)	Autoclaving	250		
		Pressure	400		
5.	Yigiter <i>et al.</i> (2012)	Water	200	>20	>25
		Steam & pressure	400		
6.	Abbas, Soliman & Nehdi (2015)		173		
7.	Kushartomo <i>et al.</i> (2015)		136	17.8	23.2
8.	Asteray, Oyawa & Shitote (2017)		57.3		
	Average	Depending on the condition & Material	57.3-800	≥17.8	≥23.2

2.2.3 Types of RPC

There are basically two types of RPC designated as R200 and R800 (Richard & Cheyrezy, 1995) but for the purpose of this research, only R200 was considered because RPC is at its infancy stage in Nigeria and no availability of instrument for pressure application as shown in Table 2.6.

Table 2 6: RPC 200 and its properties

RPC 200	Range of values
Pre-setting pressurization	None
Heat-treating	20°C to 90°C
Compressive strength	170 to 200 N/mm ²
Flexural strength	30 to 60 N/mm ²
Fracture energy	20, 000 to 40, 000 J.m ⁻²
Ultimate elongation	5, 000x10 ⁻⁶ to 7, 000x10 ⁻⁶ m.m ⁻¹
Young's modulus	50 to 60 KN/mm ²

Richard and Cheyrezy, (1995)

2.2.4 Application of reactive powder concrete

Reactive powder concrete has been recognized as a new construction material for precast prestressed concrete highway bridges due to its reduced maintenance cost compared to steel and conventional concrete bridge girders (Nematollah *et al.*, 2012) like the repairs and retrofitting on concrete element under compressive and flexural strength (Lee, Wang & Chiu, 2007). The reduction in porosity and the improved impermeability of RPC also lead

to significant durability and strength development that enables the casting of slender elements.

The RPC was first used in the construction of a footbridge in Canada known as Sherbrooke in 1997 and a footbridge spanning 120 m was constructed in Seoul, South Korea in 2002 (Nematollahi, Saifulnaz, Jaafar & Voo 2012).

Researches on the use of RPC or UHPC in China are on top gear. The present five completed bridges (made up of RPC/UHPC) in China indicate a significant milestone in this regard (Chen *et. al* 2016). These bridges comprise two railway bridges, one highway bridge and two pedestrian bridges in China.

Because of its fire resistance and large residual strength when exposed to high temperature, RPC can be used as building materials particularly in areas where high temperature is expected (Liu & Huang 2009).

2.3 General Overview on the Use of Pozzolanas in RPC

2.3.1 Silica fume

The American Concrete Institute (ACI) defines silica fume as a “very fine non-crystalline silica produced in electric arc furnaces as a by- product of the production of elemental silicon or alloys containing silicon”. It is usually a grey colored powder, somewhat similar to Portland cement or some fly ashes and exhibits pozzolanic properties. Additionally, it is an artificial pozzolana, extremely fine amorphous (non-crystalline) material difficult to handle (because of its extremely low fineness) and is relatively expensive. When added to concrete or mortar, SF has significant effect on the properties of concrete in plastic (reduces bleeding and segregation of fresh concrete) as well as the hardened (enhances strength and

durability) stage (Nayak & Jain 2012; Kosmatka & Wilson 2012; Mehrotra, 2009, Gambhir, 2006).

2.3.1.1 Production of silica fume

Silica fume (SF) is produced in electric arc-furnaces which is a waste product of silicon and ferrosilicon industry (Kadhun, 2015; Gopika, Magudeswaran & Eswaramoorthi, 2017). The SF is also known as condensed silica fume or micro silica. In a silicon metal production, a source of high purity silica (quartz or quartzite) together with wood chips and coal are heated in the electric arc furnace to remove the oxygen from the silica (reducing condition). Silica fume rises as an oxidized vapour from the 2000⁰C furnaces. When it cools, it condenses and is collected in bag filters. The condensed SF is then processed to remove impurities (Nayak & Jain 2012).

2.3.1.2 Properties of silica fume

The details of physical properties, chemical properties and mechanism of SF in concrete are as follows:

Physical properties: Amorphous silica, because of the extremely small size particles, is highly reactive with calcium hydroxide produced by hydration of Portland cement. The very small particles of SF enter the spaces between the particles of cement and thus improve the packing and the strength of concrete besides reducing its permeability and increasing resistance to a number of aggressive chemicals. Some of the SF physical properties are highlighted as follows:

Colour: Silica fume varies from light- to dark gray in colour and when mixed with water, gives slurry which is black.

Relative density: The relative density of a typical silica fume is about 2.2 as compared to about 3.1 for normal Portland cement. The SF is generally used in small quantities in concrete.

Un-compacted unit weight: The un-compacted unit weight of silica fume is of the order of 250 to 300 kg/m³ as compared with about 1200 kg/m³ for normal Portland cement. This means that a bag which contains 40 kg of cement will hold only 8 to 10 kg of loose silica fume.

Fineness: Silica fume consists of very fine vitreous particles with a specific surface area of about 20,000 m² /kg. The extreme fineness of silica fume is best illustrated by the following comparison with other fine materials:

Silica: - 20,000 m² /kg

Tobacco smoke: - 10,000 m² /kg

Fly ash: 400 to 700 m² /kg

Normal Portland cement: 300 to 400 m² /kg (Nayak & Jain, 2012).

The particle size distribution of a typical silica fume shows most particles to be smaller than 1 μm and have an average diameter of about 0.1 μm as shown in Table 2.7.

Table 2.7: Physical properties of SF

S/No.	Properties	Value
1.	Particle size (typical)	<1 μ m
2.	Bulk density	
	As-produced	130–430 kg/m ³
	Slurry	1,320–1,440 kg/m ³
	Densified	480–720 kg/m ³
3.	Specific gravity	2.22
4.	Surface area (BET)	13,000–30,000 m ² /kg
		ASTM C-1240 Limitations
	Percentage on 45 μ m 7 (No.325) sieve, max %	\leq 10
	Pozzolanic activity index % 147 at 7 days accelerated curing	\geq 105
	Specific surface, min, 21 (m ² lgm)	\geq 15

Source: Silica Fume Association (SFA, 2005)

Chemical properties: Table 2.8 gives the chemical composition of typical SF from silicon furnaces

Table 2.8: Chemical properties of SF

	Kadhu, (2015)	Mohamed, (2011)	Faseyemi , (2012)	Mounika, Kiran & Krishna, (2017)	SF Association , (2005)	ASTM C-1240 Limitations	Range of Values
Oxides	Proportion by mass (%)						
CaO	1.25	0.2	0.7	---	---	---	0.2-1.25
SiO ₂	89.16	97	89.5	86.7	>85	\geq 85	85-97.0
Al ₂ O ₃	0.36	0.2	0.8	---	---	---	0.2-0.8
Fe ₂ O ₃	1.16	0.2	2.0	---	---	---	0.2-2.0
SO ₃	0.90	0.15	0.3	---	---	---	0.15-0.9
MgO	2.45	0.5	0.3	---	---	---	0.3-2.45
Na ₂ O	0.05	0.2	---	---	---	---	0.05-0.2
K ₂ O	0.07	0.5	---	---	---	---	0.07-0.5
L.O.I	3.80	-	---	2.5	---	\leq 6.0	2.5-6.0
Moisture content	0.80	0.8	---	0.7	---	\leq 3.0	0.8-3.0

Silica fume consists of 85-99% of silicon oxides (SiO_2) with very small percentages of carbon, ferric oxide, aluminium oxide (alumina) and oxides of sodium, potassium and magnesium.

2.3.1.3 Reaction mechanism of SF

The properties of SF are best achieved through the following mechanisms:

- (i) **Pore-size Refinement and Matrix Densification:** The presence of silica fume in the Portland cement concrete mixes causes considerable reduction in the volume of large pores at all ages. It basically acts as filler due to its fineness and because it fits into spaces between grains in the same way that sand fills the spaces between particles of coarse aggregates and cement grains.
- (ii) **Reaction with Free-Lime (From Hydration of Cement):** $\text{Ca}(\text{OH})_2$ crystals in Portland cement pastes are a source of weakness because cracks can easily propagate through or within these crystals without any significant resistance affecting the strength, durability and other properties of concrete. Silica fume which is siliceous and aluminous material reacts with CH resulting in reduction of CH content in addition to forming strength contributing cementitious products which in other words can be termed as ‘‘Pozzolanic Reaction’’.
- (iii) **Cement Paste–Aggregate Interfacial Refinement:** In concrete, the characteristics of the transition zone between the aggregate particles and cement paste plays a significant role in the cement-aggregate bond. Silica fume addition influences the thickness of transition phase in mortars and the degree of orientation of the CH crystals in it. The thickness compared with mortar containing only ordinary Portland cement decreases and reduction in degree of orientation of CH crystals

in transition phase with the addition of silica fume. Hence mechanical properties and durability are improved because of the enhancement in interfacial or bond strength. Mechanism behind is not only connected to chemical formation of C–S–H (i.e., pozzolanic reaction) at interface, but also to the microstructure modification (i.e., CH) orientation, porosity and transition zone thickness) as well (Silica Fume Association, 2005).

2.3.1.4 Application of SF in RPC

Right from the inception of RPC, SF has been a major pozzolanic material used because of its great influence as filler which fill the spaces between the cement particles. The very small particles of SF enter the spaces between the particles of cement and thus improve the packing and the strength of concrete besides reducing its permeability and increasing resistance to a number of aggressive chemicals.

According to Richard and Cheyrezy (1995), the functions of silica fume in RPC are; filling the voids between the next larger class particles (cement), enhancement of rheological characteristics by lubricating effect resulting from the perfect sphericity of the basic particles and production of secondary hydrate resulting from primary hydration. It was further stated that the main quality of silica SF is the absence of aggregates/impurities and the SF/cement ratio used for the production of RPC was 0.25 which corresponds to optimum filling performance as well as close to the dosage required for complete consumption of lime resulting from total hydration of cement. This claim was supported by Mujamil, Vinay, Sikandar, Shridhar and Kulkarni (2015) where RPC was made with different proportions of SF varying from 0% up to 50% and 25% gave the best results. On the contrary, Al -Hassani, Khalil and Danha (2014) claimed that increasing SF content up to

30% caused a considerable increase in the cube and cylinder compressive strength by 34.17% and 41.04% respectively. However, the best explanation to this discrepancy could be due to change in space, materials properties, experimental conditions, precision of equipment, etc.

2.3.1.5 Influence of SF on the properties of RPC

Pozzolans are finer mineral particles that can react with a hydration product in concrete, calcium hydroxide, to make concrete microstructure denser. SF as pozzolan has a packing effect to further improve the matrix density (Li, 2011). The composition of RPC includes cement, quartz sand or powder, and silica fume. It extensively uses the pozzolanic properties of the highly refined SF and optimization of the Portland cement chemistry to produce the highest strength hydrates (Mujamil, 2015). In a research carried out by Monronliya (2012), results showed that SF gives better compressive strength and good flow at lower water/cement ratio of as low as 0.22 compare to control. The experimental results by Ahmed (2014) indicated that RPC mixes with SF gave the highest values of compressive strength and density, and lowest value of absorption in comparison with RPC using micro silica or metakaolin where metakaolin was the third in such comparisons. It can be observed that the fresh properties of RPC are highly influenced by the mixing methods (cement+silica fume for 1min, 80% of water+100% SP for 3 min and sand+quartz powder for 4 min) and this has been reported to have the highest flow of 10.5% above all other methods (Hiremath & Yaragal, 2017). Reactive powder concrete has superior structural properties; compressive strength up to 80 N/mm², tensile strength up to 10 N/mm² and flexural strength up to 20 N/mm² can be achieved with confidence using local materials (quartz powder, silica fume, sand, cement, super plasticizer and steel fibers) available in

Pakistan (Qureshi, Tasaddiq, Ali & Sultan, 2017). Manasa, Ramana and Pradeep (2017) in their attempt to introduce graded aggregate (3-8 mm) in the production of RPC, claimed that silica fume gives better compressive strength and good flow when used at lower water-cement ratio. Song and Liu (2016) in their study aimed at evaluating the properties of RPC and its application in high way bridge also used SF as the pozzolanic material which showed compressive strength of up to 200 N/mm². Many researchers across the globe used SF in RPC production (Kiran & Jayaramappa, 2017; Hou *et al.*, 2018; Lee, Koh, Kim & Ryub 2018). Due to high cost and non-availability (in some countries particularly Nigeria) of SF, researchers across the world have started using other pozzolans such as fly ash, etc. that are cheaper and more available than SF to either fully or partially replace the SF content in the production of RPC.

2.3.1.6 Challenges of using SF

Silica fume is an expensive material and also not available particularly in Nigeria. Additionally, SF causes drying shrinkage due increased heat of hydration.

2.3.2 Fly ash

The term Fly Ash (FA) is often used to describe any fine particulate material precipitated from the stack gases of industrial furnaces burning solid fuels. There are two classes of fly ash which are defined as Class F fly ash and Class C fly ash. The main difference between these classes is the amount of calcium, silica, alumina, and iron content in the ash. The chemical properties of the fly ash are largely influenced by the chemical content of the coal burned (Ambika & Shivaraja 2015).

Class F fly ash: The burning of harder, older anthracite and bituminous coal typically produces Class F fly ash. This fly ash is pozzolanic in nature, and contains less than 10%

lime (CaO). Possessing pozzolanic properties, the glassy silica and alumina of Class F fly ash requires a cementing agent, such as Portland cement, quicklime, or hydrated lime, with the presence of water in order to react and produce cementitious compounds.

Class C fly ash: Fly ash produced from the burning of younger lignite or sub bituminous coal, in addition to having pozzolanic properties, it also has some self-cementing properties. In the presence of water, Class C fly ash will harden and gain strength over time. Class C fly ash generally contains more than 20% lime (CaO). Unlike Class F, self-cementing Class C fly ash does not require an activator. Alkali and sulfate contents are generally higher in Class C fly ashes. Table 2.9 shows the chemical composition of the class F and C fly ash.

Table 2.9: Chemical composition and classification of FA

Component (%)	Bituminous (class F)	Sub-Bituminous (class C)	lignite
SiO ₂	20-60	40-60	15-45
Al ₂ O ₃	5-35	20-30	20-25
Fe ₂ O ₃	10-40	4-10	4-15
CaO	1-12	5-30	15-40
LOI	0-15	0-3	0-5

Source: Ambika and Shivaraja (2015)

2.3.2.1 Production of Fly ash

Fly Ash is a by-product of the combustion of pulverized coal in electric power generating plants which is extracted from the fuel gases by any suitable process like cyclone separation or electrostatic precipitation.

2.3.2.2 Properties of Fly ash

The physical properties, chemical properties and mechanism of FA are briefly described as follow according to Ambika and Shivaraja (2015):

Physical properties: Fly ash is a fine-grained material consisting mostly of spherical and glassy particles. Some ashes also contain irregular or angular particles.

Size and shape: The size of particles varies depending on the sources. Some ashes may be finer or coarser than Portland cement particles. Fly ash consists of silt sized particles which are generally spherical, typically ranging in size between 10 to 100 μ m.

Colour: Fly ash can be tan to dark gray, depending on its chemical and mineral constituents. Tan and light colours are typically associated with high lime content. A brownish color is typically associated with the iron content. A dark gray to black colour is typically attributed to an elevated unburned content. Fly ash colour is usually very consistent for each power plant and coal source.

Fineness: Reactivity of fly ashes increase with fineness, particularly the fraction passing 45 μ m sieve.

Specific gravity: The specific gravity of different fly ashes varies over a wide range. The specific gravity ranged from a low value of 1.90 for a sub-bituminous ash to a high value of 2.96 for an iron-rich bituminous ash. Some sub-bituminous ash had a comparatively low specific gravity of approximately 2.0, and this shows that hollow particles, such as cenospheres or plerospheres, were present in significant proportions in the ashes.

In general, the physical characteristics of fly ashes vary over a significant range, corresponding to their source. Fineness is probably influenced more by factors such as coal combustion and ash collection and classification than by the nature of the coal itself. Similarly, the type of fly ash showed no apparent influence on the specific surface as measured by the Blaine technique.

Chemical properties: The Chemical composition of FA depends on the sources of coal and also on operating parameters of boilers. Therefore, the quality of FA varies from source to source and within the source also. With the use of pulverized coal and efficient combustion system, loss on ignition (LOI) is a measurement of unburned carbon remaining in the ash. Variation in LOI can contribute to fluctuations in air content and call for more careful field monitoring of entrained air in the concrete.

Table 2.10: Chemical composition of fly ash

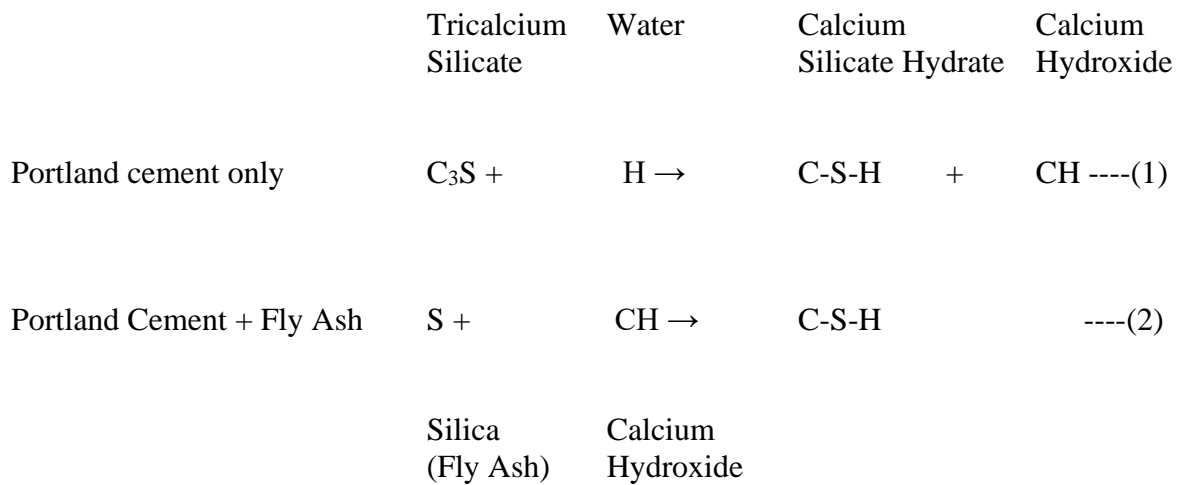
Oxides	Fly ash % by mass
CaO	0.37-27.68
SiO ₂	27.88-59.40
Al ₂ O ₃	5.23-33.99
Fe ₂ O ₃	1.21-29.63
MgO	0.42-8.79
SO ₃	0.04-4.71
Na ₂ O	0.20-6.90
K ₂ O	0.64-6.68
TiO ₂	0.24-1.73
LOI	0.21-28.37

Source: Feng and Clark, (2011)

2.3.2.3 Reaction mechanism of FA

Equation (1) below shows the chemistry of hydration of Portland cement. About 50% of Portland cement is composed of the primary mineral tri-calcium silicate, which on hydration forms calcium silicate hydrate and calcium hydroxide. With Portland cement, and the fly ash as the pozzolana, it can be represented by silica because non-crystalline silica

glass is the principal constituent of FA. The silica combines with the calcium hydroxide released on hydration of Portland cement as shown in equation 2. Calcium hydroxide in hydrated Portland cement does not contribute anything to strength, therefore it was used up with reactive silica. Slowly and gradually, it forms additional calcium silicate hydrate which is a binder, and which fills up the space, and gives impermeable and stronger concrete. This shows how the mechanism of fly ash works:



2.3.2.4 Influence of FA on the properties of RPC

Fly ash has been used by many researchers to partially or fully replace the SF content in RPC (Yazıcı, Yigiter, Karabulut & Baradan 2008; Nochaiya , Wongkeo & Chaipanich 2010; Ambika & Shivaraja, 2015; Agharde & Bhalchandr, 2015).

Research was conducted with the aim of decreasing the cement and SF content of RPC using FA by Yazici *et al.* in 2008. It was observed that the compressive strength of RPC containing FA reached up to 281 N/mm². This value increased to 324 N/mm² after the application of external pressure during setting and hardening. Yazici *et al.* (2009)

conducted another research with the aim of investigating the mechanical properties (compressive strength, flexural strength, and toughness) of RPC produced with class-C FA and ground granulated blast furnace slag (GGBFS) under different curing regime. Test results showed that RPC containing high volume FA has satisfactory mechanical performance. Although the cement and SF contents of this mixture are lower than conventional RPC, compressive strength exceeded 200 N/mm^2 after standard water curing. Autoclave and steam curing were observed to increase the compressive strength (234 N/mm^2 & 250 N/mm^2 respectively) of RPC. This can be attributed to the improvement of hydration process under these curing regimes. Furthermore, the sample has important environmental benefits in reducing cement content which reduces heat of hydration and shrinkage that are normally important problems for conventional RPC. Also, SEM micrographs revealed dense microstructure of the RPC.

In the following year, Peng, Hu and Ding (2010), undertook another study aimed at decreasing the cement and SF content of RPC by using ultra-fine fly ash (UFFA) and steel slag powder (SS). Experimental results indicated that the utilization of UFFA and SS in RPC is feasible and has prominent mechanical performance. The compressive and flexural strengths of the RPC specimens cured in 90°C water for 3 days, whose content of SS, UFFA and SF is 18%, 12% and 15% by weight of binder are 188.4 N/mm^2 and 32 N/mm^2 respectively. The microstructure analysis (SEM and TG-DTG-DSC) demonstrated that the excellent mechanical properties of RPC containing SS and UFFA were mainly attributed to the sequential hydration filling effect of the compound system.

Researches continued to flow in this direction. Demiss, Oyawa and Shitote (2018) investigated the combined effect of glass powder and FA on RPC. They showed that a

mean compressive strength of 62.9 N/mm² and flexural strength of 8.8 N/mm² were obtained using 50% glass powder 50% fly ash at 28 days standard curing with an improvement of 17.56% and 30.6% as compared to the control mix respectively. Therefore, replacing SF fully is a promising approach for local structural construction applications.

2.3.2.5 Challenges of using fly ash

Nigeria is no longer using coal to generate energy; as such FA is not much available. The non-availability of FA becomes a hindrance to its use in the production of RPC.

2.3.3 Ground granulated blast furnace slag

Grounded Granulated Blast Furnace Slag (GGBFS) is a glassy granular material that has been found to exhibit excellent cementitious properties and used as cement replacement.

2.3.3.1 Production of GGBFS

The GGBFS is a glassy granular material formed when molten GGBFS is rapidly cooled, usually by immersion in water, and then ground to improve its reactivity. Its major components are SiO₂, CaO, MgO, and Al₂O₃, and have been used as a pozzolan in Portland cement paste (Kim *et al.* 2018).

When finely ground and combined with OPC, it has been found to exhibit excellent cementitious properties. Glass particles of GGBFS are the active part and consist of mono-silicate, like those in OPC clinker, which dissolve on activation by any medium. Glass content in GGBFS is normally more than 85% of total volume. Specific gravity of GGBFS is approximately 2.7-2.90, which is lower than of OPC. Bulk density of GGBFS is varying from 1200-1300 kg/m³ (Mohd, 2005).

2.3.3.2 Properties of GGBFS

The physical and chemical properties of GGBFS are described as follows:

Physical properties: Specific gravity of GGBFS is approximately 2.7-2.90, which is lower than of OPC. Bulk density of GGBFS is varying from 1200-1300 kg/m³ (Mohd, 2005).

Chemical properties: The chemical compositions for blast furnace slags are shown in the Table 2.11. The principal constituents of blast furnace slag are silica (SiO₂), alumina (Al₂O₃), calcia (CaO) and magnesia (MgO) which make up 95% of the composition (Kalyoncu 2000).

The chemical composition of a slag varies considerably depending on the composition of the raw materials in the iron production process. Silicate and aluminate impurities from the ore and coke are combined in the blast furnace with a flux which lowers the viscosity of the slag. In the case of pig iron production, the flux consists mostly of a mixture of limestone and forsterite or in some cases dolomite. In the blast furnace the slag floats on top of the iron and is decanted for separation (Suresh & Nagaraju, 2015).

Table 2.11: Typical chemical composition of GGBF reported by different researchers

		Suresh & Kim <i>et al.</i> (2011)	Colangelo and Cioffi <i>al.</i> (2013)	Karim <i>et al.</i> (2014)	Khater (2015)	Range of Values
Properties		Proportion by mass (%)				
CaO	40	43.15	41.91	45.0	38.82	38.82-45.0
SO ₂	35	34.30	35.16	33.05	36.67	33.05-35.16
Al ₂ O ₃	13	14.50	10.76	16.36	10.31	10.31-16.36
MgO	8.0	5.61	7.68	6.41	1.70	1.70-8.00
Fe ₂ O ₃	---	0.11	1.40	0.53	0.50	0.00-1.40
Na ₂ O	---	0.26	0.11	0.13	0.48	0.00-0.48
K ₂ O	---	0.24	0.14	0.42	1.03	0.00-1.03
SO ₃	---	0.04	1.92	1.21	2.17	0.00-2.17
LOI	---	---	1.78	3.05	0.12	0.00-3.05

2.3.3.3 Reaction mechanism of GGBFS

Slag without an activator does react with water but the rate of hydration is very slow. Its hydraulic reactivity depends on chemical composition, glass phase content, particle size distribution and surface morphology. The reduction of initial strength of GGBFS cement could be overcome if the fineness of GGBFS were increased to promote hydration speed.

However, increasing the fineness of slag by pulverization could increase the manufacturing cost (Kim *et al.* 2011).

Moreover, a coating of aluminosilicate forms on the surfaces of slag grains within a few minutes of exposure to water, and these coatings were impermeable to water. Unless a chemical activator is present, further hydration is inhibited. In general, Portland cement, gypsum, and many alkalis have been used as activators and the rate of hydration is faster at high alkali concentrations. The surface of slag is amorphous, and its dissolving behavior is very similar to that of silicate glasses.

2.3.3.4 Influence of GGBFS on the properties of RPC

Some researchers used GGBFS to partially replace the SF content in an RPC with a view to cutting down cost. The effects of GGBFS and FA on mechanical properties of RPC were evaluated using standard, steam and autoclave curing at 20, 90 and 210°C respectively by Yazici *et al.* (2009). Results showed that RPC containing high volume FA has satisfactory mechanical performance. Although the cement and SF contents of this mixture are lower than conventional RPC, compressive strength exceeded 200 N/mm² after standard water curing. Autoclave and steam curing were observed to increase the compressive strength (234 N/mm² & 250 N/mm² respectively) of RPC. This can be attributed to the improvement of hydration process under these curing regimes. Furthermore, the sample has important environmental benefits in reducing cement content which reduces heat of hydration and shrinkage which are normally important problems for conventional RPC. Also, SEM micrographs revealed dense microstructure of the RPC.

Kumar, Rao and Sabhahit, (2013) conducted a research on RPC properties with cement replacement using waste materials (FA & GGBFS). The FA and GGBFS were used to replace cement content at 5%, 10% and 15%. Results showed that RPC with 5% cement replacement gave highest 28 days compressive strength of 128 N/mm² as compared to conventional RPC having 28 days strength of 126.33 N/mm². Flexural strength of RPC with 10% and 15% replacement of cement by FA ash and GGBS were higher than that of control mix (RPC). Modulus of elasticity of RPC with 5% and 10% replacement of cement by FA and GGBS were higher than that of control mix (RPC). Reactive powder concrete mix with 10% replacement of cement gave increase in compressive strength, flexural strength and modulus of elasticity of 126.67 N/mm², 25.604 N/mm² and 42.433KN/mm² respectively, when compared to the strengths of control mix.

Another study was carried out by Peng, Hu & Ding (2010) with the aim of decreasing the cement and SF content of RPC by using ultra-fine fly ash (UFFA) and steel slag powder (SS). Results showed that the utilization of UFFA and SS in RPC is possible and has prominent mechanical performance. The compressive and flexural strength of the RPC specimens cured in 90⁰C water for 3 days, whose content of SS, UFFA and SF is 18%, 12% and 15% by weight of binder are 188.4 N/mm² and 32 N/mm² respectively. The microstructure analysis (SEM and TG-DTG-DSC) demonstrated that the excellent mechanical properties of RPC containing SS and UFFA were mainly attributed to the sequential hydration filling effect of the compound system. It can be observed that GGBFS was used in combination with FA. This may not be unconnected with the fact that blast furnace slag contains more calcium and little silica while FA has a lot of silica. Therefore, silica is supplies to the GGBFS by FA. Also, GGBFS is not a pozzolan, nor in itself

cementitious, but it possesses latent hydraulic properties, which can be developed by the addition of an activator such as lime or another alkaline material.

2.3.3.5 Challenges of using GGBFS

Blast furnace slag is a non-metallic by-product produced in the process of iron production by chemical reduction in a blast furnace. Because industries like this are not properly functioning in Nigeria, waste of this nature will be very difficult to be obtained for use in the production of RPC.

2.3.4 Rice husk ash

Rice husk is an agricultural waste obtained from the outer covering of paddy rice grains during milling process. It constitutes about 20% (100 million tons) of the 500 million tons of paddy rice produced globally (Ganesan, Rajagopal & Thangavel 2008; Ramezani pour, khani & Ahmadibeni, 2009).

2.3.4.1 Production of rice husk ash

Rice husk is a residue of agricultural rice milling process. The is obtained from the brick-kiln that used rice husk as a fuel, or burnt in a ferrocement furnace or incinerator at a temperature range of 600 °C to 900 °C. The fully burnt ashes and the partially burnt ashes are separated by sieving. The ash passing 300 µm sieve size are considered as fully burnt ashes and it may be around 60% of the ashes (Uduweriya, Subash, Sulfy & Silva 2010, Kartini, 2011). It is then further ground to the required fineness and used as partial replacement of cement in concrete production. It is employed on cement composites in order to provide several advantages such as increased strength, reduced cost of materials, reduced environmental impact of waste materials and CO₂ emissions into the atmosphere.

2.3.4.2 Properties of RHA

The physical and chemical properties of RHA are described as follows:

Table 2.12: Physical properties of RHA

RHA	Bulk density (g/cm ³)		Specific Gravity	Specific surface (Blain's) (m ² /kg)	Specific surface (BET) (m ² /g)
	Dense	Loose			
	0.49	0.40	2.06	-	36.47

Ganesan, Rajagopal and Thangavel (2008)

A typical chemical composition of RHA obtained after burning and grinding is shown in

Table 2.13

Table 2.13: Chemical composition of RHA

Oxides	Ramezaniapour, khani & Ahmadibeni, (2009)	Kartini (2011)	Ganesan, Rajagopal & Thangavel (2008)	Hadipramana <i>et al.</i> (2016)	Asteray, Oyawa, & Shitote (2017)	Range of values
	Proportion by mass (%)					
SiO ₂	90.21	96.7	87.32	89.90	60	60-96.70
Al ₂ O ₃	0.06	1.01	0.22	0.46	1	0.06-1.01
Fe ₂ O ₃	0.27	0.05	0.28	0.47	0.4	0.05-0.47
CaO	0.85	0.49	0.48	1.01	4.45	0.48-4.45
SO ₃	0.25	---	---	---	---	0.0-0.25
MgO	0.49	0.19	0.28	0.79	0.71	0.19-0.79
Na ₂ O	0.08	0.26	1.02	---	0.61	0.0-1.02
K ₂ O	1.51	0.91	3.14	4.50	13	0.91-13
P ₂ O ₅	0.56	---	---	2.45	---	0.0-0.56
MnO	---	---	---	0.14	0.07	0.0-0.14
TiO ₂	0.02	0.16	---	---	0.23	0.0-0.23
LOI	5.48	4.81	2.10	---	16	0.0-16

From Table 2.13, amorphous silica is the principal oxide present in RHA. The quantity falls within the range (60 % to 96.7 %) as observed.

2.3.4.3 Reaction mechanism of RHA

The quality of RHA as an additive for cement and concrete depends on its reactivity which also depends on the fineness of the material. The reactivity of the RHA depends on amorphous silica content available and on the porous structure of the ash (Ramezaniapour,

khani & Ahmadibeni, 2009). Moreover, ground RHA mixtures depletes more calcium hydroxide, registers higher flow values, and possesses greater strength than ungrounded RHA mixtures (Venkatanarayanan & Rangaraju, 2013). These reactions produce additional amounts of calcium silicate hydrate that makes the microstructure of the RHA concrete denser as compared to that of concrete without RHA.

2.3.4.4 Influence of RHA on the properties of RPC

So far, only two studies are available to the researcher at the time of compiling this literature. Nguyen *et al.* (2011) studied the effect of RHA on the hydration and microstructure development of UHPC. The results were compared to those obtained with a control sample and a sample made with SF. The results also showed that the addition of RHA can increase the degree of cement hydration in UHPC at later ages. RHA can also refine the pore structure of UHPC and reduce the $\text{Ca}(\text{OH})_2$ content, but less significantly than SF. The thickness of the interface transition zone (ITZ) between sand particles and cement matrix of all samples was very small at the age of 28 days. The compressive strength of the sample made with RHA after 7 days was higher than that of the control sample and the sample made with SF. Also, the compressive strength of UHPC containing RHA can reach at least 175N/mm^2 and 185N/mm^2 at 28 and 91 days respectively. RHA is suitable for use as a supplementary material to make UHPC.

Asteray, Oyawa and Shitote (2017) investigated the effect of local wastes in recycled RPC for structural application, at Jomo Kenyatta University, Nairobi, Kenya. Finely dispersed waste ceramic powder was utilized to fully replace Quartz powder. Moreover, rice husk ash and finely dispersed waste glass powder were used in three different percentages (at 80-20%, 50-50% and 25-75%) as a raw material from waste stream to fully replace silica fume for the production of RRPC. It was observed that development of RRPC using hand mixing

at standard curing from local wastes was an approach to solve raw material shortage for the current generation of structural concrete and to reduce waste disposal cost and related environmental issues in Africa among others. Moreover, RRPC (fully replacing SF with 80% finely dispersed waste glass powder and 20% rice husk ash) with compressive strength of 57.3N/mm^2 (higher than the control by about 9.5%) at 28 days using standard curing was developed. No energy was involved during mixing and curing leading to reduce cost of production of the RRPC (Asteray, Oyawa & Shitote 2017).

2.3.4.5 Challenges of using RHA

Nigeria is one of the countries in Africa that cultivates rice. More than 60% of the rice produced is processed locally and the rice husks are dumped indiscriminately on open land thereby leading to environmental pollution in such areas (e.g., blocking drainages, etc.). while in some areas, the husk is converted to ashes through open burning. This practice is unhealthy. There is lack of industries in the country that can use this waste to generate energy for their electricity demand. Burning the husk to ash for concrete production only may not auger well (in terms of health and economy) for the country. As more rice is cultivated in the country, therefore, the government needs to sensitize industries on the advantages of using rice husk to generate electricity to meet their energy demands as well as putting incentive scheme for such practice. When this is done, more RHA will be available for practical application in the production of RPC and other concrete materials.

2.3.5 Metakaolin

Kaolinite is a mineral belonging to the group of aluminosilicates. It is commonly referred to as "China Clay" because it was first discovered at Kao-Lin, in China. The term kaolin is used to describe a group of relatively common clay minerals dominated by kaolinite and

derived primarily from the alteration of alkali feldspar and micas. Kaolin is an industrial mineral used primarily as inert filler and customers combine it with other raw materials in a wide variety of applications (Varga, 2007).

Kaolin is a soft, lightweight, often chalk-like sedimentary rock that has an earthy odor. Besides kaolinite, kaolin usually contains quartz and mica and also, less frequently, feldspar, illite, montmorillonite, ilmenite, anastase, haematite, bauxite, zircon, rutile, kyanite, silliminate, graphite, attapulgite, and halloysite. Kaolinite, the main constituent of kaolin, is formed by rock weathering. It is white, greyish-white, or slightly colored. Kaolinite is formed mainly by decomposition of feldspars (potassium feldspars), granite, and aluminium silicates (Varga, 2007). The process of kaolin formation is called kaolinization. Kaolinite is a hydrous aluminium silicate. It has a stable chemical structure ($\text{Al}_2\text{Si}_2\text{O}_5(\text{OH})_4$ which represents two-layer crystal (siliconoxygen tetrahedral layer joined to alumina octahedral layer exist alternately) and good physical properties for ceramic production. Metakaolin is formed from the complete thermal activation of kaolinite (Giménez, Frias, Villa & Ramírez, 2018).

2.3.5.1 Production of metakaolin

Metakaolin is essentially an anhydrous aluminosilicate with highly pozzolanic properties obtained by thermal activation of kaolin clays at a controlled temperature of between 600-900°C. The hydroxyl ions are strongly bonded to the aluminosilicate framework structure, thus only temperatures in excess of 550°C can eliminate them. When large-layer structured materials such as kaolinite are subjected to intensive thermal treatment (850°C), the material undergoes a series of transformations that enhance its subsequent reactivity with given chemical agents. At approximately 600°C, kaolinite loses most of its crystallinity.

This implies that the hexagonal layer structure in the kaolinite is partially destroyed at this temperature. The original mineral structure becomes disorganized, forming the material referred to as MK (Liew *et al.*, 2011). It is effective in increasing strength, reducing sulphate attack and improving air-void network. When MK is used in concrete production, a pozzolanic reaction takes place which changes the microstructure of the concrete and chemistry of the hydration products by consuming the released calcium hydroxide (CH), producing additional calcium silicate hydrate (C-S-H), resulting in an increased strength and reduced porosity and therefore improved durability.

2.3.5.2 Properties of MK

Some of the physical and chemical properties of MK are highlighted in Tables below:

Table 2.14: Physical properties of metakaolin

S/No.	Properties	Description
1.	Specific Gravity	2.40 to 2.60
2.	Physical Form	Powder
3.	Color	Off white, Gray to Buff
4.	Brightness	80-82 Hunter L
5.	BET	15 m ² /gram
6.	Specific Surface	8 – 15 m ² /g

Patil, Gupta and Deshpande (2013)

The Table 2.14 shows the physical properties of a typical MK where the specific gravity is between 2.40 and 2.60. Moreover, the specific surface area is between 8 and 15 m²/g.

Table 2.15: Typical chemical composition of MK

Oxides	Proportion by mass (%)						Range of Values
	Guneyisi, Gesoglu, Karaoglu & Mermerdas (2012)	Aiswaya, Prince & Dilip (2013)	Duana, Shui, Chen, & Shen (2013)	Imteyazuddin & Arafath (2014)	Vipat & Kulkarni (2016)	Khan, Imam, Srivastava & Harison (2017),	
CaO	0.780	0.06	0.29	2.0	<0.10	0.28	0.10-2.0
SiO ₂	52.68	62.62	50.27	51.52	52.2	52.86	50.27-62.62
Al ₂ O ₃	36.34	28.63	34.46	40.18	36.3	44.10	28.63-44.10
Fe ₂ O ₃	2.14	1.07	0.75	1.23	4.21	0.45	0.45-4.21
MgO	0.16	0.15	---	0.12	0.81	0.2	0-0.81
K ₂ O	0.62	3.46	---	0.53	1.41	0.2	0-3.46
Na ₂ O	0.26	1.57	---	0.08	---	0.25	0-1.57
TiO ₂	---	0.36	---	---	---	0.36	0-0.36
LOI	0.98	2.00	0.06	0.91	3.53	0.85	0.06-3.53

Table 12.15 shows a range of chemical composition of different MK by various researchers where SiO₂ (50.27-62.62%), is the major oxide, followed by Al₂O₃ (28.63-44.10%) and Fe₂O₃ (0.45-4.21%).

2.3.5.3 Reaction mechanism of MK

Calcium hydroxide accounts for up to 25% of the hydrated Portland cement and does not contribute to the concrete's strength or durability. During hydration, MK combines with the calcium hydroxide to produce additional cementing compounds (calcium silicate hydrate), the material responsible for holding concrete together (Shetty, 2015). In 2016, Shan, Rijuldas and Aiswarya observed that the addition of admixtures improves the microstructure as well as decrease the calcium hydroxide concentration through a pozzolanic reaction. This leads to the modification of the microstructure of the cement composites which improves the mechanical properties, durability and increases the service-life properties. Therefore, less calcium hydroxide and more cementing compounds means stronger and more durable concrete.

2.3.5.4 Influence of MK on the properties of RPC

Researches on the use of less costly and available pozzolanic materials that can partially or completely replace SF content in RPC are evolving every day. Smith *et al.* (2015) used refined metakaolin and replaced up to 15% of silica fume content in the production of RPC; the results showed improvement. However, the use of refined metakaolin is also expensive due to refining and beneficiation processes to remove impurities. The use of unrefined metakaolin in the production of RPC has not been reported to the best of the researcher's knowledge. Therefore, this study intends to investigate the suitability of locally sourced unrefined metakaolin in the production of RPC.

2.3.5.5 Challenges of using MK

Metakaolin has never reportedly been used alone in RPC production anywhere in the world to the best of researcher's knowledge. The use of refined MK in the production of concrete

is also expensive due the refining and beneficiation process to remove impurities associated with MK. Furthermore, there is a need to establish standard methods and clear guidelines to assess the suitability of the locally sourced unrefined MK in the production of RPC.

2.4 Performance of RPC at Elevated Temperatures

RPC has superior performance than conventional concrete and has been applied extensively in civil, petroleum, nuclear power, municipal, marine and military facilities, as well as in other projects. When RPC structures are subjected to service, there could be a time when the structures could be attacked by accidental fire. The residual compressive strength of RPC on exposure to elevated temperatures is important for the evaluation and repair of such concrete structures after fire. This is because, the compact internal structure of the RPC could probably lead to poor fire resistance. Zheng, Luo and Wang (2013), observed that when RPC is exposed to fire, the low permeability of the RPC prevent free water from escaping which led to internal pressure that resulted in spalling in addition to deterioration of strength due to the decomposition of calcium hydrate gel that causes severe deterioration (Demirel & Kelestemur, 2010). When exposed to elevated temperatures, the presence of fibre in RPC prevents proper bonding that leads to loss of strength (Peng *et al.* 2006). This temperature (400-600°C) is regarded as the critical temperature range for the strength loss of fibre concrete and the bond strength in the concrete matrix degraded significantly with increasing temperature for straight steel fibres (Abdallah, Fan & Cashell, 2017). Thus, mechanical properties and the mechanism for explosive spalling of RPC remains an important but unsolved problem particularly for materials other than SF. Literatures on the performance of RPC on fire (available to the researcher) are limited. Liu and Huang (2009) stated that the fire performance of RPC is of importance and needs to be investigated prior

to the application in building construction. Some researches show that RPC made with SF has higher fire resistance with large residual compressive strength than high performance and ordinary concretes. This is similar to what Zheng, Li and Wang, (2012) and Hiremath and Yaragal (2018) reported in their experiment on RPC exposed to elevated temperatures. But using other pozzolanic material, the performance of such RPC needs to be investigated. Table 2.16 shows the possible changes that can happen to a concrete when subjected to elevated temperatures.

Table 2.16: Changes in concrete during heating

Temperature range	Changes
20-200 °C	Slow capillary water loss and reduction in cohesive forces 80-150 °C ettringite dehydration; C-S-H gel dehydrated 150-170 °C gypsum decomposition ($\text{CaSO}_4 \cdot 2\text{H}_2\text{O}$), physically bound water loss
300-400 °C	Approximately at 300 °C break up of some siliceous aggregates (flint) 374 °C critical temperature for water
400-500 °C	460-540 °C Portlandite decomposition $\text{Ca}(\text{OH})_2 \rightarrow \text{CaO} + \text{H}_2\text{O}$
500-600 °C	Quartz phase changes β -Alpha in aggregates and sands
600-800 °C	Second phase of the C-S-H decomposition, formation of β C ₂ S
800-1000 °C	840 °C dolomite decomposition 930-960 °C calcite decomposition $\text{CaCO}_3 \rightarrow \text{CaO} + \text{CO}_2$, carbon dioxide release; ceramic binding initiation which replaces hydraulic bonds
1000-1200 °C	1050 °C basalt melting
1300 °C	Total decomposition of concrete and melting

Source: Hager (2013)

2.5

Model Development

There are various researches undertaken in this new concrete material that led to the development of some mathematical models. Some of the models developed by previous researchers are highlighted in the following paragraphs.

A study by Tai, Pan and Kung (2011) investigated the stress–strain relation of RPC in quasi-static loading after being subjected to elevated temperature. Experimental results indicate that the residual compressive strength of RPC after heating from 200–300 °C increases more than that at room temperature but, significantly decreases when the temperature exceeds 300°C. The residual peak strains of RPC also initially increase up to 400–500°C, and then decrease gradually beyond 500°C. However, Young’s modulus diminishes with an increasing temperature. Based on the regression analysis results, regression formulae were developed to estimate the mechanical properties of RPC after exposure to elevated temperatures thereby providing a valuable reference for industrial applications and design.

Mahmuda, Yang and Hassan (2013) investigated the size effects on flexural strength of similar notched ultra-high performance fibred reinforced concrete (UHPFRC) beams under three-point bending tests. Nonlinear finite element simulations using the concrete damage plasticity (CDP) model in ABAQUS were conducted, using material properties extracted from uniaxial tensile and compressive laboratory tests. The numerical simulations using the CDP model can predict load-displacement curves and crack propagation process with good agreement with the experimental data. To accurately model the crack propagation in UHPFRC, the concrete damage plasticity model in ABAQUS assumed that fibres are

uniformly distributed in the matrix and the UHPFRC is therefore modelled as a homogeneous material.

Moreover, the CDP model assumes that the failure in both tensile cracking and compressive strength of concrete is characterised by damage plasticity. It used the concept of isotropic damage evolution in combination with isotropic tensile and compressive plasticity to represent the inelastic and fracture behaviour of concrete. It allows the definition of strain hardening in compression, strain softening (or stiffening) in tension, and uncoupled damage initiation and accumulation in tension and compression.

In 2014, Zheng and Luo and Wang carried out a work on Stress–strain relationship of steel-fibre reinforced reactive powder concrete at elevated temperatures (20, 200, 400, 600, and 800°C) for ease of observation of test results, and 1%, 2% and 3 % steel fibres (by volume) were added to each batch of RPC samples. Compressive tests were performed to examine the effect of temperature on compressive strength, corresponding peak strain, elastic modulus, thermal expansion, energy absorption capacity and stress–strain curves. Using the experimental results, predictive equations were developed, and the proposed RPC models were compared with the experimental results.

$$\begin{cases} mx + (3 - 2m)x^2 + (m - 2)x^3, & x \leq 1; \\ \frac{x}{n(x-1)+x} & x > 1 \end{cases} \quad \text{(Zheng \& Luo 2014) ----- 2.1}$$

A regression equation was developed by Ahmad, Zubair and Maslehuddin (2015) with the aim of optimising the proportions of RPC mixtures within a particular range. The effect of key factors on the performance (in terms of compressive strength, modulus of rupture and modulus of elasticity) of RPC mixtures were examined. An optimum sand grading was

selected based on the maximum compressive strength and acceptable flow of a typical RPC, keeping the proportions of its ingredients constant. Then, keeping the sand grading and fiber content constant at their optimum levels, a total of 27 mixtures of RPC were selected for study by considering three levels of the three key factors (w/b ratio, cement content and silica fume content) according to a 3^3 factorial experiment design. The dosage of superplasticizer for each RPC sample was optimized to keep the flow in the desirable range of 180 mm to 220 mm. Statistical analysis of the experimental data indicated the significant effect of sand grading, water-to-binder ratio, cement content and silica fume content on flowability and mechanical properties of RPC. The regression equations were obtained as shown in equation 2.2-2.5.

(a) Effect of key factors on compressive strength

$$f'_c = 133-151W/B+0.0123C+0.564S \quad [R^2=0.99] \quad \text{-----} \quad 2.2$$

Where

f'_c = 28-day compressive strength (N/mm²).

W/B = water/binder ratio (by mass).

C = cement content (kg/m³).

S = silica fume content (% of cement content).

(b) Effect of key factors on modulus of rupture (MOR)

$$\text{MOR}=69.6-85.6W/B-0.0293C+0.332S \quad [R^2= 0.98] \quad \text{-----} \quad 2.3$$

Where

MOR = 28-day modulus of rupture (N/mm²).

W/B = water/binder ratio (by mass).

C = cement content (kg/m³).

S = silica fume content (% of cement content).

(c) Effect of key factors on modulus of elasticity

$$E=85.8-132W/B-0.0206C+0.266S [R^2=0.99] \text{ ----- } 2.4$$

Where

E = 28-day modulus of elasticity (GPa).

W/B = water/binder ratio (by mass).

C = cement content (kg/m³)

S = silica fume content (% of cement content).

(d) Correlation between compressive strength and other mechanical properties

The equation correlating MOR with compressive strength, obtained utilizing 28-day compressive strength and MOR data of the 27 RPC mixtures, is given below:

$$MOR=3.08\sqrt{f'_c} [R^2=0.86] \text{ ----- } 2.5$$

The equation correlating modulus of elasticity with compressive strength, obtained utilizing 28-day compressive strength and modulus of elasticity data of the 27 RPC mixtures is given below

$$E=4.36\sqrt{f'_c} [R^2=0.85] \text{ ----- 2.6}$$

The effect of the reinforcement ratio on the flexural behavior of ultra-high-performance fiber-reinforced concrete (UHPFRC) beams under impact loading was investigated by Yoo, Banthia, Kim and Yoon (2015). To do this, four large-sized UHPFRC beams with various reinforcement ratios were fabricated and tested using a drop-weight impact test machine. In addition, to predict impact behavior, a nonlinear analytical method, which includes (1) the determination of resistance - deflection models considering the strain rate effect based on multi-layer sectional analysis and (2) the prediction of the deflection - time response using a single-degree-of - freedom (SDOF) system, was developed and verified through comparison with the experimental results. The load-deflection relations considering strength enhancement by the strain rate effect were firstly obtained from the sectional analyses, and then these were incorporated as the dynamic resistance-deflection model into the SDOF system. The maximum deflections predicted by the SDOF analyses showed fairly good agreement with the test data, whereas the time at maximum deflection calculated by the analyses was slightly faster than that obtained from the experiments as a result of the numerous uncertainties in the test.

A study on the compressive behavior, mechanical characteristics and their application to stress-strain relationship of steel fiber-reinforced reactive powder concrete was carried out by Bae, Choi, Lee, and Bang (2016). The applicability of estimation equations for mechanical properties of concrete was evaluated with test results. From the evaluation, regression analysis was carried out, and new estimation equations were proposed and applied into stress-strain relation which was developed by previous research to describe the effects of fiber reinforcement on the material properties of interest. The analysis results

showed that the reinforcing effects of steel fibre can be expressed in terms of the fiber reinforcing index. Analysis of the test results confirmed that the relevant mechanical properties of concrete mix at a given strength level improve in proportion to the fibre reinforcement index. Linear regression analyses were performed for the mechanical properties using equations of the same form for all strength levels. The equation form was chosen so that different values of the regression coefficients were obtained for each strength level.

More so, proposed equations for mechanical properties under uniaxial compression on concrete can be used as main variables of stress-strain relation. According to comparison, ascending curve of stress-strain relation can be well fitted into experimental results. However, the short coming of this model is that descending part of stress-strain relation cannot be well fitted. This is because the prediction method did not consider the energy dissipation capacity after experiencing peak stress. In order to construct full range of stress-strain relation of fiber-reinforced concrete, boundary conditions after peak stress should be considered.

Hou, Cao, Rong, Zheng and Li (2018) studied the effects of steel fiber and strain rate on the dynamic compressive stress-strain relationship in reactive powder concrete. Outcomes of the research show that steel fiber has a significant influence on the stress-strain relationship and energy absorption of RPC. Peak strain and peak stress is proportional to steel fiber content at the identical strain rates. A dynamic compressive damage-softening model for SFRPC at high strain rates is put forward on the basis of the Weibull distribution of SFRPC strength. A theoretical formula for dynamic elastic modulus (E_d) was established in order to ascertain E_d for the proposed constitutive model. The ratio of E_d to static elastic modulus

(Es) is proportional to strain rate and inversely proportional to steel fiber content. Therefore, the proposed constitutive model captures the dynamic compressive stress-strain relationship of SFRPC, and theoretical results are in agreement with experimental data.

However, all the models described above paid attention to establishing stress-strain relationships and another drew relationship between the reinforcement ratios on the flexural behavior of ultra-high-performance fiber-reinforced concrete (UHPFRC) beams under impact loading. So also, a regression equation was developed with the aim of optimizing the proportions of RPC mixtures. The pozzolanic material used in the development of all the models was silica fume. None of these researches used another pozzolanic material other than silica fume. Moreover, they all concentrated in establishing stress-strain relationship with only one trying to optimize the constituents' materials using regression analysis. Therefore, the current research intended to use DataFit to develop models of optimised compressive strength, flexural strength and water absorption capacity of RPC using locally sourced unrefined metakaolin.

2.6 DataFit Software

DataFit is a tool used to perform nonlinear regression (curve fitting), statistical analysis and data plotting. What sets DataFit different from similar curve fitting and regression programs is its ease of use. DataFit is driven by a well-designed graphical interface, so there are no difficult instructions to remember and no programs to write. Data entry is achieved through a standard spreadsheet interface, which supports ASCII and ODBC data source import, as well as cutting and pasting data from the clipboard. With DataFit, you can perform linear or nonlinear regression on data containing up to 20 independent variables. You can choose from more than 600 pre-defined equations, which are commonly used in statistical,

scientific and engineering applications, or create your own equations. Solved equations are sorted according to goodness-of-fit. DataFit also includes forward selection, backward elimination, stepwise selection and manual variable selection modes to help determine which independent variables should be included in your regression model for multivariate datasets. Results include completely customizable 2D and 3D plots, fitted parameters with confidence intervals, input vs. estimated data and goodness-of-fit information. Plots can be saved as templates, which allow them to be applied to new plots in order to instantly give them custom appearance. Data tables, supporting interpolation and extrapolation (projections), can be exported in ASCII, Excel or HTML format. It can also automatically export source code in BASIC or C to utilize any solved equation in a program that has been written. Macro capability allows curve fitting operations to be performed non-graphically, either in batch mode or by calling DataFit from an external program. With the combination of an intuitive interface, online help and wide range of features, it is a tool that is used effectively by both beginners and experts (Oakdale Engineering, 2019)

2.7 Summary of Literature Review

The production of normal strength concrete (NSC) begun in the early 1900s. Since then, the concrete has been in use due to its versatility (despite its heterogeneous and porous nature). There is no clear demarcation between NSC and high strength concrete (HSC), any time a concrete with superior strength is produced, it is referred to as HSC. However, a concrete with strength from 41 N/mm^2 and above is acceptably regarded as HSC. Due to its brittleness, low tensile strength and durability problem associated with HSC, a high-performance concrete (HPC) was innovated.

High-performance concrete is a concrete with the ability and efficiency to perform its designed purpose with little or no maintenance. It is characterized by high strength (up to 120N/mm^2), excellent performance in the environment in which it is placed, made up with cement, aggregates, pozzolans, low water-binder ratio (0.3-0.4) and superplasticizer. The search for HPC for the construction of special structures has led to the discovery of ultra-high-performance concrete known as RPC.

Reactive powder concrete is a special coarse aggregate-free concrete material with superior properties than HPC. It is characterized by high strength of between 57.3 to 800N/mm^2 , high flexural strength ($30\text{-}60\text{N/mm}^2$) and ductility of about 25 times that of conventional concrete. It is made using cement, silica fume, fine sand, quartz sand, fiber and high dosage of carboxylate ether-based superplasticizer known as new generation superplasticizer. The advantage of RPC is that it enables the concrete industry to produce concrete materials that are strong, durable and sensitive to the environment with long slimmer sections. Moreover, some models were developed to help establish relationship between some properties of the RPC/ and or constituents' materials with the properties of the RPC, e.g., stress-strain relationship models, etc.

Table 2.17 summarizes the RPC results obtained by different researchers across the world using different materials and curing regimes (water, steam curing & autoclaving). The table also gave a range of values that can be possibly obtained using same or other pozzolanic materials provided that the conditions are closely related. Therefore, the range established here will be used as a bench mark for undertaken the research work. Reactive powder concrete is a material of choice for some special structures where high performance is very important. However, the silica fume and fibre which are the major

constituents of RPC are not available in Nigeria. The large deposit of kaolin (scattered in the country) from which metakaolin is made could serve as an alternative to the silica fume in the production of RPC.

Table 2.17: Results of researchers across the Globe using different pozzolans

S/No.	Author	Pozzolan	Results (N/mm ²)		
			Compressive	Tensile	Flexural
1.	Richard & Cheyrezy (1995)	Silica fume	200-800		30-60
2.	Song & Liu (2016)	-----	200		
3.	Qureshi <i>et al.</i> (2017)	-----	80	10	20
4.	Yazici <i>et al.</i> (2008)	Fly ash	281-324		
5.	Yazici <i>et al.</i> (2009)	-----	200 -250		
6.	Demiss, Oyawa & Shitote (2018)	-----	62.9		8.8
7.	Yazici <i>et al.</i> (2009)	GGBFS	200-250		
8.	Peng, Hu & Ding (2010)	-----	188.4		32
9.	Kumar, Rao & (2013)	-----	128.33		25.6
10.	Nguyen <i>et al.</i> (2011)		175-185		
11.	Asteray, Oyawa & Shitote (2017)	RHA	57.3		
Range of values			57.3-800	≥10	8.8-60

CHAPTER THREE

3.0 MATERIALS AND METHODS

3.1 Preamble

After undertaken an extensive literature review related to the subject matter in Chapter Two, this section (Chapter three) explains the experimental programme, materials used in this research and their characteristics. The following are the materials and methods used in carrying out this research:

3.2 Materials

The materials used were binders (Dangote blended cement, silica fume and metakaolin), fine aggregate, chemical admixture, Gear Inner Wire (GIW) as steel fiber and water. The sources and preparation treatment of the materials are described in sub-sections 3.2.1 to 3.2.6.

3.2.1 Binders (cement, silica fume and metakaolin)

As the most frequently utilized product in this area of the country, blended cement of Dangote brand that satisfies the requirements of BS EN 197-1:2011 was used throughout the experiment. Densified silica fume (SF) and Metakaolin (MK) satisfying the requirement of ASTM C618-05 for N class pozzalan were used. Unlike cement and SF which are standard materials, the MK was locally prepared in the laboratory before use. This includes dry sieving the kaolinite to obtain a fine material (less than 150 μm) using 150 μm sieve. It was then mixed with clean water to obtain a solution or slurry which was then titrated using a fabric with a pore size less than 45 μm . The characterization of cement, SF, MK and their particles size analysis carried out are presented in sub-section 4.2, Table 4.1 (Chapter Four)

3.2.2 Fine aggregates

Naturally occurring river sand with maximum particles size $600\mu\text{m}$ and retained on $150\mu\text{m}$ was used. The river sand was naturally occurring obtained from Zaria. Prior to use, the sand was sieved to reduced impurities, silt content and large particles in accordance with BS EN 12620:2003 and used in the experiment. The characterization of the sand carried out and results is presented in sub-section 4.2, Table 4.1 Chapter Four

3.2.3 Chemical admixture

Chemical admixture is a product which was added to the concrete mix during mixing for the purpose of achieving high flowability. Conplast SP 430 (as shown in Plate I) which is a 4th generation high performing polycarboxylate ether super plasticizer that conforms to ASTM C 494 was used throughout the experiment in order to achieve the required flow at constant water to binder ratio (w/b).



Plate I: Container of Conplast SP 430

3.2.4 Fibre

Light gear inner wire (GIW) was used as steel fiber. Three different GIW of *NJP* (Chinese Company) were available in the market (a sample of the *NJP* is shown in Plate II) at the time of undertaking this research. The tensile strength of each sample was determined using tensor meter (shown in Plate IV) in the Department of Mechanical Engineering, Ahmadu Bello University, Zaria. The GIW were chopped to the required length (averagely 12mm) as shown in Plate III before used in the concrete. The three samples of the GIW obtained were characterized by different diameters of 0.28 mm, 0.32 mm and 0.39 mm which was determined using digital vernier caliper. The geometry of the different samples of the GIW is presented in Table 3.1. Therefore, the GIW with highest aspect ratio (43) was selected and used in the entire experiment. Its length (L) is 12 mm and diameter (D) is 0.28 mm which conformed to the requirement of ACI 544.3R-2010. The selection was also based on the findings of Sable and Rathi (2012), who observed that the higher the aspect ratio of a fibre, the more the compressive and tensile strengths of the concrete.

Table 3.1: Properties of gear inner wire (GIW) as fiber

S/No.	Diameter (mm)	Length(mm)	Aspect Ratio (L/D)	Tensile Strength (N/mm ²)
1.	0.28	12	43	1623
2.	0.32	12	38	1888
3.	0.39	12	31	1657

Source: Experiment (2018)



Plate II: A sample pack of the GIW



GIW before Cutting

GIW after Cutting

Plate III: Sample of GIW



Plate IV: Tensor meter

3.2.5 Water

Water obtained from A.B.U. mains which satisfies the requirement of BS EN 1008:2005 was used for mixing and curing of the concrete specimens.

3.3 Preparation of Binder

All materials used in the experiment were batched by the use of digital weighing balance as shown in Plate V.

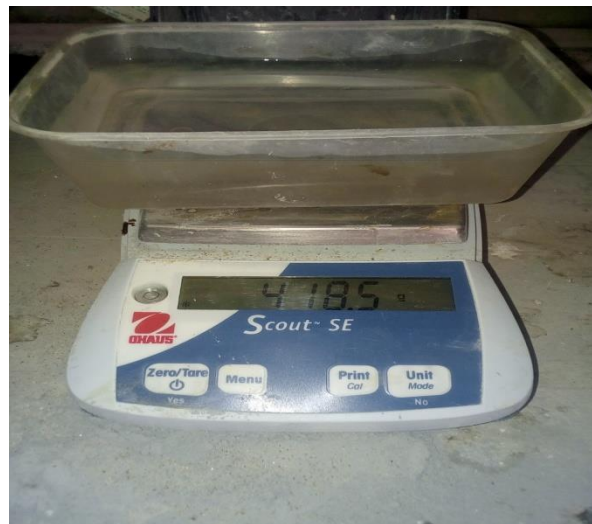


Plate V: Digital weighing balance

The MK was prepared in order to enhance its pozzolanic activity before its use. The preparation include: dry sieving, wet sieving and calcinations as described in Sub-section 3.2.1.

3.3.1 Production of MK

The MK used in this research was obtained by calcining raw kaolinitic clay (as shown in Plate VII) obtained from Getso town, Gwarzo L.G.A., Kano State. The site where the kaolin was excavated is located on the coordinates GT1 to GT5 as shown in plate VI and

were taken using UTM coordinates system as presented in Table 3.2. The reason for choosing this source of material is to test its suitability. The calcination was done using furnace in the Department of Chemical Engineering, Ahmadu Bello University, Zaria as shown in Plate VI. The calcination process required to convert the crystalline kaolin to amorphous state was done at a temperature of 700°C for 2 hours.

Table 3.2: Coordinates of kaolin site

S/No.	Coordinate	Latitude	Longitude
1.	GT1	11.870878 °	7.968568 °
2.	GT2	11.871047 °	7.968699 °
3.	GT3	11.871184 °	7.968491 °
4.	GT4	11.870879 °	7.968246 °
5.	GT5	11.871053 °	7.968180 °



Plate VI: Coordinates of kaolin site in Getso town



Plate VII: Furnance with kaolinite to be calcined

3.4 Characterization of Materials

Characterizations of the binding materials (cement, silica fume & metakaolin) were conducted in order to ensure that they satisfied the requirements of the relevant standards. This characterization will help in understanding the properties of the reactive powder concrete produced with the binders.

3.4.1 Physical properties

Some of the tests carried out to determine the physical properties of the binders are as follows:

3.4.1.1 Specific gravity and loss on ignition

The specific gravity of the binding materials was conducted using pycnometer in accordance with ASTM standard and the result is shown in sub-section 4.2, Table 4.1 in Chapter Four.

Loss on ignition (LOI) that was conducted in order to determine the mass loss from MK combustion residues upon heating in an air or oxygen atmosphere to a prescribed temperature (900°C). The mass loss can be due to the loss of moisture, carbon, and so forth, from the decomposition or combustion of the residue. The test started by first heating the

sample of the MK in an oven at a temperature 110°C for 24 hours in order to drive away the free water. The sample was then weighted using balance and was then put inside crucible and then placed inside the furnace at a prescribe temperature of 900°C for 2 hours. After that, the sample was allowed to cool, removed from the furnace and re-weighted again to determine the loss in weight. This test was conducted in the Department of Chemical Engineering, Ahmadu Bello University, Zaria in accordance with ASTM D 7348 – 08. The result is presented in sub-section 4.2, Table 4.1 in Chapter Four.

3.4.1.2 Particle size distribution

The particle size distribution of the binders (cement & metakaolin) was carried out using a particle size analyser instrument known as “Malvern Instruments” (Mastersizer) in the central laboratory of the Universiti Teknologi Malaysia (UTM). The analysis was done in order to determine the mean particle size (D_{10} , D_{50} & D_{90}) which determined the fineness of the binders used in the RPC.

3.4.1.3 Specific surface area

The specific surface area of the binders (cement & metakaolin) was also carried out using the “Malvern Instruments” as a better indication of the fineness of these materials. The specific surface area of the binders influenced the workability and dense structure of the RPC. This was also carried out in the central laboratory of the Universiti Teknologi Malaysia (UTM). The result is presented in sub-section 4.2, Table 4.1 in Chapter Four.

3.4.2 Chemical compositions

Apart from physical properties of the binders, chemical compositions analysis was also carried out using X-ray fluorescence spectrometry instruments in the Centre for Minerals

Research & Development, Kaduna Polytechnic, Kaduna. Powdered samples were placed into nylon material holder and compressed using the XRF machine. The test was conducted in order to ensure that the materials conform to ASTM C 618-2015. The instrument used in conducting the test is shown in Plate VIII.



Plate VIII: X-Ray fluorescence (Niton XL3t)

3.4.3 Mineralogical compositions of MK and sand

3.4.3.1 X-Ray diffraction (XRD) of kaolin, MK and sand

The mineral composition of the MK was carried out in order to ensure that the temperature for the calcination of kaolin to MK was sufficient enough. The mineral composition of the sand was also carried out. The test was carried out at the Multi-user laboratory, Department of Metallurgical engineering, Faculty of Engineering Ahmadu Bello University, Zaria. The result is presented in sub-section 4.2, Figure 4.1 in Chapter Four.

3.4.4 Pozzolanic activity

The pozzolanic reactivity test determined the extent of the activity of a particular material. It is normally assessed using either direct or indirect method. Direct methods analytically

monitor the presence and subsequent reduction of $\text{Ca}(\text{OH})_2$ with time as the pozzolanic reaction proceeds using methods such as X-ray diffraction (XRD), thermo-gravimetric analysis (TGA) or classical chemical titration. The Indirect test methods measure a physical property of a test sample that indicates the extent of pozzolanic activity (Donatello, Tyrer & Cheeseman, 2010). Some of the known methods are Chapelle method, Fratinni method and Strength Activity Index. However, due to the non-availability of instruments, only the Strength Activity Index (SAI) method was considered in this research. The test was carried out in accordance with ASTM C 311-05. The SAI is the ratio of the compressive strength of 50 mm x 50 mm x 50 mm standard mortar cube made with 80% reference cement plus 20% test material (MK) by mass to the compressive strength of the standard mortar cubes prepared with reference cement mix alone, when determined at the same age. If the index is greater or equal to 0.75 at 7 or 28 days, the material tested is regarded as pozzolanic. The SAI is expressed mathematically as in equation (3.1)

$$\text{SAI} = \frac{A}{B} \text{-----} 3.1$$

Where

A = compressive strength of the tested material (N/mm^2)

B = compressive strength of the control specimen (N/mm^2)

3.4.5 Characterization of fine aggregate

Tests on the fine aggregate such as specific gravity and water absorption as well as particle size distribution were carried out in accordance with ASTM C 128-15 & ASTM C 33-08. The result is presented in Sub-section 4.2, Table 4.1 and Figure 4.2 in Chapter Four.

3.5

Mix Proportion

Different mix proportions were made during the experiment which was carried out in two stages. The first stage was to come up with the optimum mix for the production of RPC which were used for the second stage to evaluate the engineering properties, microstructure and the performance of the RPC exposed to elevated temperatures.

3.6

Specimens Preparation

Reactive powder concrete specimens (cubes, cylinders & prisms) for the hardened properties tests were prepared by mixing, casting and curing. Immediately after mixing, the fresh property of the specimens (in terms of flow) was determined. The flow was fixed at 270 ± 5 mm and Conplast SP 430 was added to the material during mixing until the flow of 270 ± 5 mm was achieved.

3.6.1 Mixing

Because RPC is a new material, there is no standard method for mixing such type of concrete. However, Hiremath and Yaragal (2017) established a mixing sequence for the RPC which was used as basis for this research. The mixing sequence was used in this research. A lot of trials were carried out in order to come up with the proportioning of the new RPC under study as shown in sub-section 4.2 Table 4.2 in Chapter Four.

Mortar mixer (as shown in Plate IX) was used in order to prepare the specimens. Cementitious materials were first mixed dry in the mortar mixer for about one minute at low speed of 10 rpm. Premixed water (about 80% of the mixing water) and superplastizer (the range is shown on Table 3.3 for the SF & MK specimens) were added into the mixer and the mixing continued for three minutes at medium speed (140 ± 5 rpm). Fine sand and

GIW as fibre were then added into the mixer and mixing continued for another four minutes. The remaining mixing water (about 20%) was then added to the mixer and then mixed at high speed (285 ± 10 rpm) for additional four minutes. Finally, the mixer was returned to the medium speed (140 ± 5 rpm) and mixing continued for another three minutes. All the fresh mixes had consistency of 270 ± 5 mm. After mixing, the fresh specimens were cast and left in the moulds for 24 hours at laboratory condition ($27 \pm 2^\circ\text{C}$).



Plate IX: Mortar Mixer

Table 3.3: Range of value of SP used

S/No.	Percentage of binder	Range value of SP used
1.	20% SF	3.5-3.6%
2.	10% MK	2.8-3.2%
3.	20% MK	3.8-3.9%
4.	30% MK	4.5-5.0%

3.6.2 Specimens casting and curing

A number of specimens of different shapes (cubes, cylinders & prisms) and sizes were produced based on the type of test to be conducted (e.g., Plate X). Being a self-compacting concrete, the mixed material was poured in a single layer into the different moulds. Immediately after casting, the specimens were covered with damp hessian for 24 hours before demoulding. The demoulded specimens were then cured in fresh clean water at 27 ± 2 °C for the required period (7, 14, 28, 90 & 180 days) of curing before testing.



Plate X: Sample of RPC after casting

3.7

Fresh Property of RPC

After mixing, fresh property in terms of concrete flow was determined in according to ASTM C143 as shown in Plate XI. The result is presented in sub-section 4.3, Plate XIX in Chapter Four.



Plate XI: Measuring the Flowability of the RPC

3.8 Hardened Properties of RPC

At each curing age, the hardened properties of the specimens were tested in accordance with the relevant standards. The tests include compressive strength, tensile strength, flexural strength, absorption and sorptivity. The sorptivity test involved immersing the sample in water at an average ambient temperature of $27\pm 2^{\circ}\text{C}$. This procedure was adopted from (Richard & Cheyrezy 1995; Cwirza, Penttala & Vornanen 2008, Peng *et al.*, 2012; Bashandy, 2013; Aghard & Bhalchandra 2015; Faizan *et al.*, 2015).

3.8.1 Compressive strength

The compressive strength test was carried out (as shown in Plate XII) based on the requirements of {BS EN 12390-3 (2009)}, at 7, 14, 28, 90, and 180 days of curing. The compressive strength was computed using equation 3.2. This test was carried out in the Department of Building Faculty of Environmental Design, Ahmadu Bello University, Zaria

$$F_c = \frac{F}{A} \text{-----} 3.2$$

Where:

F_c = compressive strength (N/mm²)

F = maximum failure load (KN)

A = cross-sectional area of the specimen (mm²)



Plate XII: RPC samples under compressive strength test

3.8.2 Tensile strength

Tensile strength was conducted (as shown in Plate XIII) in accordance with {BS EN 12390-3(2009)-1:2000} at 7, 14, 28, 90, and 180 days of curing and was computed using equation 3.3. The test was carried out in the Department of Building Faculty of Environmental Design, Ahmadu Bello University, Zaria.

$$F_t = \frac{2P}{\pi ab} \text{-----3.3}$$

Where:

F_t = split tensile strength (N/mm²)

P = maximum failure load (KN)

a= length of the specimen (mm)

b= breadth of the specimen

π = a constant with value 22/7



Plate XIII: RPC samples under tensile strength test

3.8.3 Flexural strength

Reactive powder concrete samples produced were subjected to flexural strength test (as shown in Plate XIV) which was carried out at 7, 14, 28, 90, and 180 days of curing in accordance with the relevant standards and was computed using equation 3.4. The test was carried out in the Department of Building Faculty of Environmental Design, Ahmadu Bello University, Zaria.

$$F_f = 0.0028P$$

Where:

F_f = flexural strength (N/mm²)

P = maximum failure load (KN)



Plate XIV: RPC samples under flexural strength test

3.9

Water Absorption Capacity

One of the most important properties of a good quality concrete is low permeability. A concrete with low permeability resists ingress of water and is not susceptible to freezing and thawing. Water enters pores in the cement paste and even in the aggregate. A set of three cube specimens (50 mm x 50 mm x 50 mm) each of the RPC was used for carrying out the water absorption test. The test procedure according to BS 1881-122:(1983) was adopted which involves drying a specimen to a constant weight in an oven at 105⁰C for 72 hours. The sample was allowed to cool in the oven, weighed and the mass recorded. Each sample was then immersed in water for 30 minutes. After that, the specimens were removed from the water and dried with a cloth as rapidly as possible until all free water was removed from the surface and re-weighed again. The increase in weight as a percentage of the original weight is expressed as its absorption (in percent) using equation 3.5. The test was carried out in the Department of Building Faculty of Environmental Design, Ahmadu Bello University, Zaria

$$Absorption = \frac{m_2 - m_1}{m_1} \text{-----} 3.5$$

Where:

m_1 = mass before immersion in water

m_2 = mass after immersion in water

3.10 Sorptivity Test

Permeability is a measure of the flow of water under pressure in a saturated porous medium while sorptivity is characterized by the material's ability to absorb and transmit water through it by capillary suction. The specimens of the RPC were removed from the curing tank and allowed to dry. They were then put inside an oven and dried at temperature of $50 \pm 2^\circ\text{C}$ for 72 hours. After, Abro 2000 RTV silicone sealant was applied on the sides of the specimens in order to prevent water ingress through the sides of the specimens. The specimens were then weighted and the masses recorded. The specimens were subjected to sorptivity test as shown in Plate XV at 1, 5, 10, 20, 30, 60 minutes, 1, 2, 3, 4, 5, 6 and 24 hours and the change in masses were recorded after each testing period. This test was conducted in accordance with the ASTM C 1585. Results of the test were calculated using equation 3.6



Plate XV: Samples subjected to Sorptivity test

$$I = \frac{mt}{axd} \text{-----3.6}$$

Where:

I= the absorption,

mt= change in specimens mass (g) at the time t

3.11 Elevated Temperature

The elevated temperature test on the specimens was carried out on the RPC specimens cured at 28 days using an automatic electric furnace. Before heating, the specimens were oven dried at 105 ± 5 °C for 24 hours to minimize the effect of explosive spalling. The specimens were heated to 200, 400, 600 and 800 °C in the furnace at a heating rate of 2.5° Cmin⁻¹. In order to achieve a thermal steady state, the specimens were maintained for 2 hours at the peak temperature. After heating, the furnace was switched off and the specimens were allowed to cool in the furnace environment for about 2 hours with the furnace door closed. Later, the specimens were removed from the furnace and allowed to cool to ambient temperature in the laboratory environment before testing. The RPC samples

were then subjected to the following tests: using ultra sonic pulse velocity (UPV), compressive strength, absorption, sorptivity and microstructure analysis using SEM, XRD and FTIR. Details of the afore mentioned tests are as follows:

3.11.1 Ultrasonic pulse velocity

Ultrasonic pulse velocity (UPV) was carried out on the specimens exposed to elevated temperatures in order to determine the quality of the internal structure. The apparatus used were electrical pulse generator, pair of transducers (transmitter and receiver) amplifier, electrical timing device and calibrator bar as shown in Plate XVI.



Plate XVI: UPV instrument

Petroleum jelly was applied on two opposite surfaces of the specimens after being exposure to the elevated temperatures so as to serve as couplant between transducers and concrete surface. The time taken for the transmission of the ultrasonic pulse was then recorded. The result of the UPV is calculated using equation 3.7

$$V = \frac{L}{T} \text{-----3.7}$$

Where:

V = pulse velocity (mm/ μ s)

L = Path length (mm)

T = time taken by the pulse to transverse the length (μ s)

3.11.2 Microstructure analysis of RPC

Microstructure of the RPC was investigated using the scanning electron microscope (SEM) technique which identifies the morphology of the structure; X - Ray Diffraction (XRD) was used to identify the compounds and minerals present in powdered specimens; and Fourier Transform Infrared Spectroscopy (FTIR) which was used to provide qualitative (through fingerprinting), semi-quantitative, quantitative information on chemical structures and physical characteristics of the RPC. The SEM, XRD and FTIR were carried out in Malali Kaduna and the multi-user laboratory in the Department of Metalogical engineering, Department of chemistry A.B.U. Zaria respectively. The results of the microstructure analysis are discussed in sub-section 4.6 to 4.6.3 in Chapter Four.

3.12

Development of Models

In order to develop the models, experimental works were carried to determine the variables. Percentage (%) of metakaolin (MK) and steel fibre (gear inner wire) were used as independent variables for all the models while compressive strength, flexural strength and water absorption capacity were used as dependent variables.

3.12.1 Processes of models' development using DataFit software

After double clicking the DataFit software icon on the desktop of the computer, a small dialogue box appeared. The dialogue box contains information where number of independent variables can be entered by the user. Two (2) was entered, as shown in Plate XVII, representing the two independent variables (% MK and % SF) for the development of these models (compressive strength, flexural strength and water absorption capacity). After that, three columns X1, X2 and Y were displayed as shown in Plate XVIII (a). X1 and X2 represent the independent variables while Y represents the dependent variable. For the compressive strength model, % MK and % SF were used as X1 and X2 respectively while compressive strength was used as Y, so also, the flexural strength and water absorption capacity models. After entering X1, X2 and Y results obtained from the experiment, the models were generated by clicking solve button as shown in Plate XVIII (b).

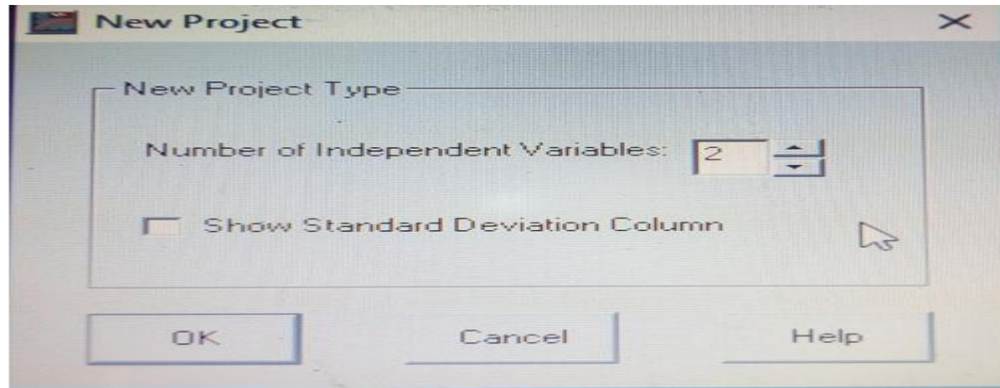
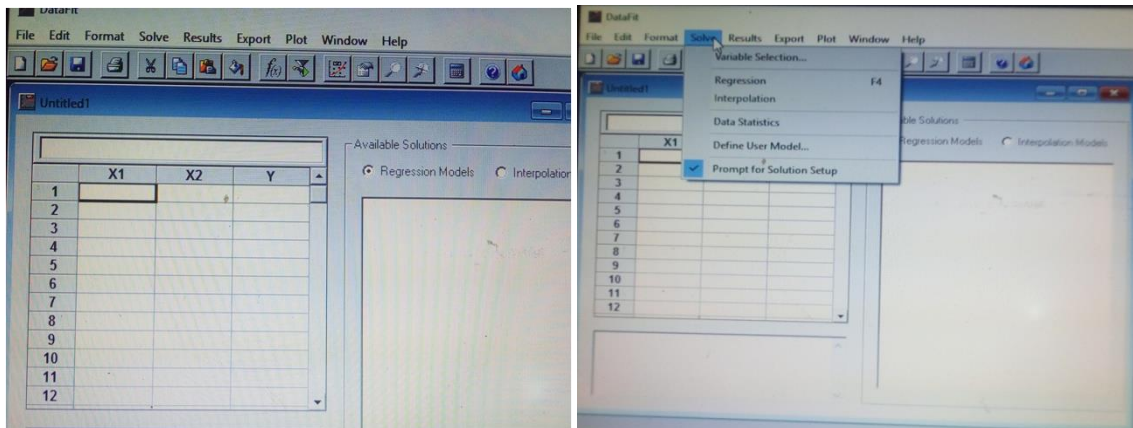


Plate XVII: Display of number of independent variables



(a) X1, X2 and Y results

(b) Solution & generation of models

Plate XVIII: Display of Interface; (a) entrance X1, X2 and Y, (b) solving and generation of models

3.13.2 Assumption on the use of the models

- i. The RPC was made up of limestone Portland cement
- ii. Unrefined metakaolin used was restricted to 30% MK
- iii. Fine aggregate of 150 μ -600 μ m particle size was used
- iv. The RPC was cured under ambient environment
- v. Steel fibre used was gear inner wire (GIW).

3.14

Data Analysis

Results obtained from the experiment were analysed statistically using mean, percentages and correlations.

3.14.1 Correlation analysis

Correlation analysis was used to study the relationship between ultrasonic pulse velocity and residual compressive strength, ultrasonic pulse velocity and water absorption capacity of fibred and unfibred RPC samples exposed to elevated temperatures. The coefficient of relation (R^2 -value) tells how much variation is explained by the model. For example, 0.1 R^2 means that the model explains 10% of variation within the data. The greater the R^2 the better the model. The coefficient of relation (R^2) was established by plotting a scattered plot of ultrasonic pulse velocity, residual compressive strength and water absorption capacity of both fibred and unfibred RPC samples using the Microsoft excel software which automatically generated the R^2 value.

3.14.2 Probability (P-value)

P-value was used statistically to determine the significance of the three models developed. Table 3.4 shows the interpretations of different p-values.

Table 3.4: Interpretation of p-values

S/No.	P-value	Interpretation
1.	$P \leq 0.01$	Highly significant
2.	$P \leq 0.05$	Significant
3.	$P > 0.05$	Not significant

Source: Masqood and Ibrahim (2015)

CHAPTER FOUR

4.0 RESULTS, ANALYSIS AND DISCUSSIONS

4.1 Preamble

This chapter presents the results of the various tests conducted and as explained in chapter three. The tests include characterization of the constituent materials of reactive powder concrete (RPC) using unrefined metakaolin, fresh and hardened properties of the concrete. The chapter also includes results of the RPC samples exposed to elevated temperatures. The results of the different experiments carried out are presented and discussed as follow:

4.2 Characterization of the Constituent Materials of RPC

4.2.1 Chemical compositions and physical properties of RPC constituents

This section present results related to the oxides compositions and physical properties of the RPC constituents' materials in Table 4.1.

Table 4.1: Oxide compositions and physical properties of RPC constituents

Oxide (%)	Sand	Cement	Silica fume	Metakaolin
SiO ₂	86.53	17.519	92.00	65.05
Fe ₂ O ₃	2.94	2.768	0.50	2.59
Al ₂ O ₃	1.64	4.74	0.70	20.65
CaO	0.40	71.297	0.50	0.82
CuO	0.00	0		0.02
NiO	0.00	0	0.015	0.03
MnO	0.01	0.072	0.128	0.08
Cr ₂ O ₃	0.00	0	0.006	0.03
TiO ₂	0.00	0.105	0.071	0.00
MgO	0.60	0	0.50	1.66
SO ₃	0.10	0.00	0.00	0.18
ZnO	0.00	0.007	0.006	0.01
SiO ₂ + Al ₂ O ₃ + Fe ₂ O ₃				88.29
LOI	0.84	3.492	3.00	1.80
<i>Physical properties</i>				
Surface area (m ² /kg)		561.9	2 0, 000	509.0
Strength activity index (%)			-	87
Specific gravity			2.21	2.53

Source: Experiment (2019)

Table 4.1 shows the chemical compositions of the constituent materials of RPC. For unrefined metakaolin, the summation of the major oxides (SiO₂ + Al₂O₃ + Fe₂O₃) as shown in the Table is 88.29%. The percentage (%) of the oxides is above the minimum (70%)

specified by ASTM C 618-05 for class N pozzolanic materials. Furthermore, the proportion of SO_3 (0.18%) is below the maximum (4%) specified by ASTM C 618-05 for class N pozzolanic materials. Also, the loss on ignition (LOI) is 1.80% which is below the maximum (10%) states by ASTM C 618-05 for class N pozzolanic materials. Therefore, the MK used for this research satisfied the requirement of ASTM C 618-05 for class N pozzolanic materials. The result of the Dangote blended cement and silica fume is also shown on the table. Moreover, the surface area of the cement, MK and SF are $561.9 \text{ m}^2/\text{kg}$, $509 \text{ m}^2/\text{kg}$ and $20000 \text{ m}^2/\text{kg}$ respectively. It can be observed that the SF has the highest surface area while MK has the lowest. This means that the SF is finer than the MK which could lead to more reactivity and filling effect.

4.2.2 Mineral composition of kaolin, calcined kaolin and fine sand

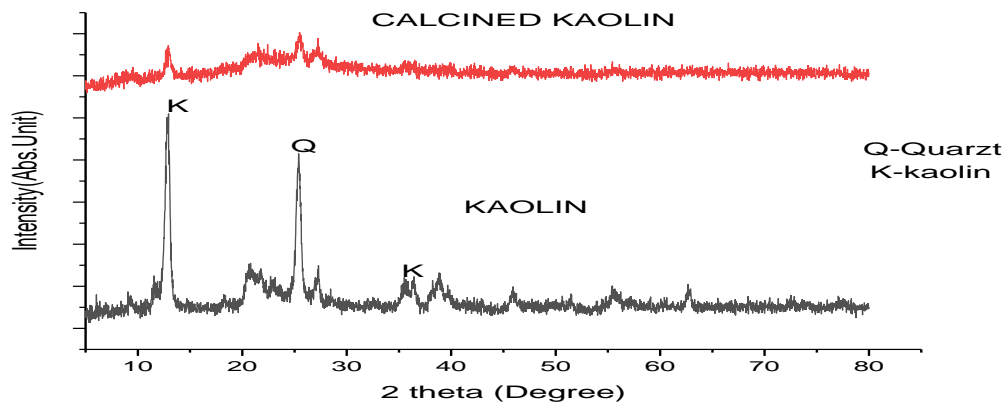


Figure 4.1: X-Ray diffraction result of metakaolin

Figure 4.1 shows the XRD pattern of kaolin and calcined kaolin (MK). It can be observed that the kaolin has kaolinite quartz as the major minerals. The peak at 2θ represent the existence of the kaolinite. However, after calcining, the peak or kaolinite drastically

reduced to a point of banishing. This indicated the partial transformation of kaolinite from crystalline to amorphous as can be seen the hallow shape nature of the calcined kaolin.

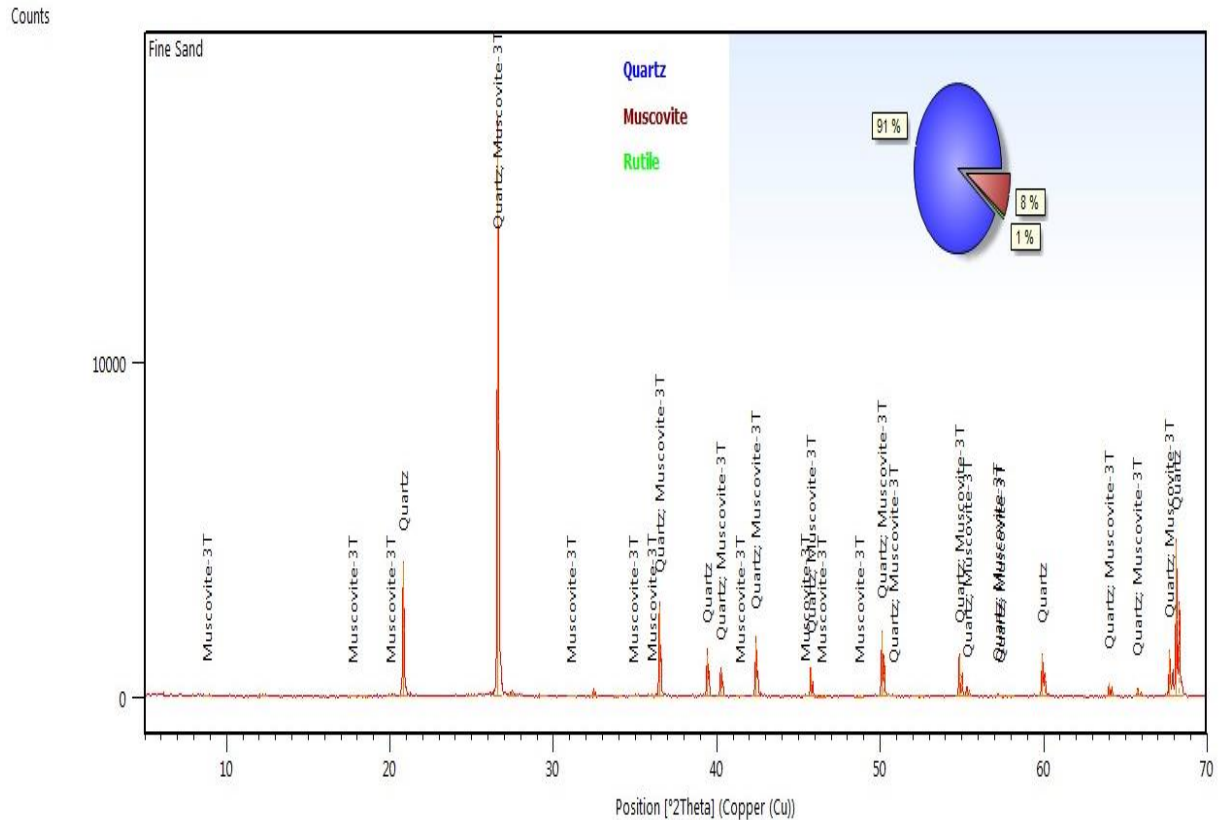


Figure 4.2: XRD of fine sand

Figure 4.2 shows the XRD result of fine sand used in the research. It can be observed that the major mineral is quartz with highest peak at 2θ value (27). However, muscovite and particles are present in the minor minerals. The minor mineral serves as impurities which is expected of any natural materials.

4.3

Mix Proportion of RPC

Table 4.2: Mix proportion of RPC

	Richard and Cheyrezy (1995) RPC 200					Experimental			
	Non fibred		Fibred			Non fibred		Fibred	
Portland cement	1	1	1	1	Dangote cement	1	1	1	1
Silica fume	0.25	0.23	0.25	0.23	Silica fume/Metakaolin	0.20	0.20	0.20	0.20
Sand 150-600 µm	1.1	1.1	1.1	1.1	Sand 150-600 µm	1.1	1.1	1.1	1.1
Crushed quartz	-	0.39	-	0.39	Crushed quartz	-	-	-	-
Superplasticizer (Polyacrylate)	0.016	0.01	0.01	0.01	Superplasticizer Conplast 430	0.032	0.033	0.035	0.036
Steel L=12 mm	-	-	0.17	0.17	GIW L=12 mm	-	-	0.02	0.02
Steel aggregates <800 µm	-	-	-	-		-	-	-	-
Water	0.15	0.17	0.17	0.19	Water	0.3	0.3	0.3	0.3
Compacting pressure	-	-	-	-	Compacting pressure	-	-	-	-
Heat treatment temp. (°C)	20	90	20	90	Heat treatment temp. (°C)	27	27	27	27

Table 9 depicts the proportions of RPC constituent materials as proposed by Richard and Cheyrezy (1995) and the one arrived at after series of trials. It is from this proportion that the experiment was conducted. The proportion containing SF served as control while that containing MK (by completely replacing the SF) as specimen. It should be noted that the percentage of the MK was then varied (10%, 20% and 30%) in order to find the optimum % of the MK that can best be used for the production of the RPC.

4.3

Flowability of RPC



(a) During pouring

(b) During measuring

Plate XIX: Flowability of RPC

Plate XIX shows the flowing nature of the RPC produced. RPC is considered to be self-flowing concrete. ASTM C143 (AASHTO T119) states that for concrete to be regarded as self-compacting concrete, the flow value or workability of such concrete should not be less than 190 mm and ASTM C1611 states that the value should not be greater than 600 mm. Therefore, it was based upon this range and series of trials that the flow value of the RPC produced was fixed at 270 ± 5 mm. This value was achieved by the addition of superplasticizer. It was observed that the superplasticizer (SP) dosage for RPC increased with the increasing MK content. The dosage of SP required for the RPC specimens produced with 10% MK, 20% MK, 30% MK and 20% SF, were in the range of 2.8-3.2%, 3.8-3.9%, 4.5-5.0% and 3.5-3.6% respectively. The increasing SP demand by MK can be ascribed to its high surface area. Therefore, the use of MK in RPC production requires more SP which may likely affect the cost of the mix.

4.4

Hardened Properties of RPC

4.4.1 Compressive strength unrefined RPC

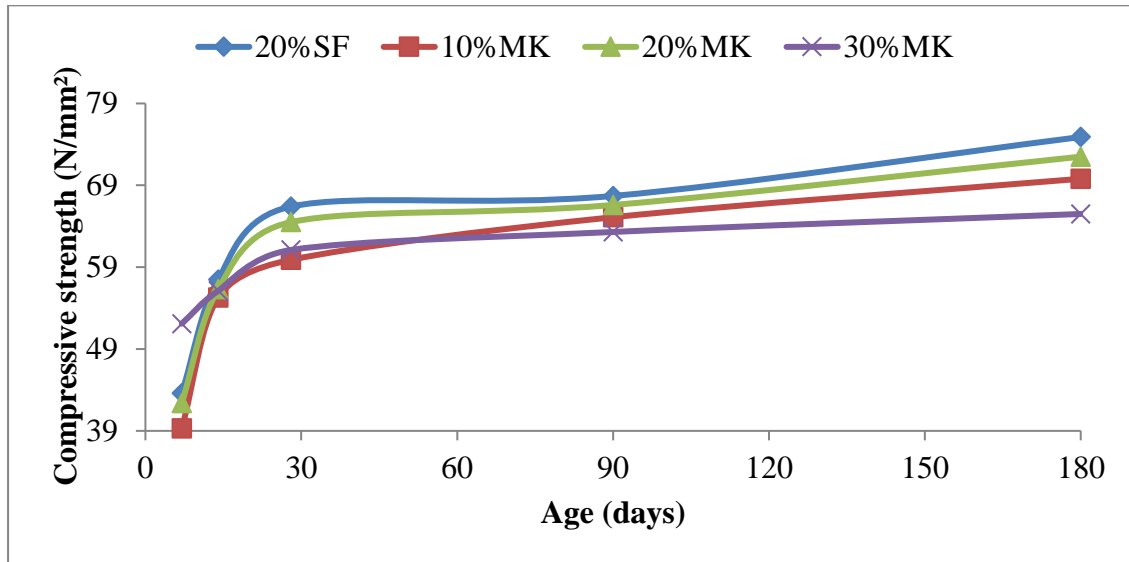


Figure 4.3: Effect of MK content on the compressive strength of unfibred RPC

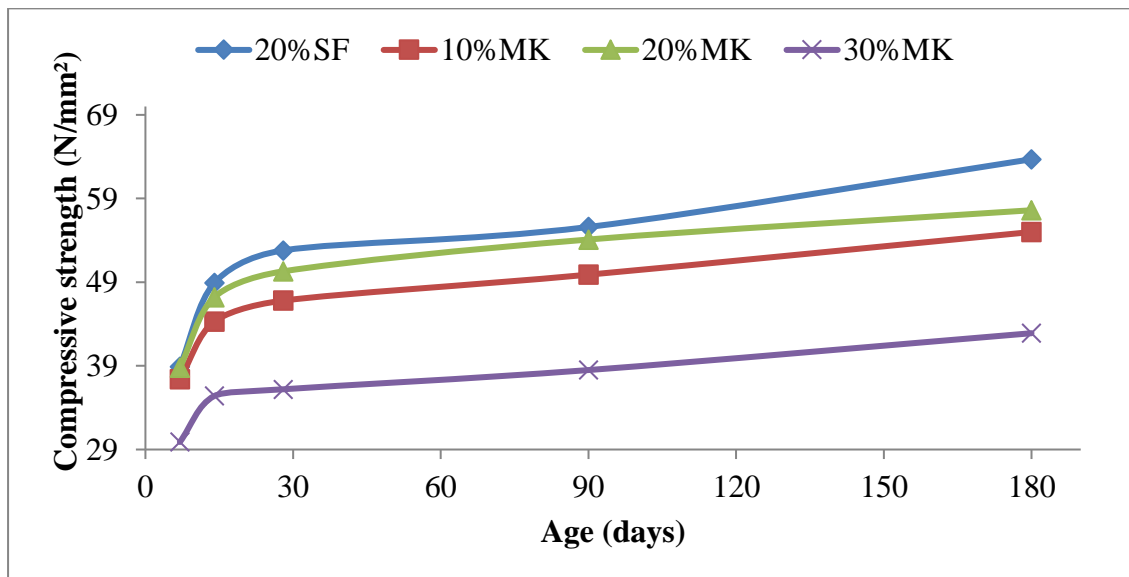


Figure 4.4: Effect of MK content on the compressive strength of fibred RPC

Figures 4.3 and 4.4 show the effect of MK content on the compressive strength of unfibred and fibred RPC at 7, 14, 28, 90 and 180 days respectively. For the unfibred and fibred specimens of the RPC, increase in compressive strength with age can be observed. The average compressive strengths of 20% SF, 10% MK, 20% MK and 30% MK of unfibred RPC at 7 days were 43.6, 39.3, 42.4 and 52.1 N/mm² respectively. At 28 days, the compressive strengths were 66.4, 59.9, 64.5 and 61.1 N/mm², at 90dys, the compressive strength were 67.7, 65.1, 66.6 and 63.3N/mm², respectively and at 180 days, the compressive strengths were 74.9, 69.8, 72.5 and 65.5 N/mm² respectively.

At 7 and 28 days, the compressive strengths of unfibred specimen with 20% MK were comparable to those of the control (20% SF). However, the specimen with 30% MK showed higher strength at 7 days but lower at 28 days. The improved strength exhibited by the specimen with 30%MK could be due to the fast pozzolanic reaction of MK at 7 days due to the presence of more SiO₂ that reacted with the Ca (OH)₂ liberated during hydration to produce additional cementitious compounds such as C-S-H and C-S-A-H. On the other hand, the control concrete has higher early compressive strength compared to 10% MK due to high pozzolanic activity and finer particle sizes of the SF than the MK. At 28 days, the compressive strengths of the unrefined RPC with 10% MK, 20% MK and 30% MK were 66.4, 59.9,64.5 and 61.1 N/mm² respectively (90.2%, 97.1% and 92% than that of the control with 66.4 N/mm²). At 180 days, the compressive strengths of the unfibred specimens with 10% MK, 20% MK and 30% MK were 69.8, 72.5 and 65.5 (93.2%, 96.8% and 87.4% of the control, 74.9 N/mm²). It was found out that at 90 and 180 days, the compressive strengths of unfibred specimen with 20% MK were comparable to those for

the control (20% SF). It means that the MK has similar compressive strength effect with SF at all ages. This agrees with the findings of Guneyisi, Gesoglu, Karaoglu and Mermerdas (2012) and Ding and Li (2002) who observed that MK reacts (in terms of strength) in similar way to SF. Also, MK helps in enhancing the early age and long-term mechanical properties of concrete (Siddique & Klaus, 2009). Hence, 20% is the optimum content of MK to produce RPC with comparable compressive strength to that of the control.

However, the fibred specimens showed variation in compressive strength compared to the unfibred as shown in Figure 4.5. At 7 days, the compressive strengths of the fibred specimens with 20% SF, 10% MK, 20% MK and 30% MK are 38.9N/mm², 37.4 N/mm², 38.8 N/mm² and 29.9 N/mm² respectively. While at 28 days, the compressive strengths of the specimens with 10% MK, 20% MK and 30% MK were 88.6%, 95.3% and 69.1% lower than that of the control (52.8N/mm²). At 90 days, the compressive strength of the fibred RPC specimens (20% SF, 10% MK, 20% MK and 30% MK) was 55.6, 49.9, 54.1 and 38.5N/mm² respectively and those of 180 days were 63.7, 55, 57.6 and 42.9N/mm² respectively. It can be observed (Figure 4.5) that there is increase in strength in all the ages across the specimens with 20% MK recording a comparable strength to that of the control (20% SF). For example, at 7, 28, 90 and 180 days the 20% MK has 99.7%, 95.3%, 97.3% and 90.4% respectively of the strength of the control (20% SF). For the fibred samples, the introduction of the fibre material caused reduction in strength probably due to its slippery surface that could hinder adequate bond between the fibres and the cement paste. This is line with what Iqbal, Ali, Holschemacher and Bier, (2015) who reported that there is around 12% reduction in compressive strength with increase of steel fiber content from 0% to 1.25% in RPC. Meaning that steel fibre inclusion reduces

compressive strength. The compressive strength of RPC produced with 20% MK in this study is superior to those obtained when rice husk ash (RHA) and fly ash were separately used in the production of RPC as reported by Asteray, Oyawa and Shitote (2017); Demiss, Oyawa and Shitote (2018) respectively. Therefore, the use of unrefined MK in RPC production gives better compressive strength result than fly ash and RHA.

4.4.2 Tensile strength of unrefined RPC

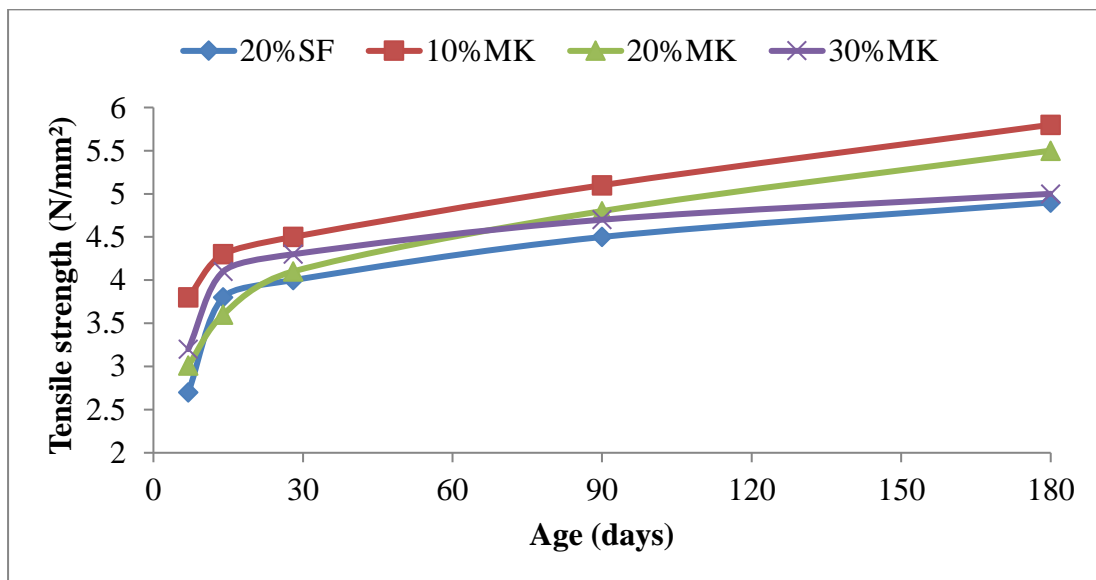


Figure 4.5: Effect of MK content on the tensile strength of unfibred RPC

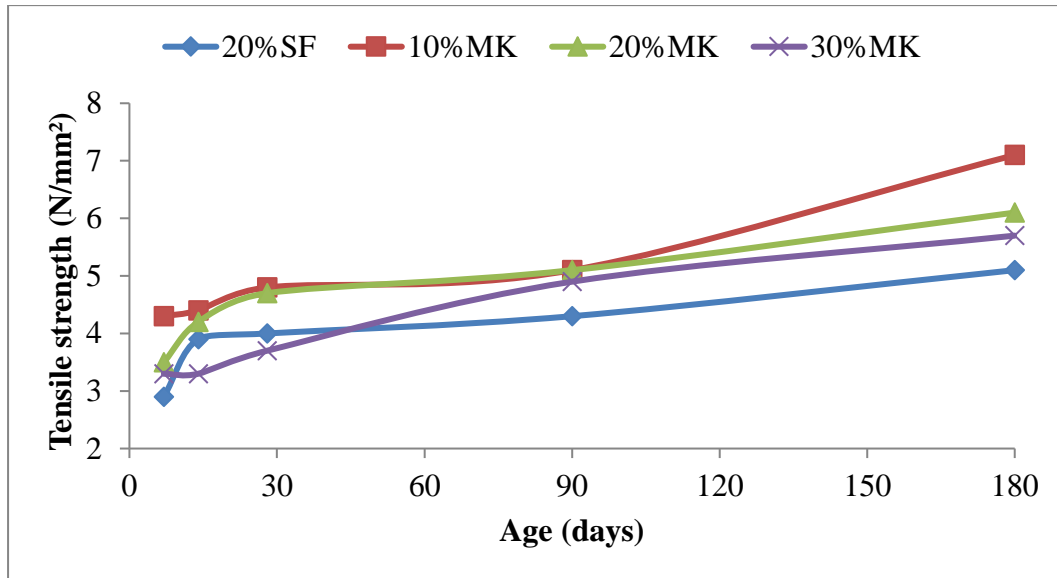


Figure 4.6: Effect of MK content on the tensile strength of fibred RPC

Figures 4.5 and 4.6 depict the split tensile strength of unfibred and fibred RPC respectively. For the fibred and unfibred specimens, increase in tensile strength with age can be observed. As shown in Figure 4.5, the tensile strength of unfibred specimens with MK at all ages were generally higher than that of the control. At 7 days, the tensile strength of the 20% SF, 10% MK, 20% MK and 30% MK were 2.7 N/mm², 3.8 N/mm², 3.01 N/mm² and 3.2 N/mm² respectively. At 28 days, the tensile strengths for 10% MK and 30% MK were 4.5, 4.1 and 4.3 N/mm² which is higher than that of the control by 12.5% and 2.5% respectively and 20% MK is lower than the control by 10%. At 90 and 180 days, all the specimens showed higher tensile strength than the control sample. For example, at 90 days, 10% MK, 20% MK and 30% MK tensile strength (5.1, 4.81 and 4.7 N/mm²) were higher than the control by 13.3%, 6.7% and 4.4% respectively. At 180 days, 10% MK, 20% MK and 30% MK were also higher than the control by 18.4%, 12.2% and 2% respectively. The improvement in the tensile strength of the specimens with MK could be due to the filler and

pozzolanic effects of MK that enhance the microstructure of the RPC. This agrees with what Vipat and Kulkarni, (2016) reported that MK enhances the properties of normal concrete through filler and pozzolanic effects.

For the fibred specimens, as shown in Figure 4.6, it is clear that the inclusion of fibre improves the tensile strengths of all the specimens. And that the tensile strength improvement reduces with the increasing MK content above 10% at all ages. The tensile strengths of the specimens with 20% SF, 10% MK, 20% MK and 30% MK at 7 days were 2.9 N/mm², 4.3 N/mm², 3.5 N/mm² and 3.3 N/mm² while those at 28 days were 4 N/mm², 4.8 N/mm², 4.7 N/mm² and 3.7N/mm² respectively. Moreover, at 90 days, the tensile strength (5.1, 4.8 and 4.7 N/mm²) of 10% MK, 20% MK and 30% MK were higher than the control by 18.6%, 18.6%, and 14% respectively. So also, at 180 days, the tensile strength (7.1, 6.1 and 4.7 N/mm²) of 10% MK, 20% MK and 30% MK were higher than the control by 39.2%, 19.6% and 11.8%. Hence, up to 30% MK can be used to develop fibred RPC with improved tensile strength.

4.4.3 Flexural strength

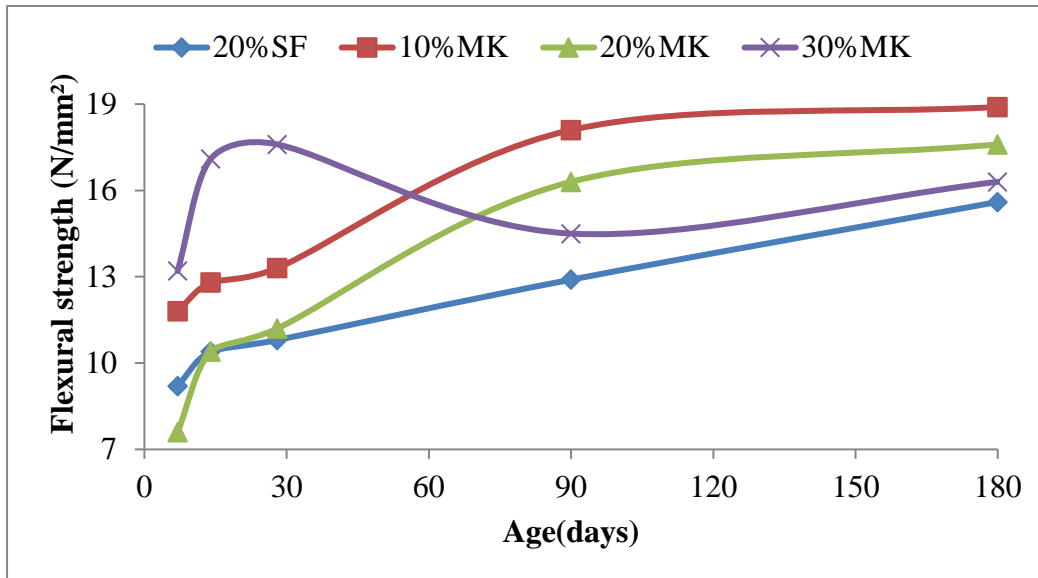


Figure 4.7: Effect of MK content on the flexural strength of unfibred RPC

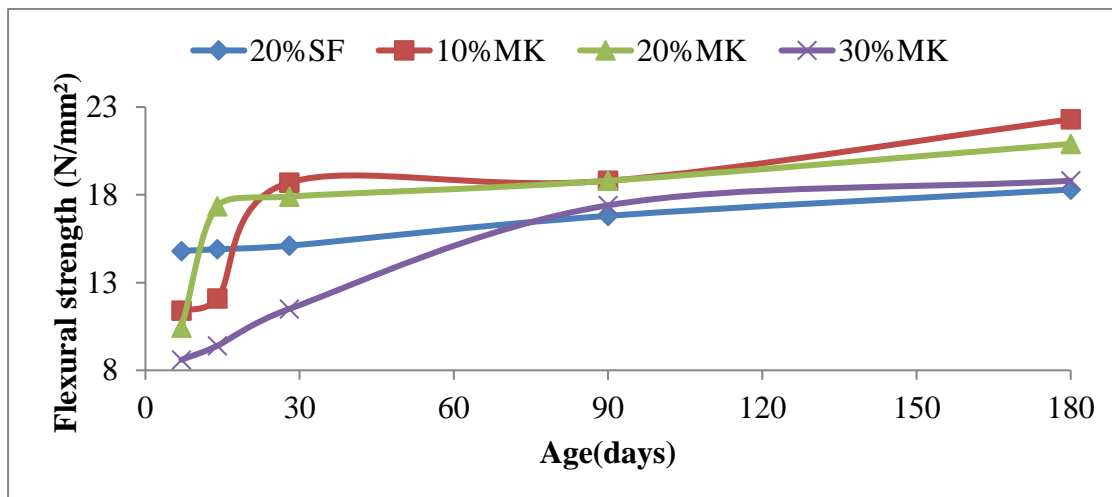


Figure 4.8: Effect of MK content on the flexural strength of fibred RPC

Figures 4.7 and 4.8 demonstrate the flexural strengths of fibred and unfibred RPC. Compared to the control, MK improved the flexural strength of unfibred RPC, and the improvement goes along with the increase in MK content. At 7 and 28 days, the range of flexural strength of the MK based RPC is 7.6 – 13.2 N/mm² and 11.2- 17.6 N/mm² respectively. However, the flexural strength of the control is 10.8 N/mm². Similar trend was observed at 90 and 180 days. At 90 days, the flexural strength of the MK-based RPC specimens (10% MK, 20% MK & 30% MK) was higher (in the range of 14.5 N/mm² to 18.1 N/mm²) than the control (20% SF) by 40.3%, 26.4% and 12.4% respectively. Also, at 180 days, the 10% MK, 20% MK and 30% MK were higher than the referenced (20% SF) by 21.2%, 12.8%, and 4.5% respectively. As shown in Figure 4.8, fibre improves the flexural strengths of all the specimens. For example, at 7 days, the flexural strength of 20% SF, 10% MK, 20% MK and 30% MK were 14.8, 11.4, 10.44 and 8.6 N/mm² respectively. However, the extent of improvement over curing ages is more pronounced with the specimens made with MK than with SF. At 180 days, the 10% MK, 20% MK and 30% MK were higher than the control by 21.9%, 14.2% and 2.7% respectively. Overall, 10% MK inclusion outperformed the other specimens at all ages. The improvement in the flexural strength of the specimens with MK could be due to the filler and pozzolanic effects of MK that enhance the microstructure of the RPC. Vipat and Kulkarni, (2016) reported similar findings that MK enhances the properties of concrete through filler and pozzolanic effects. Results similar to these findings were reported by Haroon, Ashad, Vikas and Alvin (2017); Demiss, Oyawa and Shitote (2018).

4.5 Performance of the RPC Exposed to Elevated Temperature

This section presents the result of the RPC cured at 28 days and exposed to elevated temperatures (200-800°C).

4.5.1 Physical observation

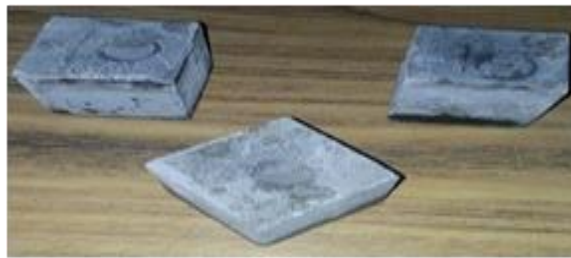


Plate XX: Control @ 27 °C



Plate XXI: Sample exposed to elevated temperatures

Plate XX shows the different RPC samples exposed to elevated temperatures 200°C, 400°C, 600°C and 800°C at 28 days curing age. It can be observed that at 200°C there is no colour change and visible crack development on various RPC surfaces. Up to 600°C there is no visible crack development on the surfaces of the various RPC sample. However, colour changes were noticed as can be seen from Plate XXI. At 400°C and 600°C, the colour

changed from grey to light brown. At 800°C, the colour changed from light grey to light green with very minor micro cracks on the RPC surfaces. The change in colour at different temperatures could be attributed to the dissolution and oxidation of iron contained in the fine aggregates. Similar observation was made by Lee, Choi and Hong (2010) that colour change in concrete exposed to high temperature is due to oxidation of iron and dissolved hydrates contain in the fine or coarse aggregates. From the above observation, it can be noticed that the presence of the micro cracks (instead of large cracks) could be due to the presence of the pozzolanic materials (SF & MK) as well as the GIW as fibre in the production of the RPC that enhanced the physical performance of the RPC specimens through filler and pozzolanic effect.

4.5.2 Residual and normalized compressive strengths

This section explains the residual compressive strength of unfibred and fibred RPC after exposure to elevated temperatures of 200°C to 800°C.

4.5.2.1 Unfibred RPC

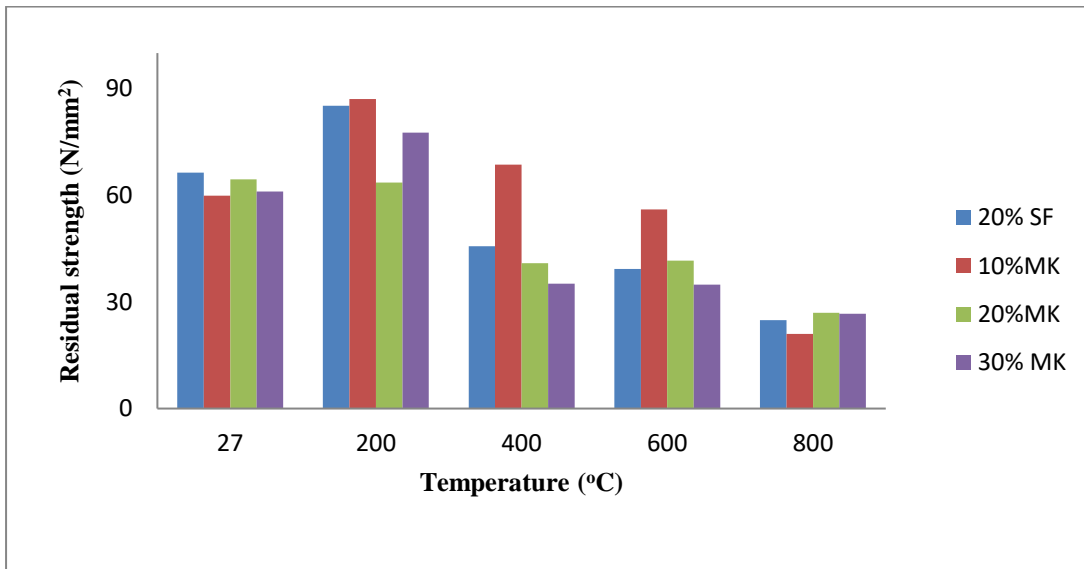


Figure 4.9: Residual strengths of unfibred RPC exposed to elevated temperatures

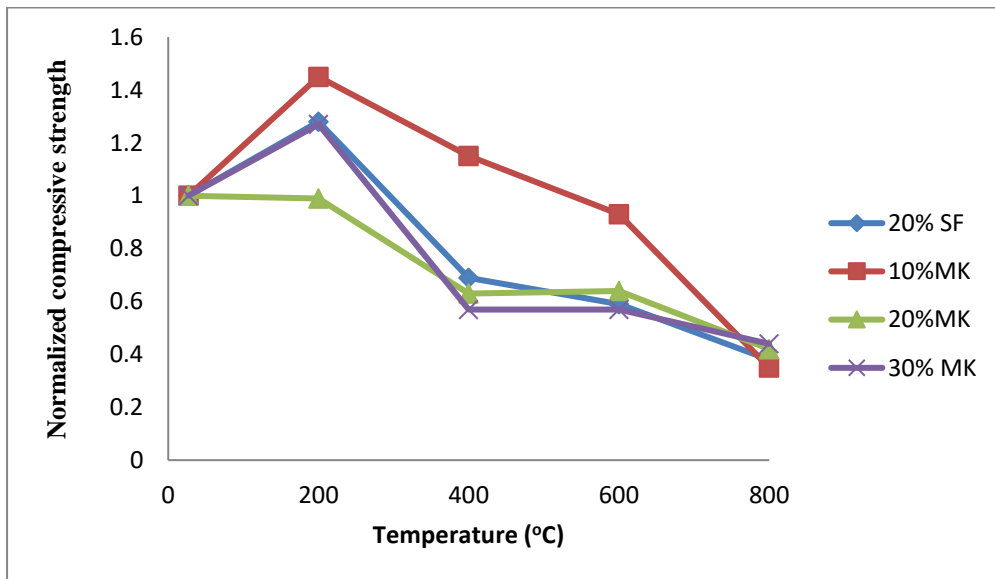


Figure 4.10: Normalized compressive strength results of unfibred RPC exposed to elevated temperature

Figures 4.9 and 4.10 show the residual and normalized compressive strength of the unfibred RPC. It can be observed that each temperature range has a different pattern of strength gain or loss. At 200 °C, 20% SF, 10% MK and 30% MK samples show 28%, 45% and 27% higher compressive strength compared to the RPC at room temperature respectively while 20% MK sample is 1% lower strength than the one at ambient temperature (27°C). The increase in the compressive strength of these samples could be due evaporation of free water that leads to strengthening of hydrated cement paste at 200 °C which in line with the findings of Hiremath and Yaragal (2018). At 400°C, there was an increase in the compressive strength of 10% MK RPC (indicating endurance to higher temperature) while a decrease in the compressive strength of all other RPC was observed. A loss of strength was observed at 600°C. The strength loss was within the range of 7-43%. All samples have no visible micro cracks on their surfaces but the 10% MK performed better than all other samples. At 800°C, there was greater loss of strength and hair-like micro cracks on the surfaces of all the RPC samples. The residual strength at this temperature was between 56% and 65%.

Generally, the strength loss decreases with increase in MK content (10-30%) in the RPC when the temperature was varied between 200°C and 800°C. This is an indication of better performance of MK in retaining strength at elevated temperature. The benefit of replacing MK with SF was more observed when 10% MK was used. The deterioration of strength at elevated temperature could be due to the decomposition of calcium hydrate gel that causes severe deterioration in the RPC (Demirel & Kelestemur, 2010). Moreover, the normalized strength of the unfibred RPC followed the same trend as the residual strength and it is the percentage of the strength retained by concrete with respect to the strength of the unheated sample at 27°C.

4.5.2.2 Fibred RPC

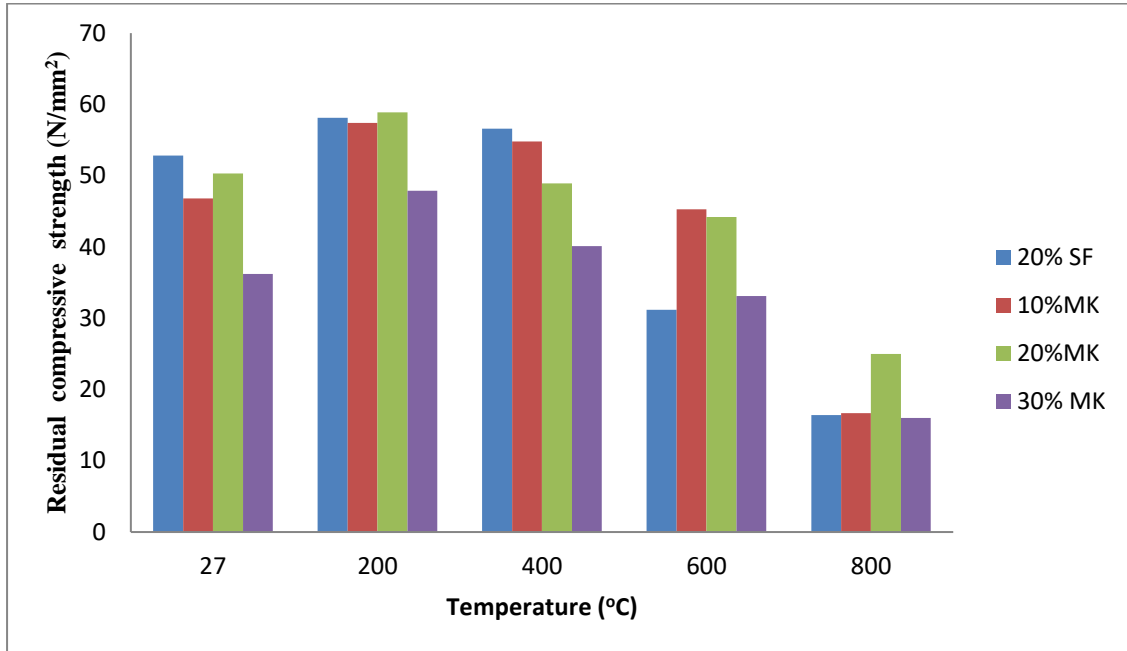


Figure 4.11: Residual compressive strength of fibred RPC exposed to elevated temperatures

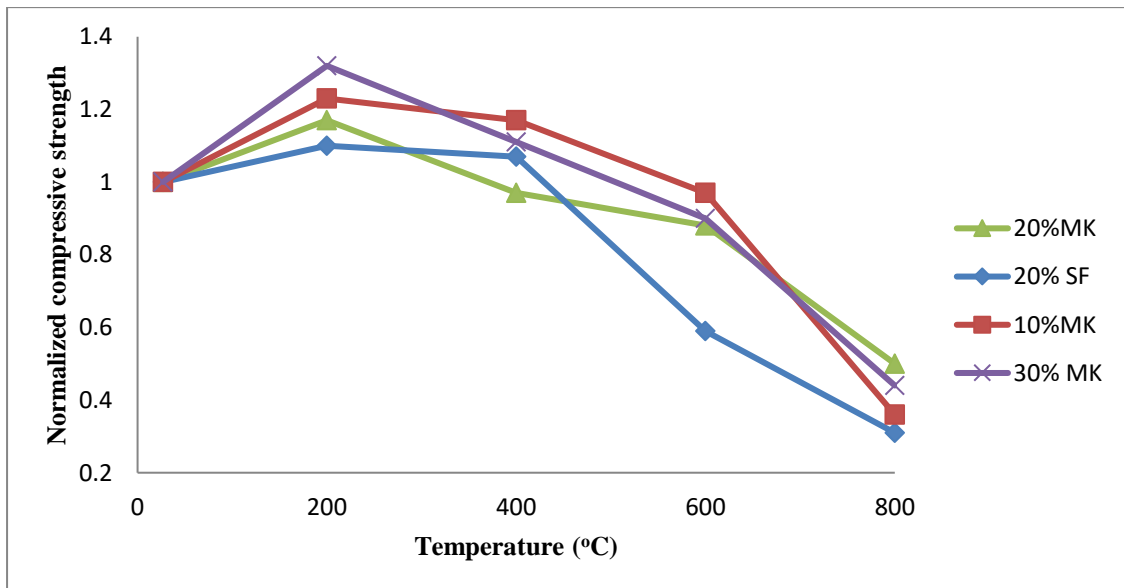


Figure 4.12: Normalized compressive strength of fibred RPC exposed to elevated temperatures

Figures 4.11 and 4.12 show the residual and normalized compressive strength of the fibred RPC samples. Also, it can be noticed that each temperature range has a different pattern of strength gain or loss. At 200°C, the RPC specimens (20% SF, 10% MK, 20% MK and 30% MK) have shown 10%, 23%, 17% and 32% higher compressive strength respectively compared to the RPC at ambient temperature. The increase in the compressive strength of these samples at 200°C could be due to the evaporation of free water that strengthened hydrated cement paste (Peng *et al.*, 2012, Tian *et al.*, 2012, Zheng *et al.*, 2013, So *et al.*, 2014, Hiremath and Yaragal 2018). The 20% MK has similar residual compressive strength with 20% SF.

At 400 °C, there was an increase in the compressive strength of 20% SF, 10% MK and 30% MK in the range of 7-17% with 10% MK recording the highest (17%) while 20% MK RPC relatively remained the same which somehow contradict the findings of Peng *et al.* (2012), Tian *et al.*, (2012), Zheng *et al.*, (2013) and So *et al.*, (2014) in their studies. A loss of strength was noted at 600°C. The strength loss was within the range of 3-41%. All samples had no visible micro cracks on their surfaces but 10% MK performed better (with just 3% loss) than all other samples. The 20% SF recorded the highest loss of strength (41%). At 800 °C, there was greater loss of strength and hair-like micro cracks on the surfaces of all the RPC samples. The residual strengths at this temperature were 50-69% with 20%SF and 20%MK recording the highest and the least respectively.

Therefore, it was observed that the strength loss decreased with increase in MK content (10-30%) in the RPC when the temperature was varied between 200°C to 400°C. This is an indication of better performance of MK and fibre in retaining strength at elevated temperature. The benefit of replacing SF with MK was more when 20% MK addition was used. The deterioration of strength at elevated temperature (400–800°C) could be due to the

decomposition of calcium hydrate gel that causes severe deterioration in the RPC (Demirel & Kelestemur, 2010) as well as the presence of fibre which prevented proper bonding and may also be regarded as the critical temperature range for the strength loss of fibre concrete (Peng *et al.* 2006). The bond strength in the concrete matrix degraded significantly with increasing temperature for straight steel fibres (Abdallah, Fan & Cashell, 2017). Additionally, the normalized strength of the fibred RPC followed the same trend as the residual strength and it was calculated as the percentage of the strength retained by concrete with respect to the strength of the unheated sample at 27°C.

4.5.3 Ultrasonic pulse velocity (UPV) of RPC exposed to elevated temperatures

The UPV was done in order to determine the quality of the internal structure of the RPC exposed to elevated temperatures (200-800°C). The UPV results of the unfibred and fibred RPC exposed to elevated temperatures are discussed in sub-sections 4.5.3.1 and 4.5.3.2 respectively.

4.5.3.1 Unfibred RPC

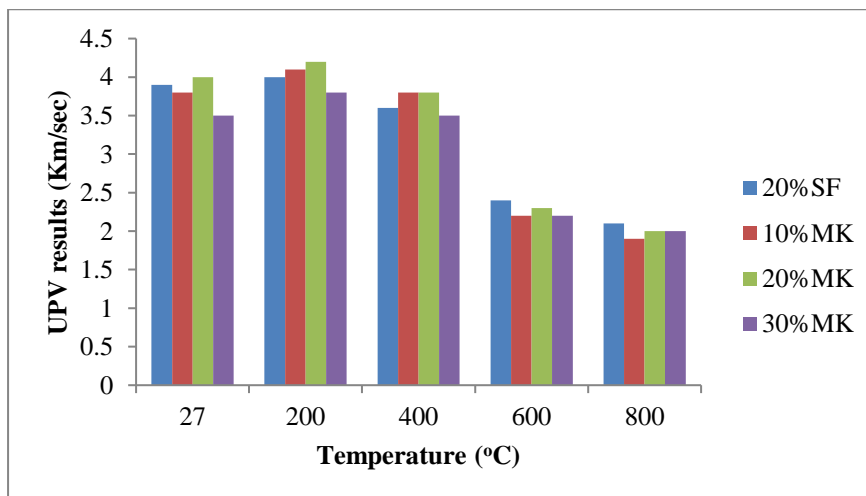


Figure 4.13: Ultrasonic pulse velocity results of unfibred RPC

Figure 4.13 depicts the Ultrasonic Pulse Velocity (UPV) of unfibred RPC made from 20% SF, 10% MK, 20% MK and 30% MK exposed to elevated temperatures. It can be seen that the UPV value increased at 200°C as compared to that at ambient temperature (27 °C). The increase in strength could be due to steam curing caused by hot vapour which leads to further hydration of the cement paste. This agreed to the finding of Houa, Abid, Zheng and Waqar (2017). There was loss in UPV value in the range of 1.9-3.8 km/s at 400 °C, which indicated decrease with an increasing temperature. Therefore, it can be concluded that at the temperatures of 200 °C and 400 °C all the RPC samples were good while at 600 °C to 800 °C the RPC samples were in doubtful condition based on an International Atomic Energy Agency, (IAEA, 2010) classification of concrete exposed to elevated temperatures. Generally, the 20% MK performs better than the 20% SF, 10% MK and 30% MK by having higher UPV values across the temperature.

4.5.3.2 Fibred RPC

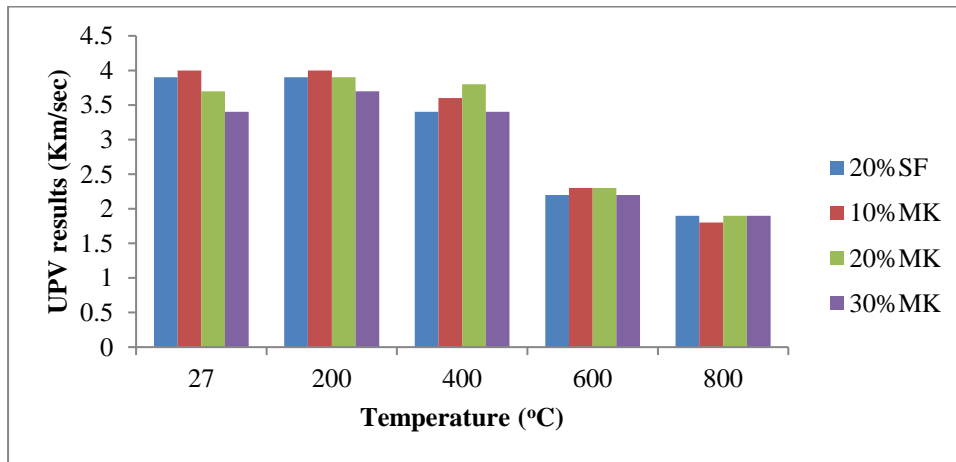


Figure 4.14: Ultrasonic pulse velocity results of fibred RPC

Figure 4.14 shows the Ultrasonic Pulse Velocity (UPV) of fibred RPC made from 20% SF, 10% MK, 20% MK and 30% MK exposed to elevated temperature. It can be observed that

the UPV value increased at 200 °C as compared to that at ambient temperature. The increase in strength could be due to further hydration of cement paste caused by hot vapour (Houa, Abid, Zheng & Waqar 2017). However, for 10% MK and 20% MK at 400°C, their UPV values are still in good condition (IAEA2010). Therefore, the high UPV values could be due to the presence of the WGIW fibre that tends to strengthen the RPC samples. At 600°C to 800°C, the RPC were in doubtful conditions.

4.5.4 Water absorption capacity (%) of RPC exposed to elevated temperatures

Water absorption capacity was carried out in order test the degree of permeability of the RPC exposed to elevated temperature. Low permeable concrete resists ingress of water and is not susceptible to freezing and thawing. The abbreviation ‘U’ and ‘F’ represent unfibred and fibred RPC specimens respectively. Results of the water absorption capacity of the unfibred and fibred RPC are presented and discussed below:

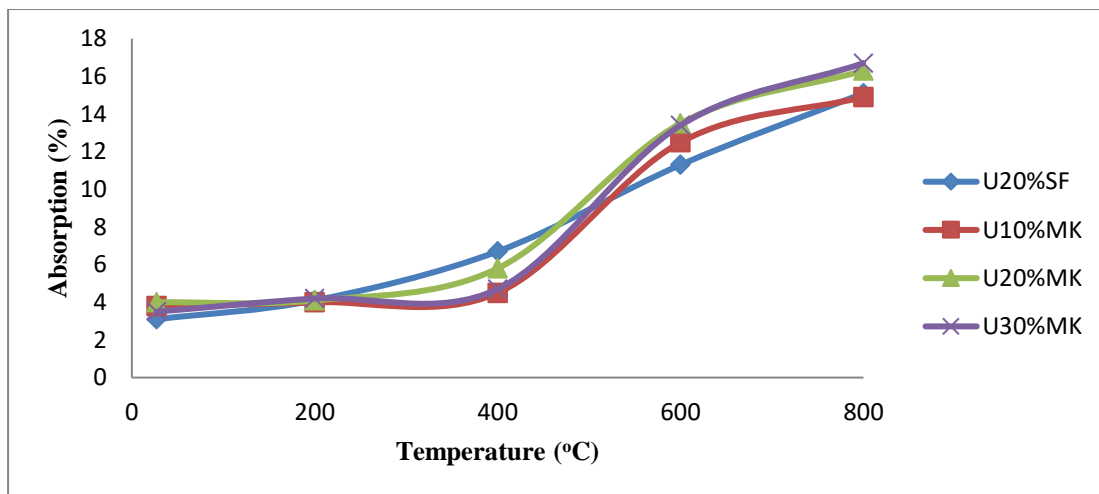


Figure 4.15: Water absorption of unfibred RPC exposed to different elevated temperature

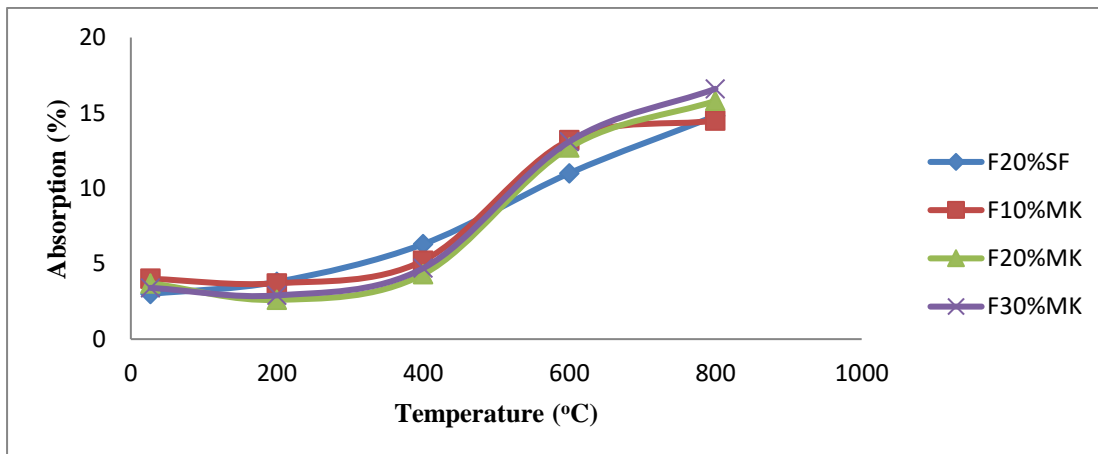


Figure 4.16: Water absorption of fibred RPC exposed to different elevated temperature

Figure 4.15 and 4.16 show the water absorption of the unfibred and fibred RPC exposed to elevated temperature. At 27°C, the water absorption of the unfibred samples (20% SF, 10% MK, 20% MK and 30% MK) were 3.1%, 3.8%, 4.0% and 3.5% respectively with 20% SF recording the least and 20% MK recording the highest absorption. When the samples were exposed to 200 °C, an increase in water absorption of between 2.5 and 20% was observed in RPC made with MK, with an even more pronounced increase (32%) in RPC made with SF. Significant increase in the water absorption was noticed in all the samples of the RPC when the temperature was raised between 400°C and 800°C. The 20% SF recorded the least (15.1%) and 30% MK recording the highest (16.7%). Therefore, above 200 °C RPC made with MK was observed to absorb more water than the 20% SF sample. This means that there are more pores present (which are responsible for the higher absorption) in the RPC made with MK than the control (20% SF). Similar finding was reported by Aghabaglou, Sezer and Ramyar (2014) in their research.

4.5.5 Relationship between ultrasonic pulse velocity and residual strength of RPC

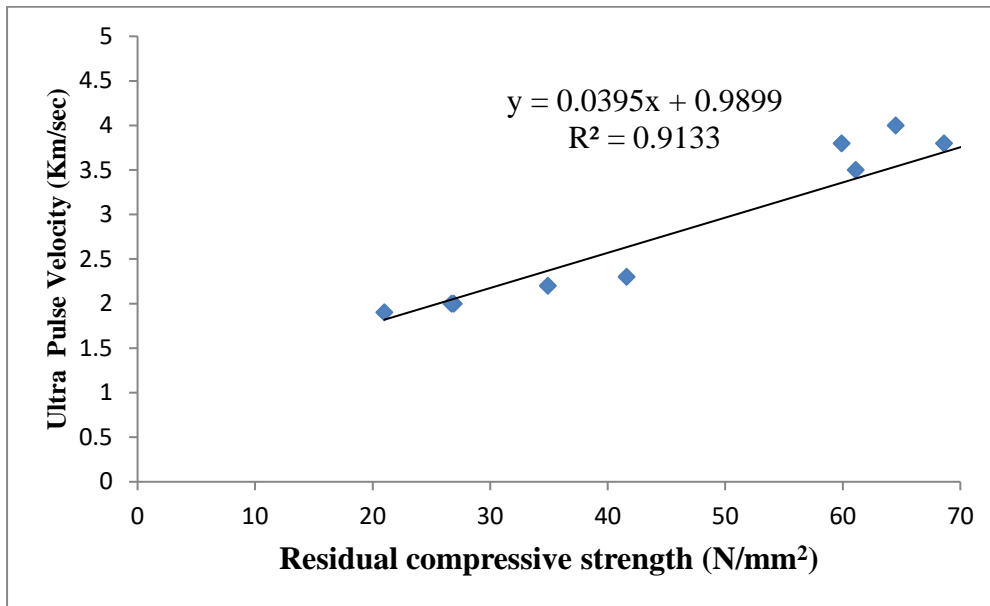


Figure 4.17: Relationship between UPV and residual compressive strength of unfibred RPC

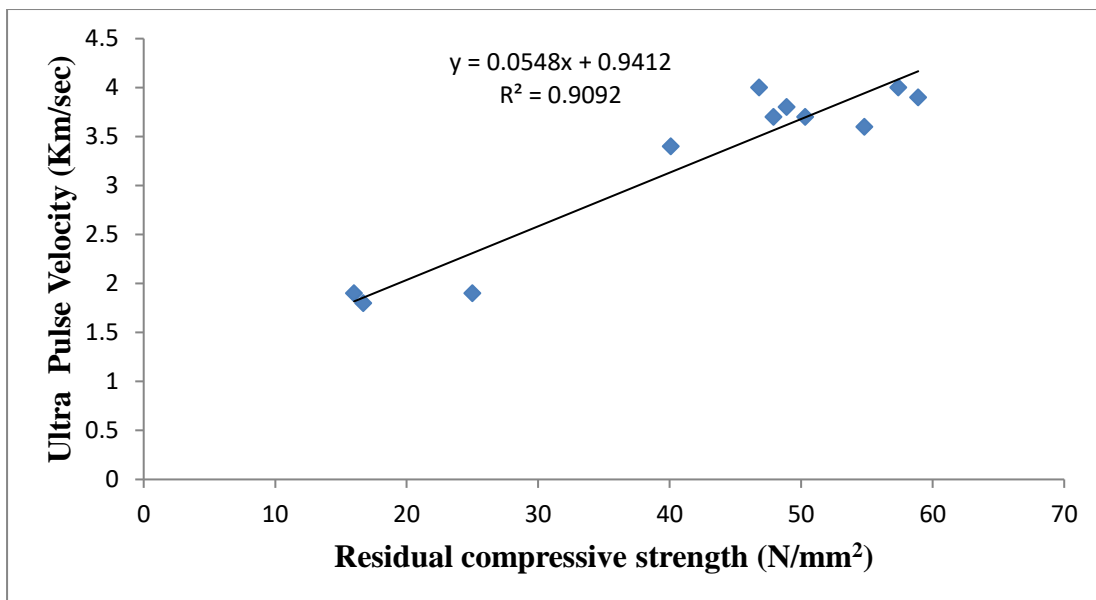


Figure 4.18: Relationship between UPV and residual compressive strength of fibred RPC

Figures 4.17 and 4.18 show the relationship between residual strength and ultrasonic pulse velocity for the unfibred and fibred RPC samples made from different percentages of MK. It can be seen that a linear relationship exists between the residual compressive strength and ultrasonic pulse velocity having coefficient of correlation (R^2) value of 0.913 and 0.909 for unfibred and fibred RPC respectively. This means that there is strong linear relationship between residual strength and ultrasonic pulse velocity of the RPC. Therefore, UPV can be used to describe the residual compressive strength of RPC made with unrefined MK.

4.5.6 Relationship between ultrasonic pulse velocity and water absorption of RPC

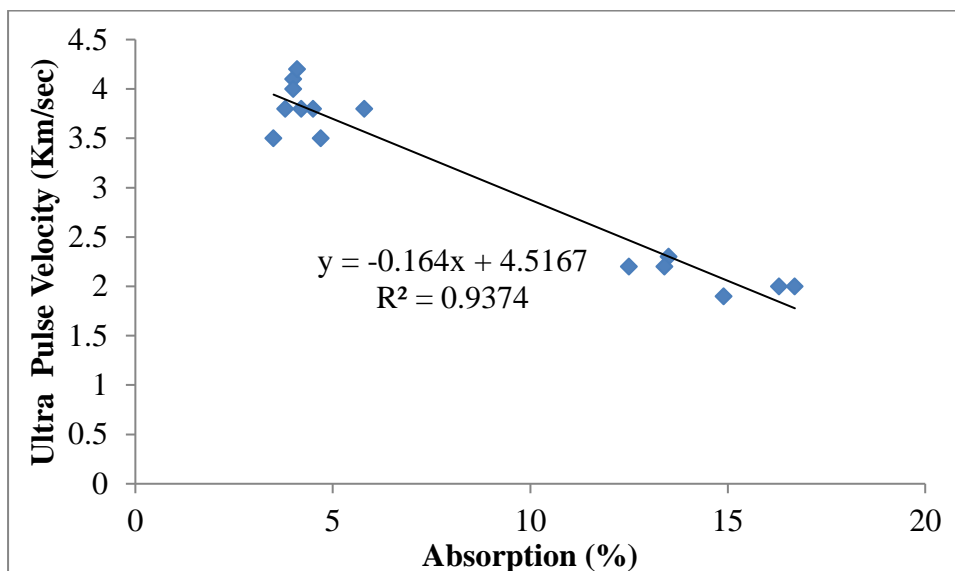


Figure 4.19: Relationship between UPV and water absorption of unfibred RPC

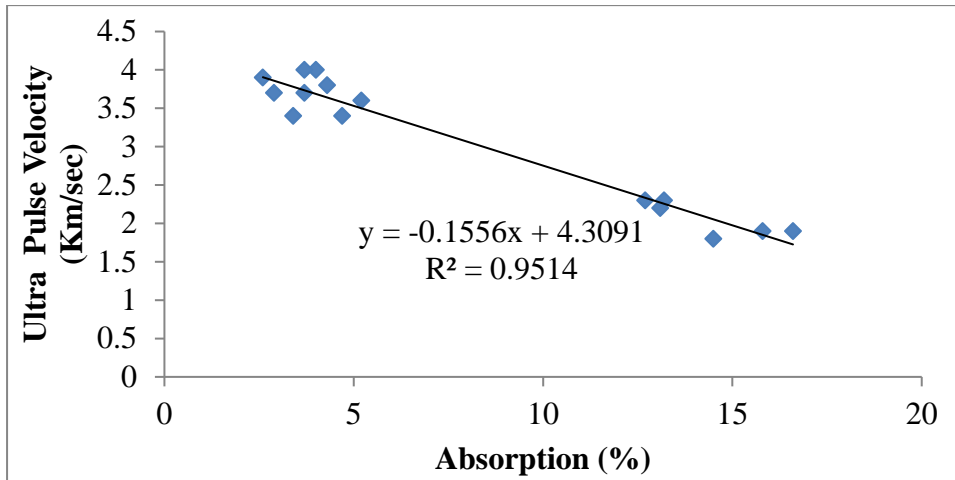


Figure 4.20: Relationship between UPV and water absorption of fibred RPC

Figures 4.19 and 4.20 show the relationship between water absorption and ultrasonic pulse velocity for the unfibred and fibred RPC samples made from different percentages of MK. It can be noticed that a linear relationship exists between the water absorption and ultrasonic pulse velocity having coefficient of correlation (R^2) value of 0.937 and 0.951 for unfibred and fibred RPC. Therefore, a relationship between absorption and ultrasonic pulse velocity of the RPC means that UPV can be used to describe the absorption of such samples.

4.5.7 Sorptivity of RPC exposed to elevated temperatures

The results of sorptivity of the RPC specimens (as shown in appendix G) made from locally sourced unrefined MK (unfibred and fibred) are presented and discussed in Subsections 4.5.7.1 to 4.5.7.5

4.5.7.1 Sorptivity of RPC at ambient temperatures

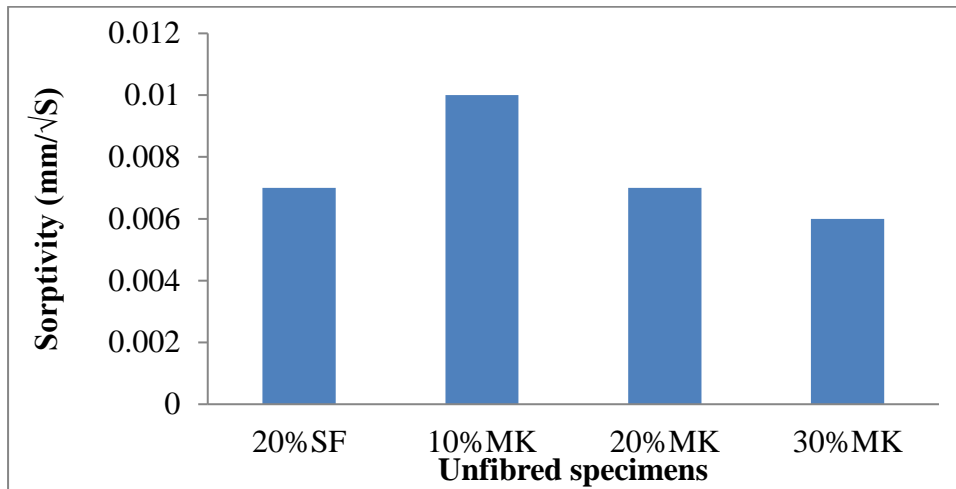


Figure 4.21: Sorptivity of unfibred specimens exposed to ambient temperature

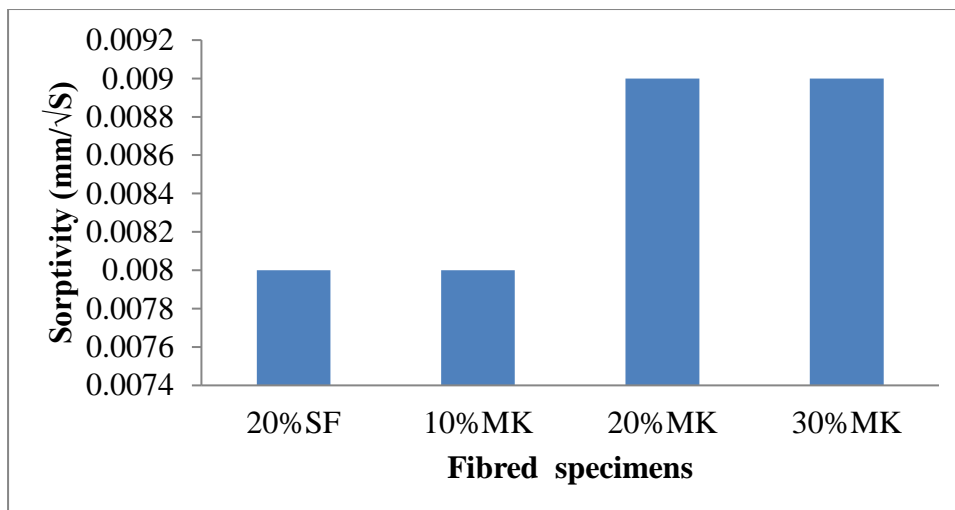


Figure 4.22: Sorptivity of fibred specimens exposed to ambient temperature

Figure 4.21 and 4.22 show the initial water absorptions rates of unfibred and fibred RPC specimens (20% SF, 10% MK, 20% MK and 30% MK) exposed to ambient temperature. For Figure 4.21 (unfibred RPC), the initial water absorptions rates of the 20% SF, 10% MK, 20% MK and 30% MK are 0.007, 0.01, 0.007 and 0.006 mm/√s respectively. The 20%

MK recorded a similar result with the reference sample (20% SF), 10% MK shows higher absorptions rates and 30% MK records lower absorptions rates than the control.

For fibred RPC (as shown in Figure 4.22), the initial water absorptions rates of the sample with 20% SF, 10% MK, 20% MK and 30% MK are 0.008, 0.008, 0.009 and 0.009 mm/ \sqrt{s} respectively. The 10% MK recorded similar result with that of the reference (20% SF) while 20% MK and 30% MK have higher absorptions rates than the reference. It can be noted that the rate of water absorption decreases with increase in metakaolin content for the unfibred specimens and increases with increase in metakaolin content for the fibred RPC. The decrease in the absorptions rates for the unfibred RPC could be due to reduction in volume of capillary pores as a result of the filling effect by the MK that retard the water absorption in the unfibred RPC made with metakaolin. This finding affirms what Ganesh and Murthy (2019) observed in their study. For the fibred specimens cured at ambient temperature, the increase in absorptions rates could be due to the presence of the fibre material as shown by Hiremath and Yaragal (2018) that is responsible for more pores within the concrete structure.

4.5.7.2 Sorptivity of RPC samples at 200°C

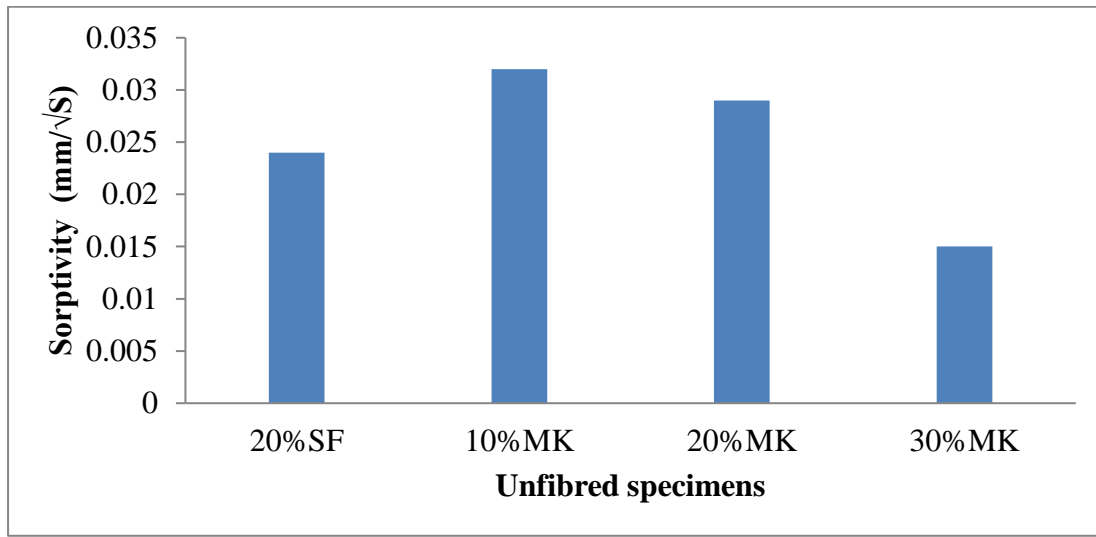


Figure 4.23: Sorptivity of unfibred specimens exposed to 200°C

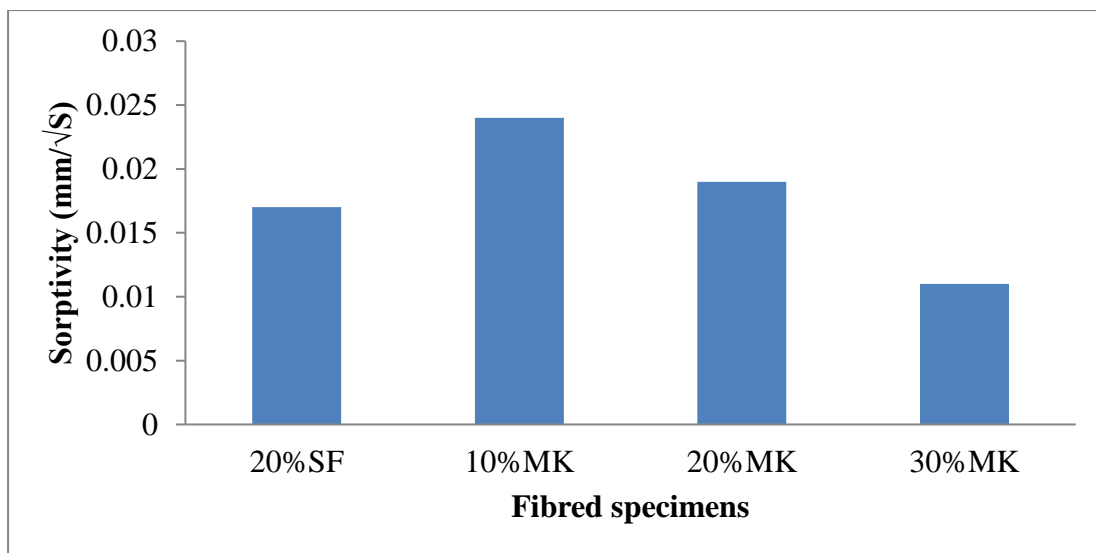


Figure 4.24: Sorptivity of fibred specimens exposed to 200°C

Figures 4.23 and 4.24 depict the sorptivity of unfibred and fibred RPC specimens exposed to 200°C. For unfibred (Figure 4.23), the initial water absorptions rate of 20% SF, 10% MK, 20% MK and 30% MK are 0.024, 0.032, 0.029 and 0.015 mm/√s. The reference specimens (20% SF) have lower water absorptions rate than 10% MK and 20% MK and

higher than 30% MK. It can be observed that the water absorptions rate decreases with the increase in MK content as a result of the filler effect. Compared with the RPC specimens cured at ambient temperature, the specimens exposed to 200°C had higher water absorptions rate. This is in agreement with what Hiremath and Yaragal (2018) who states that as the temperature of exposure increases, water absorptions rate increases.

Figure 4.24 indicates the sorptivity of fibred RPC with 20% SF, 10% MK, 20% MK and 30% MK as 0.017, 0.024, 0.019 and 0.011 mm/ \sqrt{s} respectively. The 20% SF (control sample) has lower water absorptions rate than 10% MK and 20% MK as a result of filler effect of the silica fume but lower than 30% MK. The lower water absorptions rate by the 30% MK could be due to the presence of more pozzolanic materials that enhance the pore filler effect of the MK. As compared with the specimens cured at ambient temperature, water absorptions rate increases with increase in temperature as explained by Hiremath and Yaragal (2018). However, the fibred RPC show lower water absorptions rate. The reason for the lower water absorptions rate could be due to the fact that at 200°C, more hydration products (C-S-H and C-A-H) are produced which help in refining pore system of the RPC and the fibre helps in achieving a better bond.

4.5.7.3 Sorptivity of RPC samples at 400°C

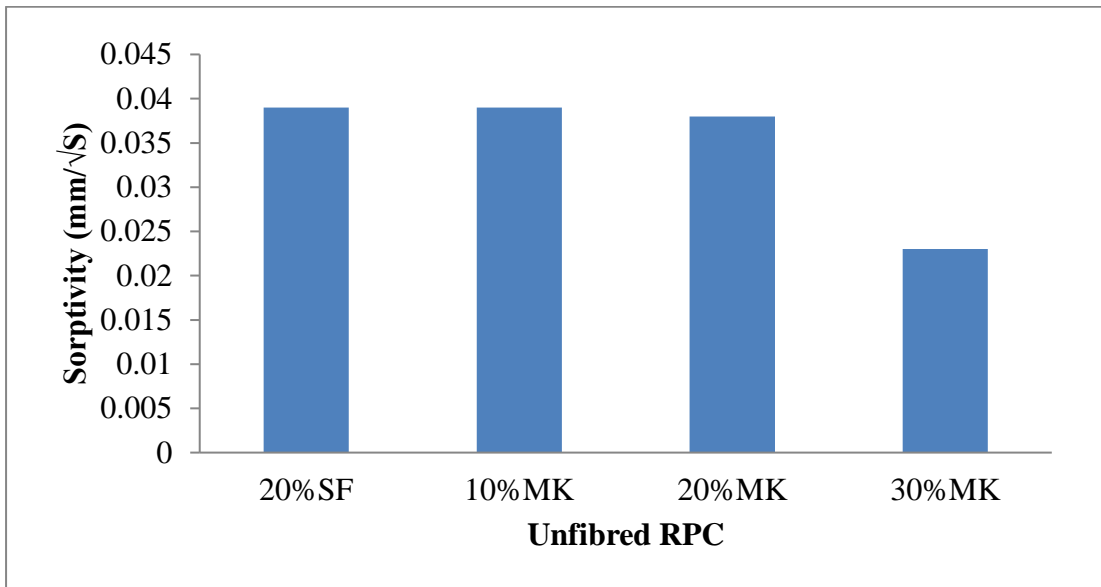


Figure 4.25: Sorptivity of unfibred specimens exposed to 400°C

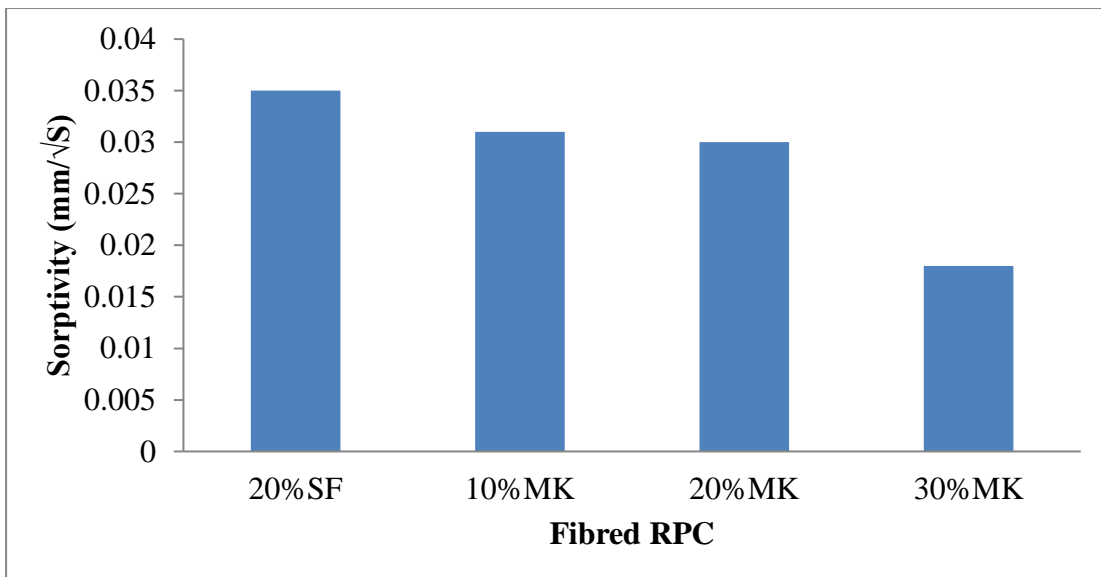


Figure 4.26: Sorptivity of fibred specimens exposed to 400°C

Figures 4.25 and 4.26 show the sorptivity of unfibred and fibred RPC exposed to 400°C.

Figure 4.25 (unfibred) indicates that the water absorptions rate of 20% SF, 10% MK, 20%

MK and 30% MK are 0.039, 0.039, 0.038 and 0.022 mm/ \sqrt{s} respectively. It can be observed that the reference specimen (20% SF) has similar water absorption rate with 10% MK while 20% MK and 30% MK recorded lower water absorption rate by 3.4% and 43.6% respectively than the control specimen. It can be concluded that water absorption rate decreases with increase in MK content at 400°C.

For the fibred specimens (shown in Figure 4.26) the water absorptions rate of 20% SF, 10% MK, 20% MK and 30% MK are 0.035, 0.031, 0.030 and 0.018 mm/ \sqrt{s} respectively. The reference specimen (20% SF) has higher water absorption rate than the 10% MK, 20% MK and 30% MK by 11.4%, 14.3% and 48.6% respectively. It can be observed that the specimens with MK have lower sorptivity than the reference and decreases with increase in MK content. Therefore, it can be concluded that the fibred specimens have lower water absorption rate than the unfibred specimens at 400°C. The reason for the lower water absorptions rate could be due to the fact that at 400°C there is relatively increase in strength compared to the specimens at ambient temperature, more hydration products (C-S-H and C-A-H) were produced which help in refining pore system of the RPC and the fibre helps in achieving a relatively better bond.

4.5.7.4 Sorptivity of RPC samples at 600°C

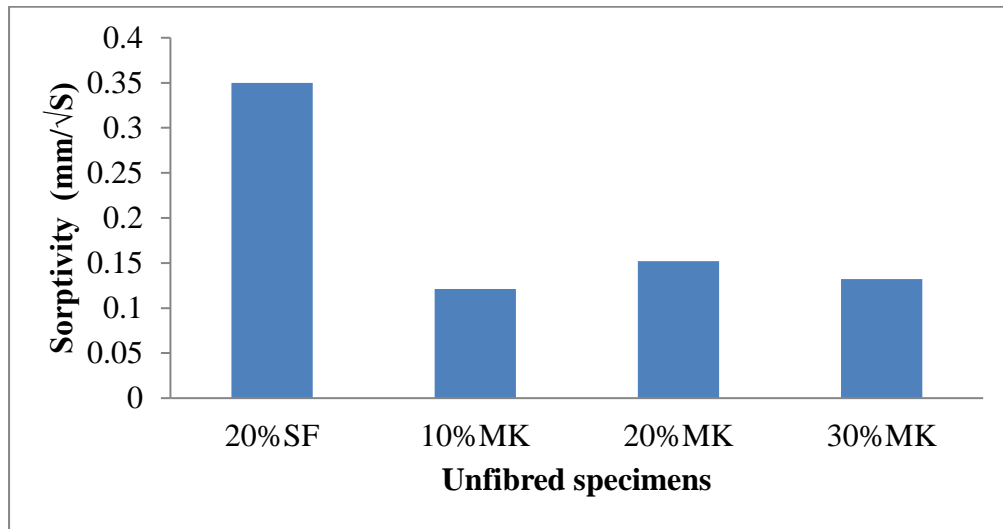


Figure 4.27: Sorptivity of unfibred specimens exposed to 600°C

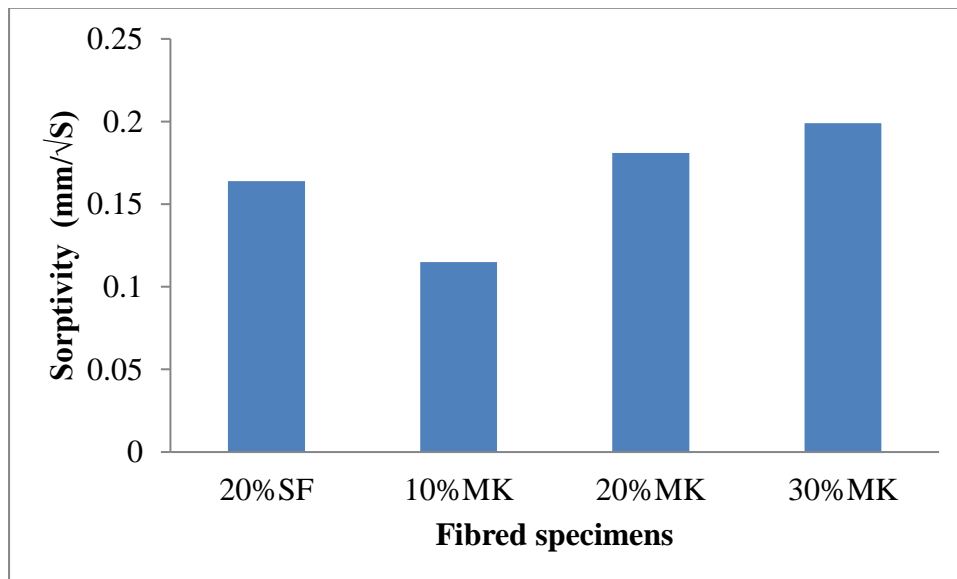


Figure 4.28: Sorptivity of fibred specimens exposed to 600°C

The sorptivity of unfibred and fibred RPC exposed 600°C are presented in Figures 4.27 and 4.28. It can be observed (as in Figure 4.27) that unfibred RPC specimens show the water absorptions rate of 20% SF, 10% MK, 20% MK and 30% MK at 600°C are 0.35, 0.121, 0.152 and 0.132 mm/√s respectively. From the results, it can be observed that the control

sample (20% SF) has higher water absorptions rate than the 10% MK, 20% MK and 30% MK by 65.4%, 56.6% and 62.3% respectively while 10% MK recorded the least water absorptions rate.

For the fibred specimens (shown in Figure 4.28), the water absorptions rate of 20% SF, 10% MK, 20% MK and 30% MK are 0.16, 0.115, 0.181 and 0.199 mm/ \sqrt{s} respectively. The 20% SF specimen has higher water absorptions rate than 10% MK by 28.1% and lower than 20% MK and 30% MK by 11.6% and 19.6% respectively. It can be inferred from the results that there is increase in water absorptions rate with the increase in temperature which supports the earlier findings of Hiremath and Yaragal (2018) that the water absorption rate of RPC increases with increase in temperature above 200°C.

4.5.7.5 Sorptivity of RPC samples at 800°C

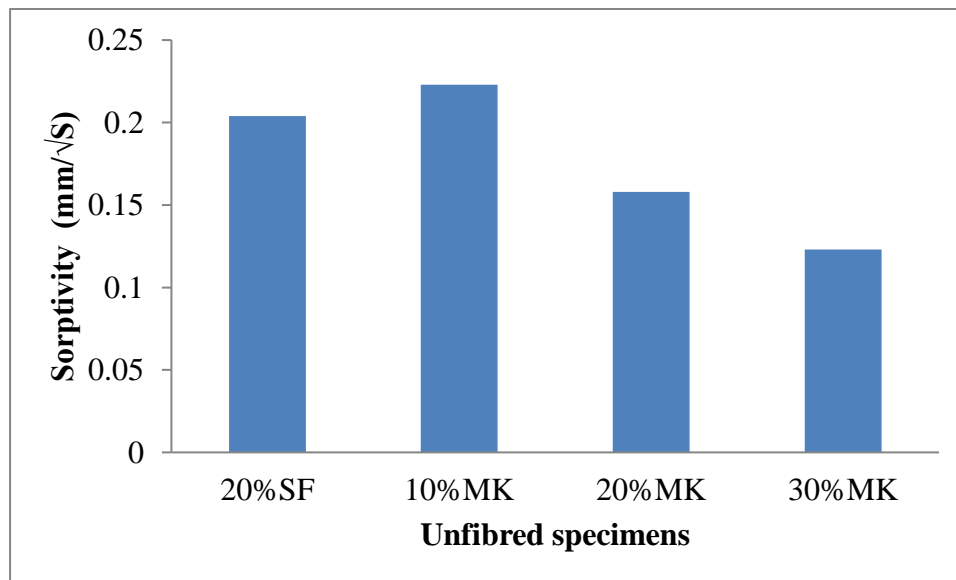


Figure 4.29: Sorptivity of unfibred specimens exposed to 800°C

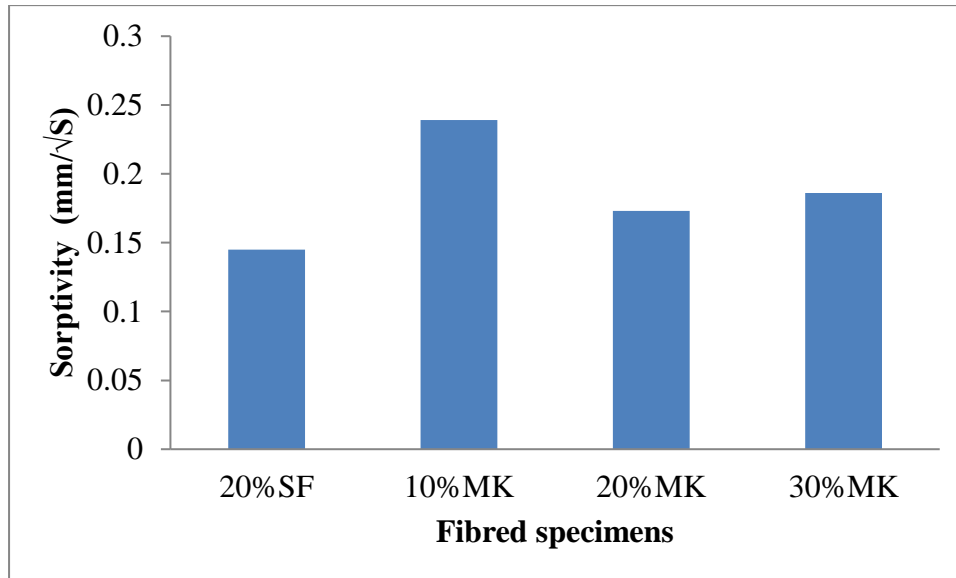


Figure 4.30: Sorptivity of fibred specimens exposed to 800°C

Figures 4.29 and 4.30 depict the sorptivity of unfibred and fibred RPC exposed to 800°C. Figure 4.29 (unfibred) shows the water absorptions rate of specimens with 20% SF, 10% MK, 20% MK and 30% MK are 0.204, 0.223, 0.158 and 0.123 mm/√s respectively. It can be noted from the results of the unfibred RPC that 20% SF recorded lower water absorption rate by 8.5% than 10% MK while it is higher by 22.5% and 39.7% than 20% MK and 30% MK respectively.

For the fibred specimens (shown in Figure 4.30) the water absorptions rate of 20% SF, 10% MK, 20% MK and 30% MK are 0.145, 0.239, 0.173 and 0.186 mm/√s respectively. The results show that 20% SF has lower water absorptions rate by 39.3%, 16.2% and 22% than 10% MK, 20% MK and 30% MK respectively. It can be noted that there is more increase in water absorptions rate at 800°C compare to other temperatures. Fibred RPC with 20% SF seems to have less pores within the concrete structure than specimens with MK. This finding is similar to what Hiremath and Yaragal (2018) reported in their study.

4.6

Microstructure Analysis of RPC

This section discusses the microstructure analysis of RPC produced with locally sourced unrefined MK at 27°C, 200 °C and 800 °C using X-Ray diffraction (XRD), Fourier transform infrared spectroscopy (FTIR) and scanning electron microscopy (SEM). The reason for selecting these temperatures is that at 27°C, the specimens were assessed for compressive strength where the reference (20% SF) was taken because of its highest strength compared with 20% MK (recording similar strength with the reference) and 10% MK. This is to enable scientific explanation for the varied behaviour. The results for the analysis are highlighted in Subsection 4.6.1, 4.6.2 and 4.6.3.

4.6.1 X-Ray diffraction (XRD) analysis

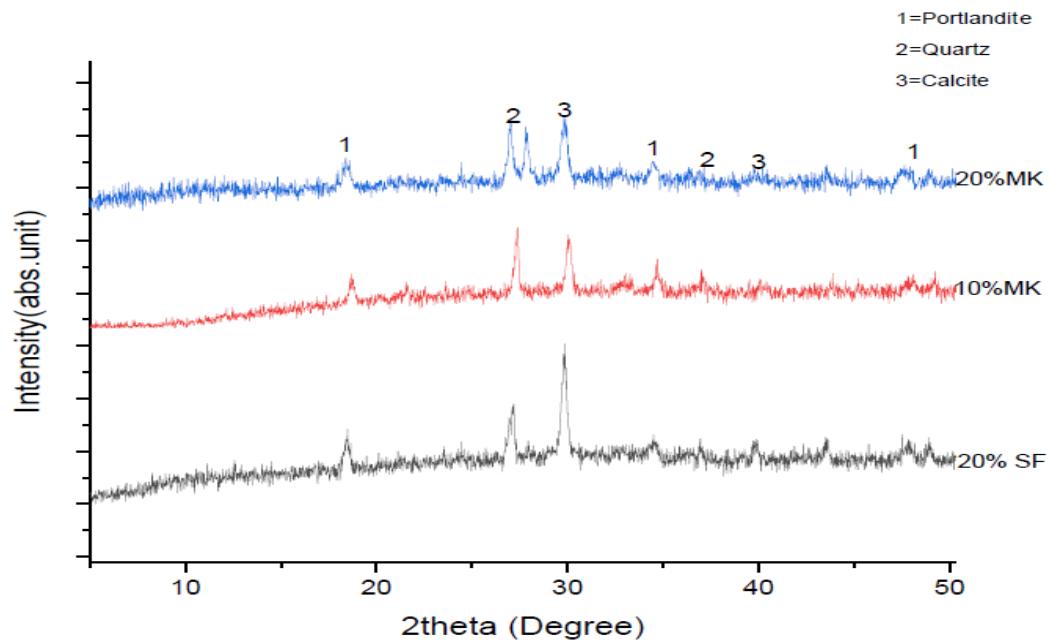


Figure 4.31 XRD patterns of RPC specimens at 27°C

Figure 4.31 shows the XRD patterns of RPC at 27°C. The crystalline phases present in the RPC are $\text{Ca}(\text{OH})_2$ (Portlandite) at $2\theta = 18.5^\circ$, quartz (at $2\theta = 27.5^\circ$) and calcite (at $2\theta = 30^\circ$). The diffraction peak of interest is that of Portlandite as its reduction is considered to

contribute to strength and durability properties. Compressive strength result at 28 days shows that 20% SF recorded higher strength followed by 20% MK while 10% MK recorded the least strength. It can be observed from Figure 4.31 that 20% MK have reduced diffraction peaks (Portlandite) than the 20% SF while 10% MK has lower peak than 20% SF. The reason for the higher peak than that of 20% MK could be due to agglomeration effect of silica fume at a percentage higher than 10% which prevented proper dispersion that can lead to the presence of un-reacted $\text{Ca}(\text{OH})_2$ as indicated in the UPV result for unfibred specimens. This effect of the SF has been demonstrated by Mitchell, Hinczak and Day (1998); Zhang, Zhang and Yan (2016).

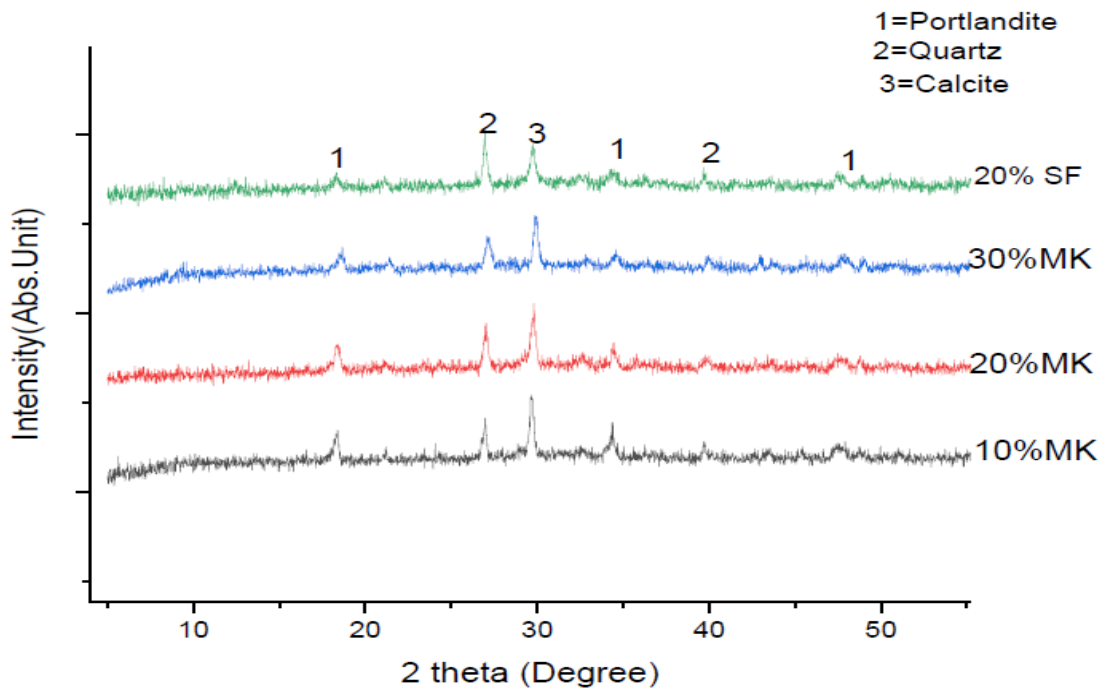


Figure 4.32 XRD patterns of RPC specimens at 200°C

Figure 4.32 shows the XRD patterns of RPC at 200°C. The crystalline phases present in the RPC are $\text{Ca}(\text{OH})_2$ (Portlandite) at $2\theta=18.5^\circ$, quartz (at $2\theta=27.5^\circ$) and calcite (at $2\theta=30^\circ$).

The Portlandite remains detectable at this temperature but at a lower peak than the one at ambient temperature. The lower peak of the Portlandite indicates further hydration at this temperature that leads to improvement in compressive strength in all the specimens. This is evident in the residual strength and UPV of RPC specimens exposed to 200°C.

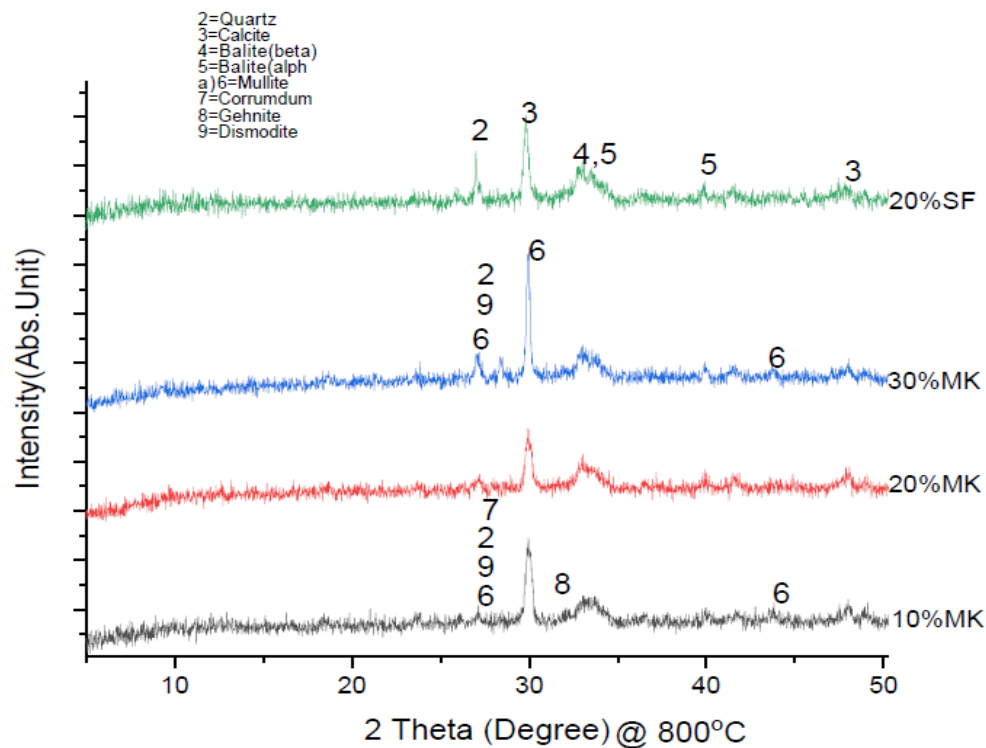


Figure 4.33 XRD patterns of RPC specimens at 800°C

Figure 4.33 shows the XRD patterns of RPC at 800°C. The crystalline phases present at 800°C quartz, calcite, belite, mullite, corrumdum, gahnite and dismodite. Portlandite has completely vanished at this temperature because of the decomposition of CH and water. There is also formation of ceramics minerals (refractories) which are useful in enhancing thermal resistance capacity. In the specimens with MK, the newly formed refractory phases

different from the reference (20% SF) are mullite (at $2\theta = 27^\circ, 30^\circ$ and 44°), corundum (at $2\theta = 27^\circ$), gahnite (at $2\theta = 32^\circ$) and dismodite (at $2\theta = 27^\circ$). The presence of the refractories in the RPC specimens containing MK is an indication of the higher residual strength compared to the control at 800°C .

4.6.2 Fourier transforms infrared spectroscopy (FTIR) results

This section discusses the analysis of RPC specimens by the use of FTIR method at ambient temperature, 200°C and 800°C after curing at 28 days. The essence of the FTIR studies is to identify different interactions of $\text{Ca}(\text{OH})_2$ with SiO_2 .

4.6.2.1 FTIR result at 27°C

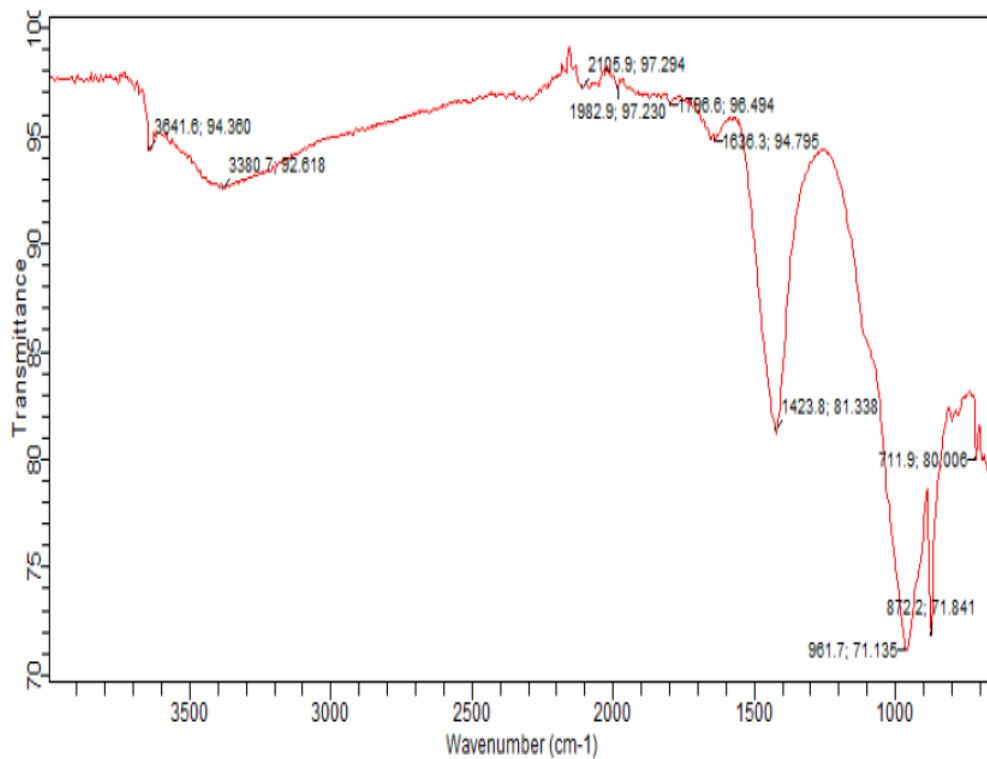


Figure 4.34: FTIR result of 20% SF

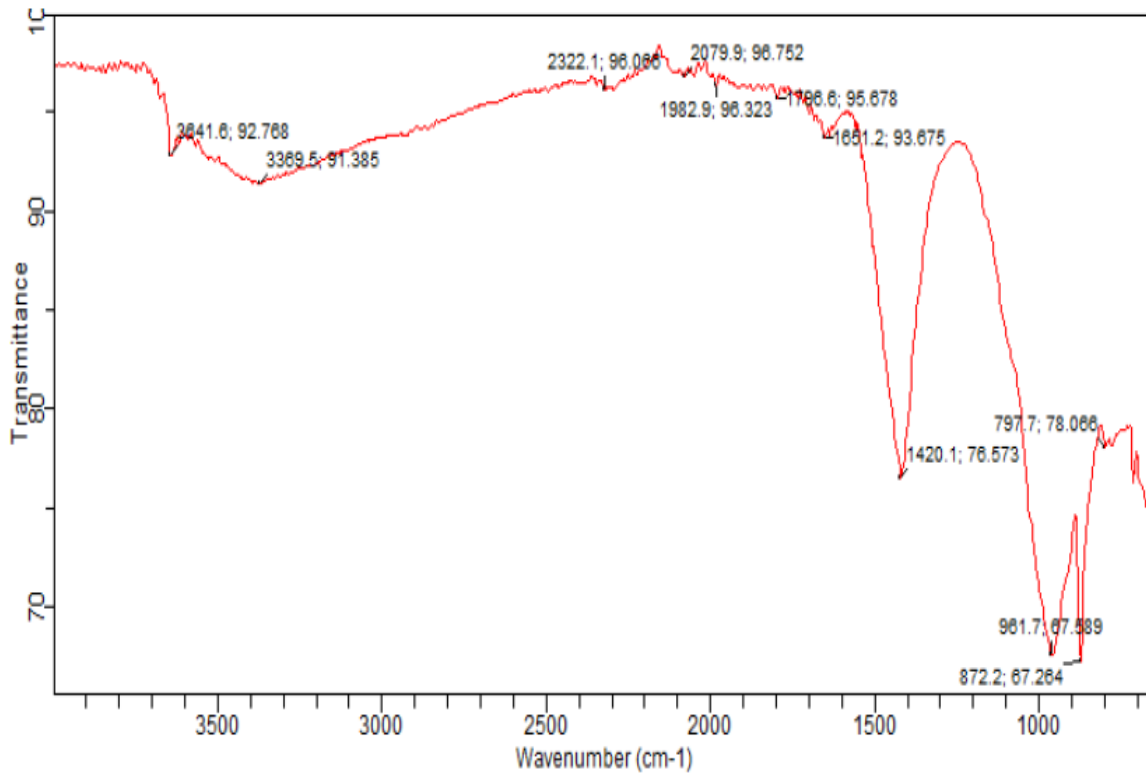


Figure 4.35: FTIR result of 20% MK

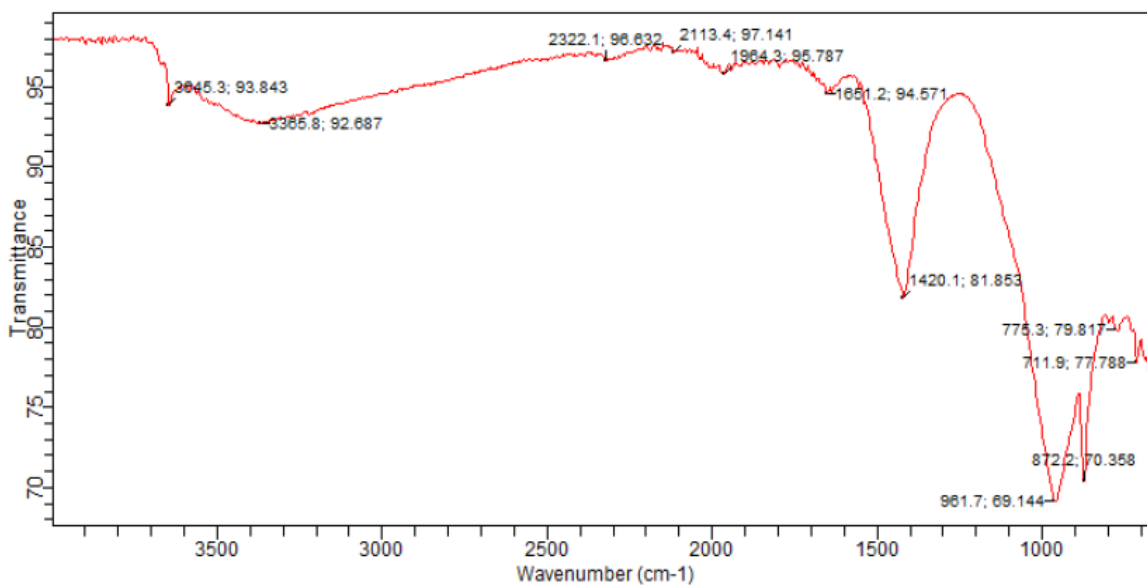


Figure 4.36: FTIR result of 10% MK

Table 4.2: Summary of FTIR results at 27°C

Specimen	Product	Wave number (cm ⁻¹)	Transmittance T (%)
20% SF	CSH gel	962	71.135
	CH	3642	94.360
	CaCO ₃	872/ 1424	71.84/ 81.338
20% MK	CSH gel	962	67.539
	CH	3642	92.768
	CaCO ₃	872/ 1420	67.264/ 76.573
10% MK	CSH gel	962	69.144
	CH	3645	93.843
	CaCO ₃	872/ 1420	70.358/ 81.853

Table 4.2 summarises the FTIR results (shown in Figures 4.34, 4.35 & 4.36) of RPC specimens cured at ambient temperature (27°C). The peaks at 3642 cm⁻¹ to 3645 cm⁻¹ are due to O-H stretching vibrations related to Ca(OH)₂ while the asymmetric Si-O stretching band (ν_3) at 962 cm⁻¹ indicates the formation of polymerized calcium silicate hydrates (C-S-H) which is the most significant infrared spectra. The C-O stretching (ν_3) and bending (ν_2) bands at 872 and 1420 to 1424 cm⁻¹ are assigned to calcite (CaCO₃). The intensity of the bands (associated with CaCO₃) is higher in 20% SF than 10% MK and 20% MK. The variation in intensities is due to the pozzolanic efficiency of the materials that influences the rate and amount of C-S-H formed as stated by Usman, Sam and Hussin (2016) while the frequencies of the Si-O-Si bands are an indication of the overall degree of polymerization of the silica network (Baltakys, Jauberthie, Siauciunas & Kaminskas, 2007). Generally, a lower frequency corresponds to a lower degree of polymerization. This finding validated

the XRD result shown in Figure 4.33 XRD where the 20% SF and 20% MK show similar peaks.

4.6.2.2 FTIR results at 200°C

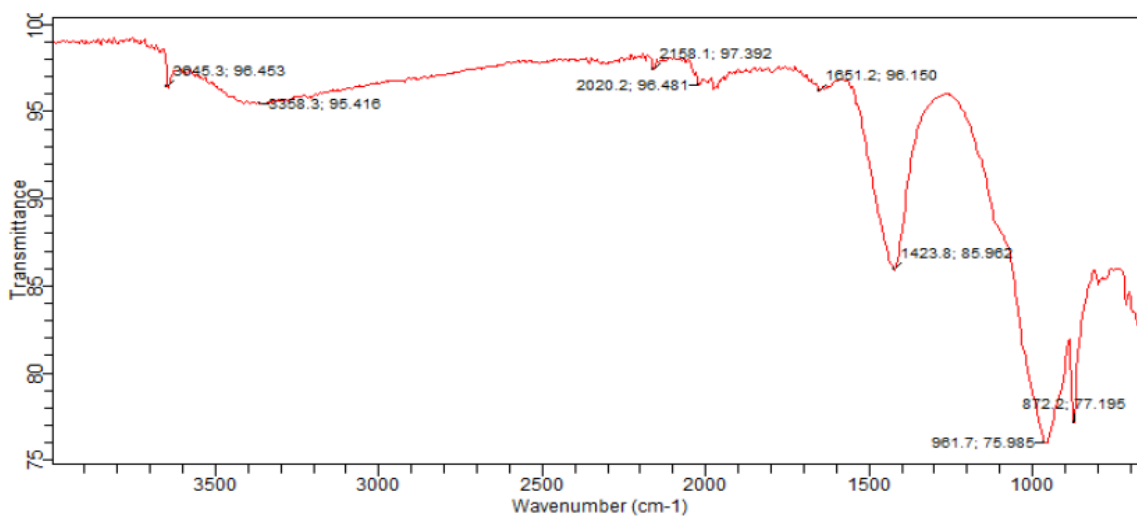


Figure 4.37 FTIR result of 20% SF\

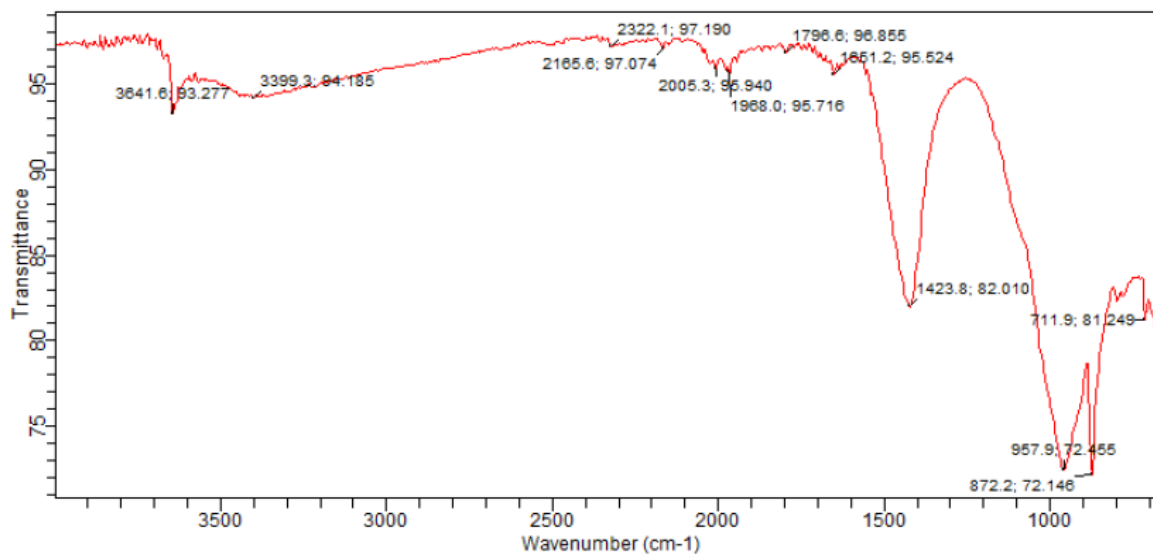


Figure 4.38: FTIR result of 10% MK

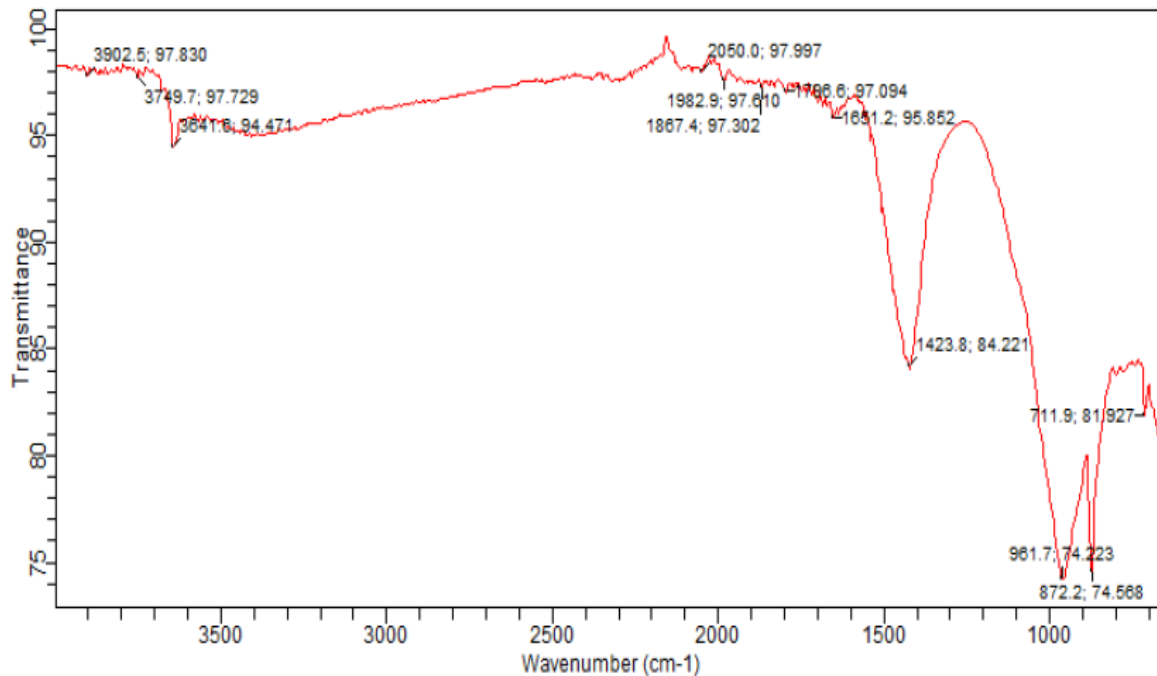


Figure 4.39: FTIR result of 20% MK

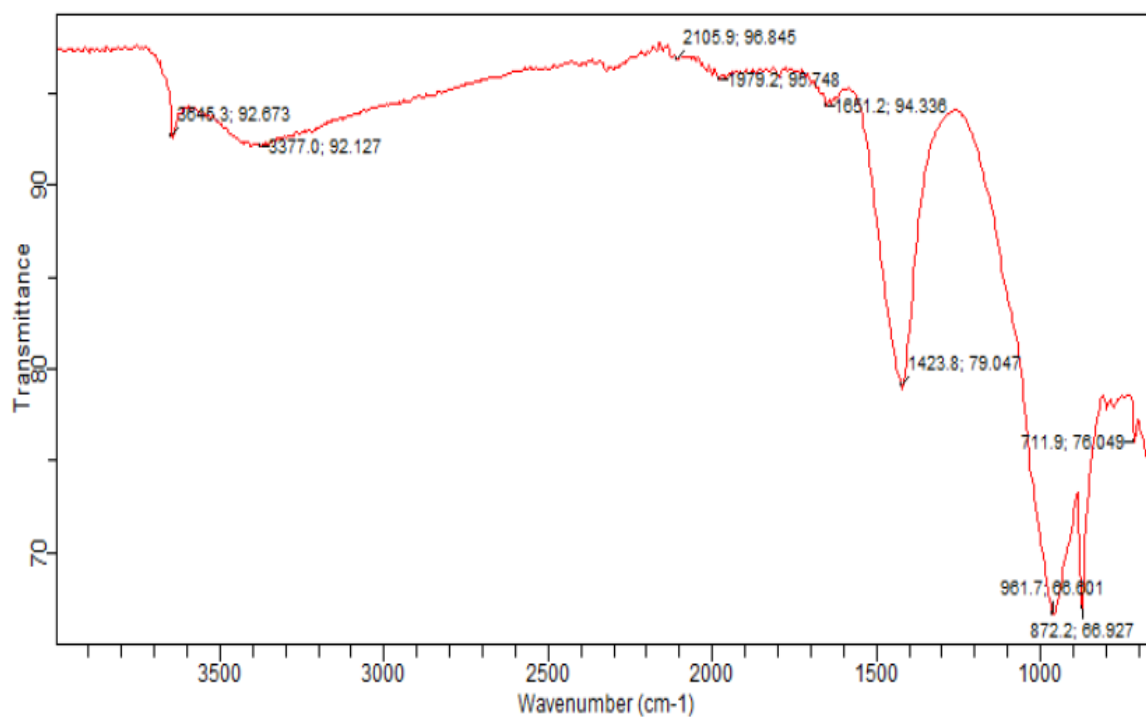


Figure 4.40: FTIR result of 30% MK

Table 4.3: Summary of FTIR results at 200°C

Specimen	Product	Wave number (cm ⁻¹)	Transmittance T (%)
20% SF	CSH gel	962	75.985
	CH	3645	96.453
	CaCO ₃	872/ 1424	77.195/ 85.962
10% MK	CSH gel	958	72.455
	CH	3642	93.277
	CaCO ₃	872/ 1424	72.146/ 82.010
20% MK	CSH gel	962	74.223
	CH	3642	94.471
	CaCO ₃	872/ 1424	74.668/ 84.221
30% MK	CSH gel	962	66.601
	CH	3645	92.673
	CaCO ₃	872/ 1424	66.927/ 79.047

Table 4.3 shows the summarised FTIR results (shown in Figure 4.37, 4.38, 4.39 & 4.40) of RPC specimens (20% SF, 10% MK, 20% MK & 30% MK) heated at 200°C. The peaks at 3642 cm⁻¹ to 3645 cm⁻¹ are due to O-H stretching vibrations related to Ca(OH)₂ while the asymmetric Si-O stretching band (ν_3) at 958 cm⁻¹ to 962 cm⁻¹ indicate the formation of polymerized calcium silicate hydrates (C-S-H) which is the most significant infrared spectra. The C-O stretching (ν_3) and bending (ν_2) bands at 872 and 1424 cm⁻¹ are assigned to calcite (CaCO₃). The 20% SF and 20% MK recorded similar intensity (75.985% & 74.223%) of the band while 30% MK recorded the lowest (66.927%). The variation in the intensities is due to the pozzolanic efficiency of the materials used in terms of rate and

amount of C-S-H formed as reported by Usman, Sam and Hussin (2016) while the frequencies of the Si–O–Si bands are an indication of the overall degree of polymerization of the silica network (Baltakys, Jauberthie, Siauciunas & Kaminskas, 2007). Generally, a lower frequency corresponds to a lower degree of polymerization. This confirmed the XRD patterns in Figure 4.34 where the 20% SF and 20% MK show similar and reduced peak than any 10% MK and 30% MK.

4.6.2.3 RFTIR results at 800°C

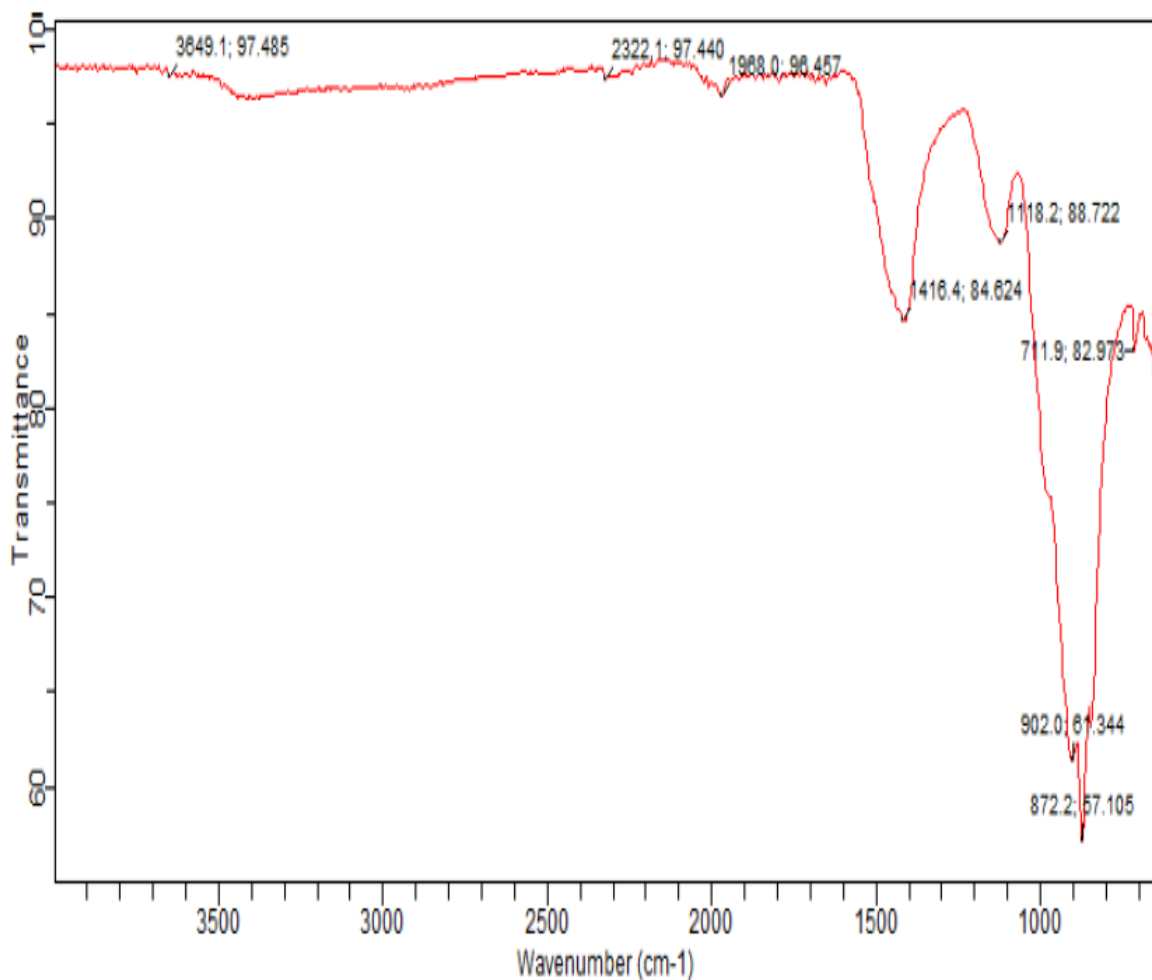


Figure 4.41: FTIR result of 20% SF

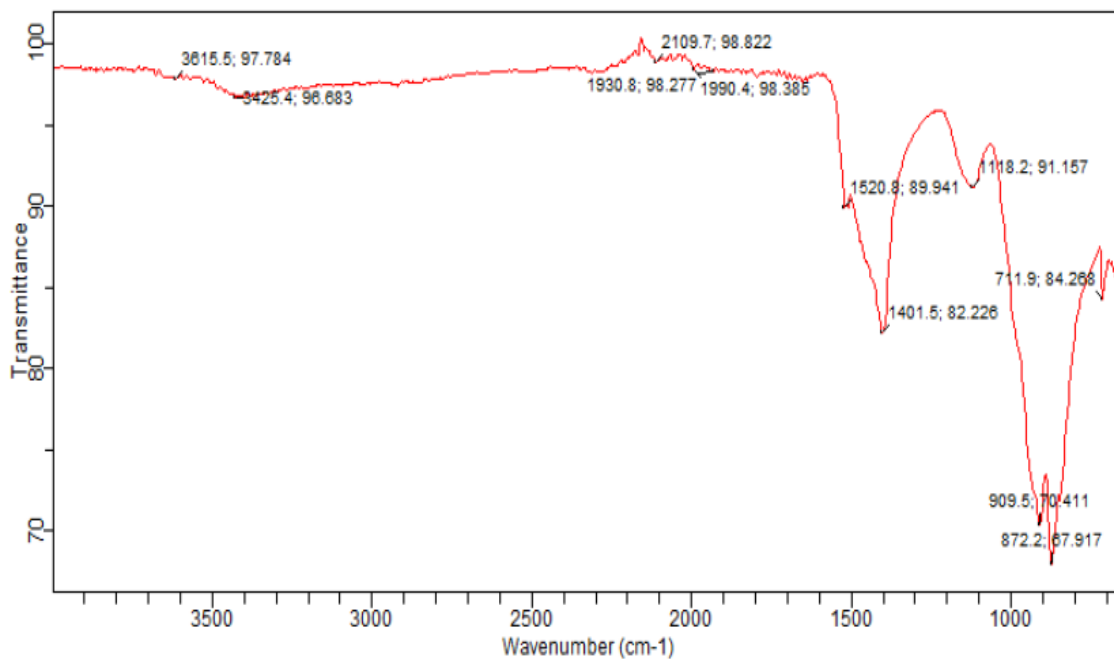


Figure 4.42: FTIR result of 10% MK

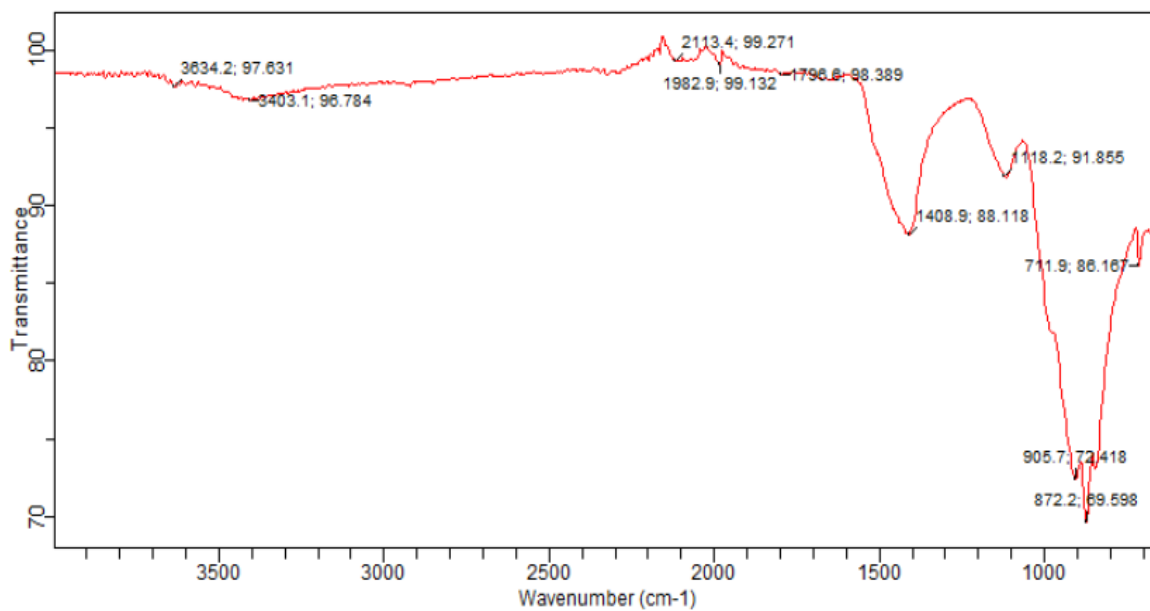


Figure 4.43: FTIR result of 20% MK

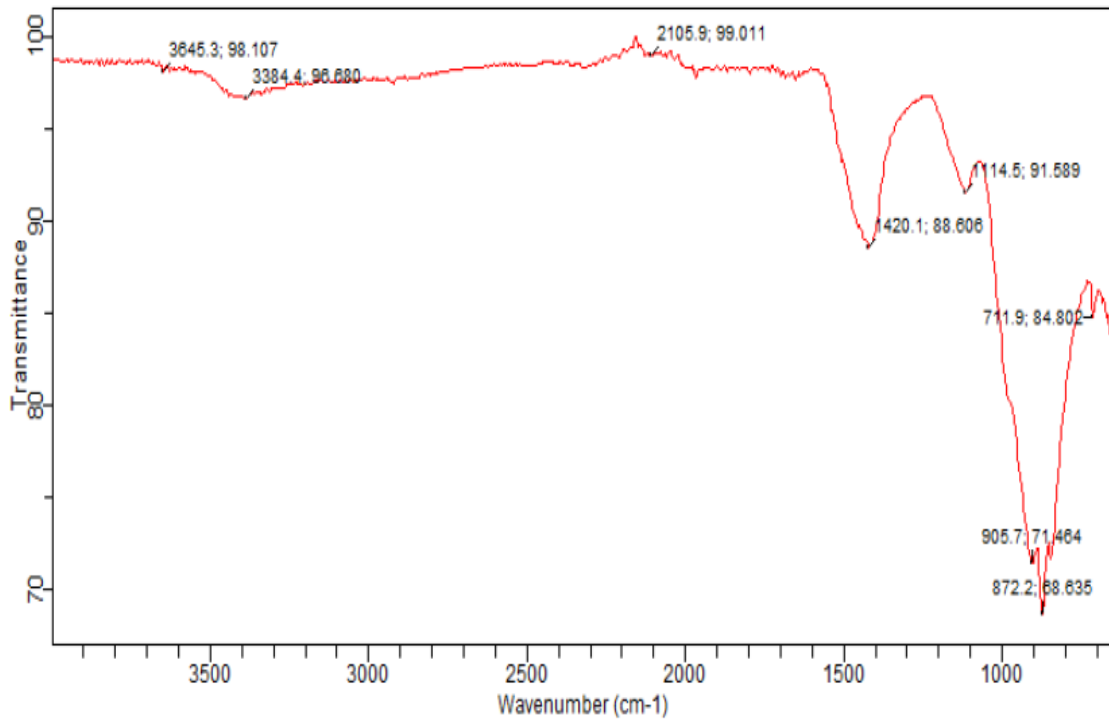


Figure 4.44: FTIR result of 30% MK

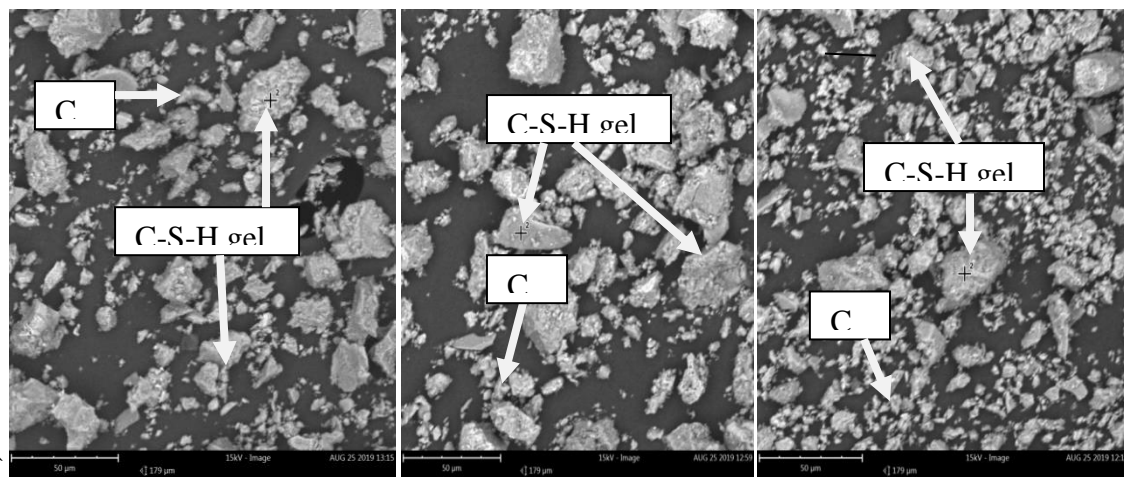
Table 4.4: Summary of FTIR results at 800°C

Specimen	Product	Wave number (cm ⁻¹)	Transmittance T (%)
20% SF	C ₂ S	902	61.344
	CaCO ₃	872/ 1416	57.105/ 84.624
10% MK	C ₂ S	910	70.411
	CaCO ₃	872/ 1402	67.917/82.226
20% MK	C ₂ S	906	72.418
	CaCO ₃	872/ 1409	69.598/ 88.118
30% MK	C ₂ S	906	71.464
	CaCO ₃	872/ 1420	68.635/ 88.606

Table 4.4 shows the summarised FTIR results (shown in Figure 4.41, 4.42, 4.43 & 4.44) of RPC specimens (20% SF, 10% MK, 20% MK & 30% MK) heated at 800°C. At this temperature of exposure, a new absorption band surfaced at 902 cm^{-1} to 910 cm^{-1} and the band assigned to CSH disappeared as can be observed from the Figures. The disappearance of the C-S-H is an indication of decomposition of CSH as reported by Usman, Sam and Hussin (2016). This is evident in the XRD patterns where the peaks of re-crystallization products of CSH resurface at 800°C.

4.6.3 Scanning electron microscopy (SEM) analysis

4.6.3.1 SEM of RPC specimens exposed to 27°C



(a) 20% SF

(b) 20% MK

(c) 10% MK

Figure 4.45: Scanning electronic microscopy (SEM) of RPC specimens at 27°C

Figure 4.45 shows the SEM images of RPC specimens at ambient temperature. The image shows that CSH and crystal of CH are visible in the microstructure but more pronounced in 20% SF (a) and 20% MK (b). This confirms the higher strength recorded by 20% SF and 20% MK RPC specimens.

4.6.3.2 SEM of RPC specimens exposed to 200°C

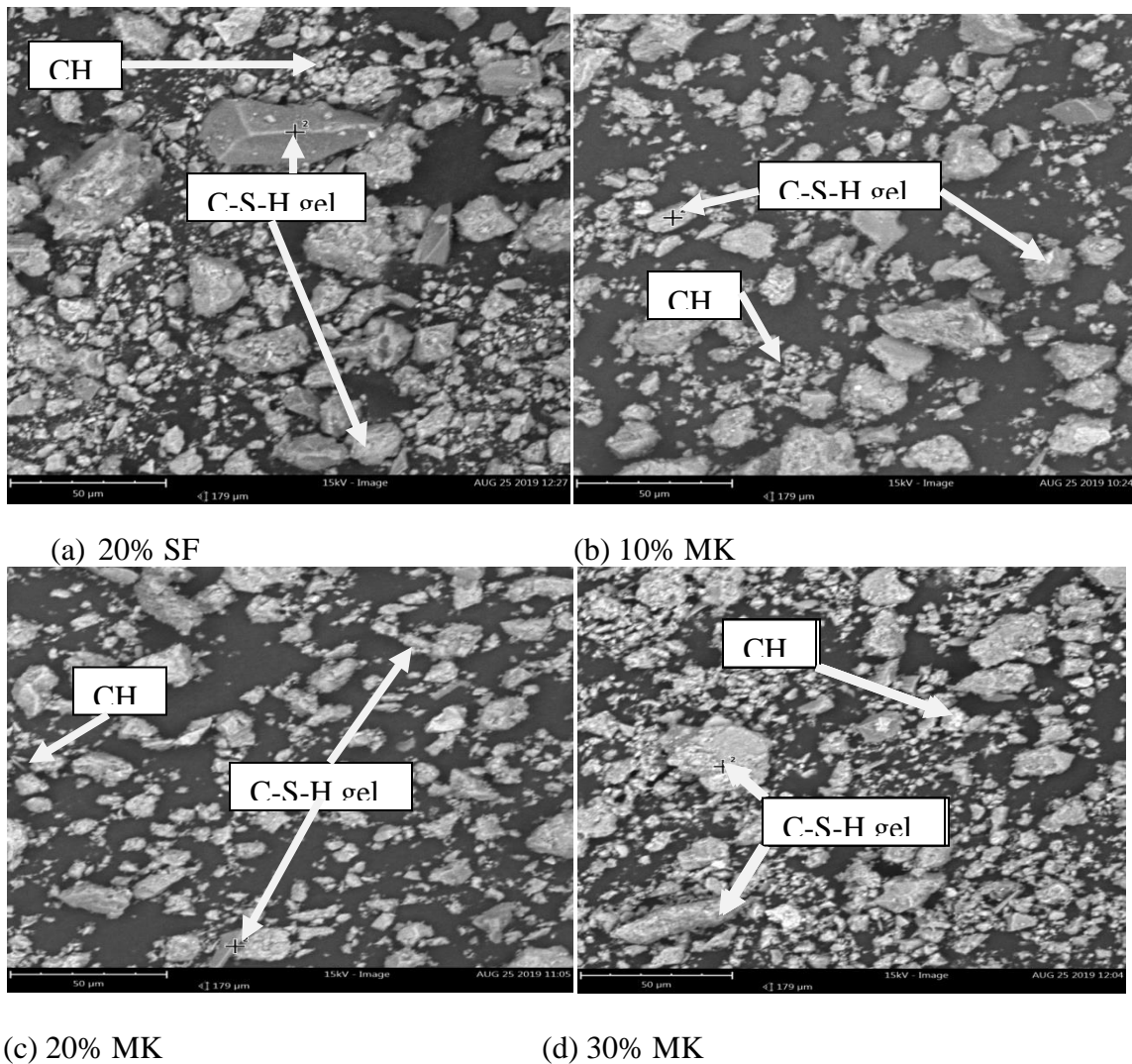


Figure 4.46: Scanning electronic microscopy (SEM) of RPC specimens at 200°C

Figure 4.46 shows the SEM images of RPC specimens exposed to 200°C. The image shows that CSH and crystal of CH are visible in the microstructure. A higher strength is observed in all the RPC specimens at this temperature. The increase in the compressive strength could be due to un-reacted SF and MK reacted with cement and hydrates: SO_2 serves as catalyst and accelerates the hydration reaction by producing CSH which enhances the

compressive of the RPC (Hiremath & Yaragal 2018). This is evident in the UPV and XRD results of the specimens.

4.6.3.3 SEM of RPC exposed to 800°C

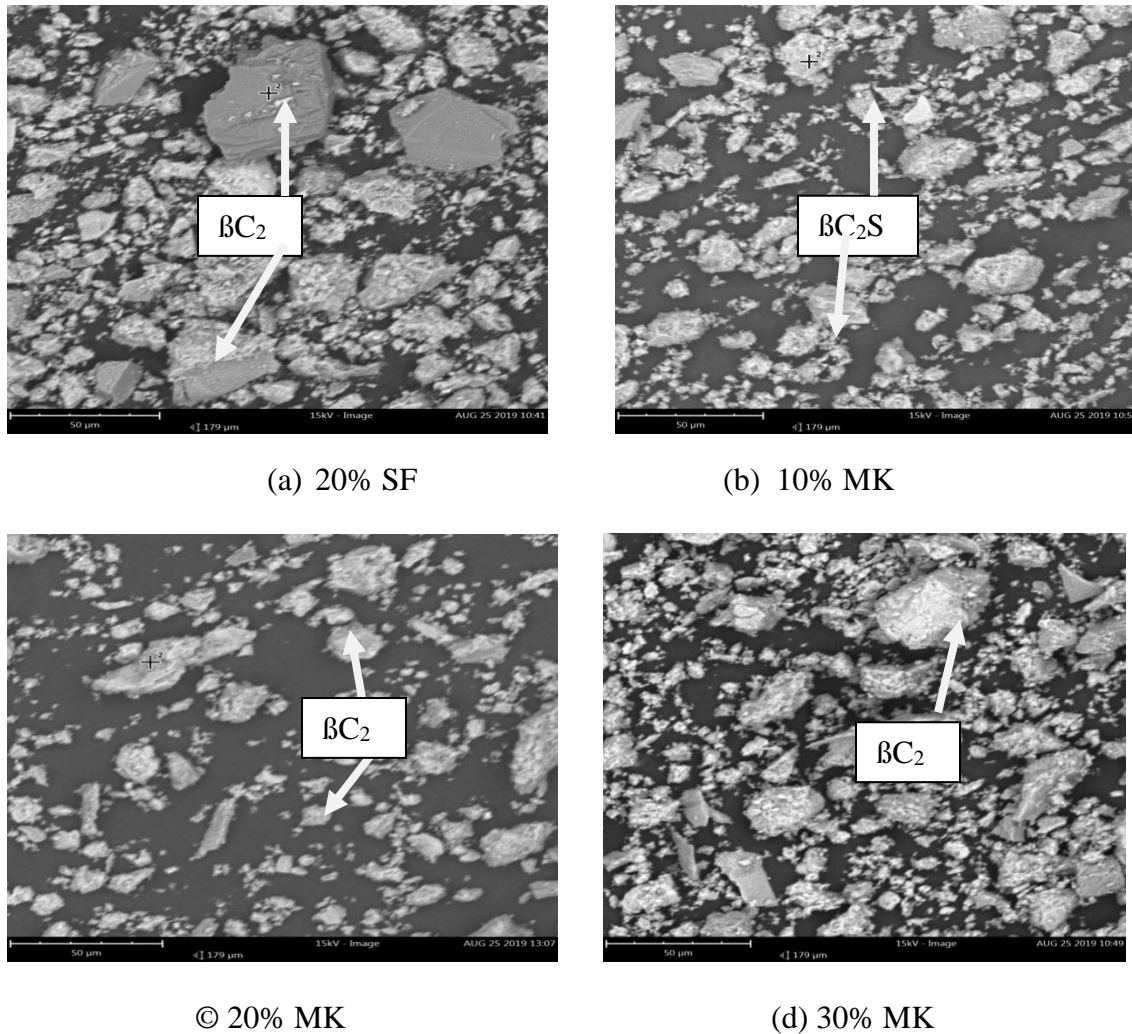


Figure 4.47: Scanning electronic microscopy (SEM) of RPC specimens at 800°C
Figure 4.47 shows the SEM images of RPC specimens exposed to 800°C. At this temperature the CSH disappeared and new images appeared indicating the decomposition of CSH and formation of $\beta\text{C}_2\text{S}$. This is consistent with the XRD and UPV. The result also agreed with the findings of Usman, Sam and Hussin (2016) and Hager (2013) who stated that at temperature up to 800°C decomposition of C-S-H and formation of $\beta\text{C}_2\text{S}$ occur.

Therefore, the loss of strength observed at higher temperatures may be attributed to the loss of bound water, increased porosity, and, consequently, increased permeability.

4.7 Models Development for the Optimised RPC Samples

This section presents the models development for the RPC samples cured using the conventional methods under ambient environment. The procedures of how the models were developed were presented in Chapter 3 (sub-section 3.3).

4.7.1 Model development for the prediction of compressive strength of RPC with optimised proportions.

Percentage of metakaolin and fibre were used as independent variables while compressive strength was used as dependent variable. After inserting all the variables in the Datafit software, about 250 models were generated by the software out of which the model presented in equation 4.1 was chosen based on the highest and lowest R² and P-values.

$$f'_c = 67.825 - 1.91MK + 0.167MK^2 + 0.00385MK^3 - 65.8GIW \text{-----} 4.1$$

Where:

f'_c = Compressive strength (N/mm²)

MK= % metakaolin

GIW= % gear inner wire

The R² and P-value of the model are 0.93 and 0.04 respectively as can be seen in Appendix H. The R²-value shows the degree of variation of the data to the proposed model while P-value shows the statistical significance of the model. For a P-value ≤0.05, the relationship is significant. This shows that there is significant relationship between independent and

dependent variables that were used in developing the model which is presented graphically in Figure 4.21

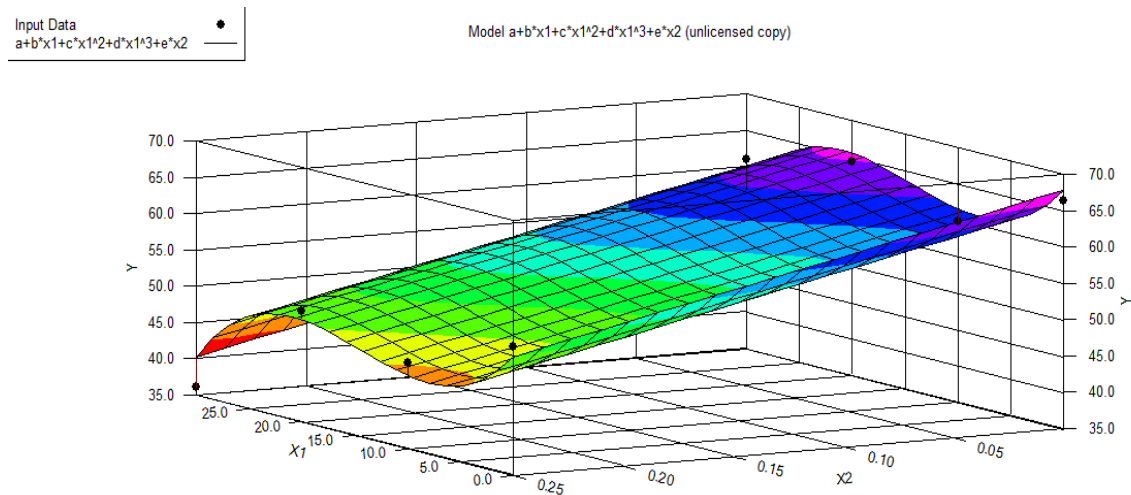


Figure 4.48: Model plot for compressive strength

4.7.1.1 Validation of compressive strength model

The validation was achieved through experimental and statistical methods. Two sets of concretes were produced for the experimental work using (7.5% MK+0.3% steel fibre) and (15% MK+0.2% steel fibre). At the end of 28 days curing period, the RPC specimens were subjected to compressive test and the results are presented in table 4.5. It can be observed from Table 4.5 that the experimental results are close to the estimated values with minimum and maximum percentage errors as -0.17 and 9.74 respectively which are within the range of 90% confidence level.

Table 4.5: Experimental versus predicted compressive strength of RPC

Sample	Input data		Output data		Percentage (%) error
	% of MK	% of fibre	Experimental compressive strength (N/mm ²)	Estimated compressive strength (N/mm ²)	
1.	7.5	0.3	55.3	61.3	9.74
2.	25	0.1	64.4	63.8	-0.17

4.7.1.2 Model development for the prediction of flexural strength of RPC with optimised proportions

The percentage of MK and fibre (GIW) were used as independent variables while flexural strength was used as dependent variable. After putting all the variables in the Datafit software, there were about 250 models generated by the software out of which the model presented in equation 4.2 was chosen based on the highest value of R² and lowest P-value.

$$f'_f = 10.25 + 0.51875MK - 0.0219MK^2 + 21.7GIW \quad \text{-----} \quad 4.2$$

Where:

f'_f = Flexural strength (N/mm²)

MK= % metakaolin

GIW= % gear inner wire

The R² and P-value of the model are 0.98 and 0.03 respectively as can be seen in Appendix H. R²-value relate to the degree of function of the data to the proposed model while P-value indicates the statistical significance of the model. For a P-value ≤0.05, the relationship is significant. This shows that there is significant relationship between independent and

dependent variables that were used in developing the model and is presented graphically in Figure 4.49.

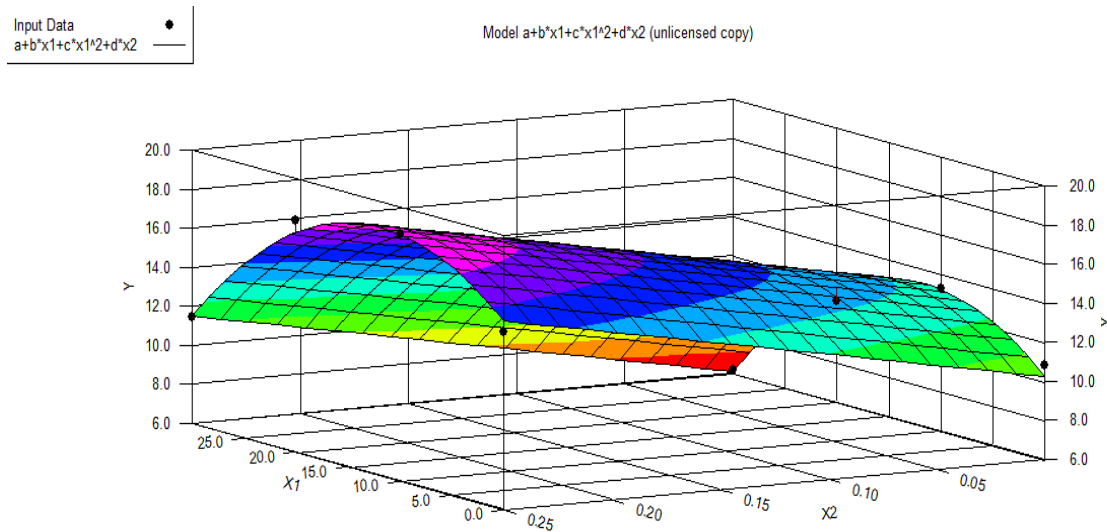


Figure 4.49: Model plot for flexural strength

4.7.1.3 Validation of flexural strength model

The validation was carried out through experimental and statistical method. Two sets of concretes were produced for the experimental work using 7.5% MK+0.3% steel fibre, and 15% MK+0.2% steel fibre. At the end of 28 days curing period, the RPC specimens were subjected to flexural strength test and the results are presented in table 4.6. It can be observed from the table that the experimental results are much closed to the estimated values with minimum and maximum percentage errors as -3.8 and 1.7 respectively that is within the range of 90% confidence level.

Table 4.6: Experimental versus predicted flexural strength of RPC

Sample	Input data		Output data		Percentage (%) error
	% of MK	% of fibre	Experimental flexural strength (N/mm ²)	Estimated flexural strength (N/mm ²)	
1.	7.5	0.3	20.2	19.5	-3.8
2.	15	0.2	17.14	17.44	+1.7

4.7.1.4 Model development for the prediction of water absorption capacity of RPC with optimised proportions

For the water absorption capacity model, the percentage of the MK and fibre (GIW) were also used as independent variables while water absorption capacity was used as dependent variable. After inserting all the variables in the Datafit software, about 250 models were generated by the software out of which the model presented in equation 4.3 was chosen based on R² and P-value.

$$A'_c = 3 - 0.0708MK + 0.00425MK^2 - 0.0000667MK^3 + 0.8GIW \text{ ----- } 4.3$$

Where:

A'_c =Water absorption capacity (%)

MK= % metakaolin

GIW= % gear inner wire

The R² and P-value of the model are 0.95 and 0.02 respectively as can be seen in Appendix H. For a P-value ≤0.05, the relationship is significant. This shows that there is significant relationship between independent and dependent variables that were used in developing the model which is presented graphically in Figure 4.50.

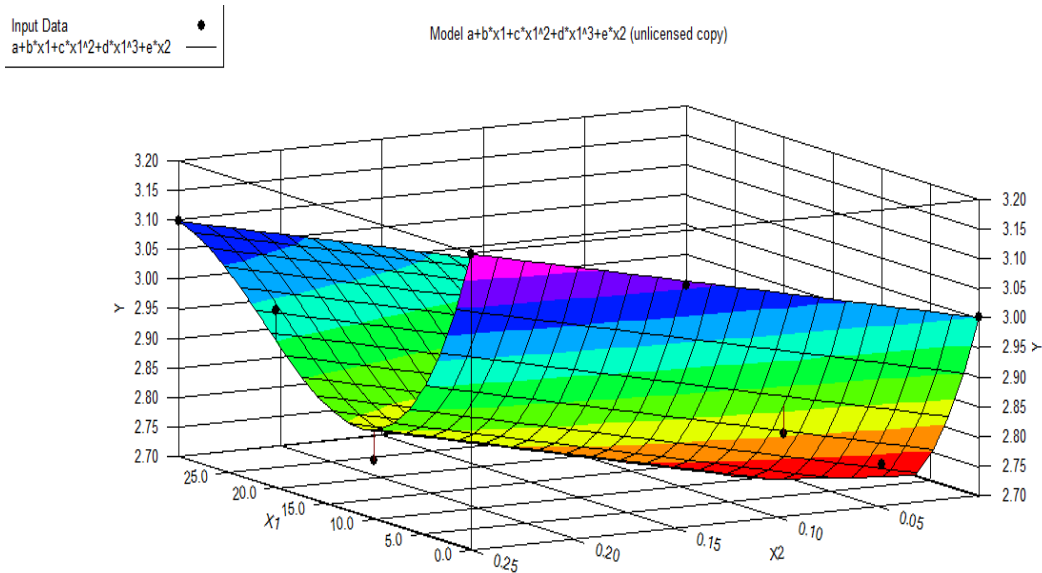


Figure 4.50: Model plot for water absorption capacity

4.7.1.5 Validation of water absorption capacity model

The validation was achieved through experimental and statistical method. Two sets of concretes were produced for the experimental work using 7.5% MK+0.3% steel fibre, and 15% MK+0.2% steel fibre. At the end of 28 days curing period, the RPC specimens were subjected to water absorption capacity test and the results are presented in Table 4.7. It can be observed from the table that the experimental results are closed to the estimated values with minimum and maximum percentage errors as -2.8 and 4.6 respectively that are within the range of 90% confidence level.

Table 4.7: Experimental versus predicted absorption of RPC

Sample	Input data		Output data		Percentage (%) error
	% of MK	% of fibre	Experimental absorption capacity (%)	Estimated absorption capacity (%)	
1.	7.5	0.3	3	2.9	-2.8
2.	15	0.2	2.7	2.8	+4.6

4.7.2 Limitations of the models

- (i) The models could not be used for other pozzolanic materials
- (ii) It could not be used for heat treated RPC
- (iii) It could not be used for RPC produced with other types of fibres

CHAPTER FIVE

5.0 SUMMARY, CONCLUSIONS AND RECOMMENDATIONS

5.1 Summary

The research evaluated the suitability of locally sourced unrefined MK and GIW for the production of reactive powder concrete (RPC). The highlights of the major findings are as follow:

- i. Chemical compositions of unrefined MK ($\text{SiO}_2 + \text{Al}_2\text{O}_3 + \text{Fe}_2\text{O}_3$) are 88.29%, LOI is 1.8%, SAI is 0.87 and surface area is $509 \text{ m}^3/\text{kg}$.
- ii. Mix proportion of the RPC using 20% unrefined MK and 0.25% GIW has been developed
- iii. Unrefined metakaolin and gear inner wires have been found to be suitable in the production of RPC.
- iv. Reactive powder concrete made with 20% SF and 0.25% GIW has a maximum compressive strength of up to 74.9 N/mm^2 , tensile strength of 5.1 N/mm^2 and a flexural strength of 18.3 N/mm^2 .
- v. Reactive powder concrete made with 20% Unrefined MK 0.25% GIW has a maximum compressive strength of 72.5 N/mm^2 , tensile 7.1 N/mm^2 and flexural strength of 22.3 N/mm^2 .
- vi. Reactive powder concrete with 20% MK has better performance in terms of residual strength, water absorption capacity and ultrasonic pulse velocity (UPV) when exposed to elevated temperatures.

- vii. At ambient temperature, the fibred RPC specimens have lower rate of water absorption than the fibred ones while at 200°C and above, the fibred specimens show lower rate of water absorption than the unfibred.
- viii. At higher temperature of 800°C, all RPC specimens experienced drastic reduction in strength but 20% MK and 30% MK showed relatively better strength retention capacity.
- ix. The strength retention capacity of the 20% MK and 30% MK is attributed to the formation of some refractories as shown by the XRD results compared to the 20% SF and 10% MK specimens.
- x. The maximum compressive strength, flexural strength and water absorption capacity estimated by the DataFit analysis showed fairly good agreement with the test data.

5.2 Conclusions

Based on the outcomes of the research, the following conclusions are drawn:

- i. The unrefined metakaolin and gear inner wires can be used in the production of RPC.
- ii. Unrefined MK of up to 20% by weight of cement can be used to produce RPC with 72.5 N/mm² compressive strength and using 0.25% GIW by weight of concrete can give tensile strength and flexural strength of 7.1 N/mm² and 22.3 N/mm² respectively.
- iii. Reactive powder concrete with 20% MK performed better than 20% SF, 10% MK and 30% MK in terms of residual strength, absorption and ultrasonic pulse velocity (UPV) when exposed to elevated temperatures.

- iv. Ultrasonic pulse velocity can be used to predict residual strength and water absorption capacity of RPC.
- v. Reactive powder concrete made with locally sourced unrefined MK and GIW has more resistance to sorptivity than the one made with SF.
- vi. It is concluded that at higher temperature of 800°C, all RPC specimens experienced drastic reduction in strength but specimens containing 20% MK and 30% MK showed relatively better strength retention capacity. The strength retention capacity of the 20% MK and 30% MK is attributed to the formation of some refractories as shown by the XRD results compared to the 20% SF and 10% MK specimens.
- vii. Moreover, the use of the unrefined MK and GIW can lead to production of strong, durable, cheaper and sustainable RPC by cutting down importation cost of both silica fume and fibre materials.

5.3

Recommendations

- i. Nigerian unrefined MK can be used in making RPC as mineral admixture.
- ii. Gear inner wire can be used to reinforce RPC elements exposed to high tensile and flexural strengths, e.g., beams.
- iii. Reactive powder concrete produced from unrefined MK can be used in structures to be exposed to elevated temperatures less than 800°C.
- iv. An optimised compressive strength of RPC made from unrefined MK can be predicted using the equation

$$f'_c = 67.825 - 1.91MK + 0.167MK^2 + 0.00385MK^3 - 65.8GIW$$

- v. An optimised flexural strength of RPC made from unrefined MK can be predicted using the equation

$$f'_f = 10.25 + 0.51875MK - 0.0219MK^2 + 21.7GIW$$

- vi. An optimised water absorption capacity of RPC made from unrefined MK can be predicted using the equation

$$A'_c = 3 - 0.0708MK + 0.00425MK^2 - 0.0000667MK^3 + 0.8GIW$$

5.4 Recommendations for Further Study

- i. Optimised models for the prediction of other durability properties of RPC (e.g., exposed to aggressive media, like sulphate environment) cured conventionally and made from locally sourced unrefined MK should be developed.
- ii. An optimised model for the prediction of mechanical and durability properties of RPC (under pressure and heat treatment) made from locally sourced unrefined MK should be developed.
- iii. Durability properties of RPC made from unrefined MK exposed to sulphate and acid environment using other parameters such as Sorptivity, permeability, etc. should be studied.
- iv. Other locally sourced pozzolanic materials other than MK e.g., rice husk ash, saw dust, etc. should be used in the production of RPC

5.5 Contribution to Knowledge

Outcomes of the research have established the following contributions to knowledge:

- i. An optimised compressive strength of RPC made from unrefined MK can be predicted using the equation

$$f'_c = 67.825 - 1.91MK + 0.167MK^2 + 0.00385MK^3 - 65.8GIW$$

- ii. An optimised flexural strength of RPC made from unrefined MK can be predicted using the equation

$$f'_f = 10.25 + 0.51875MK - 0.0219MK^2 + 21.7GIW$$

- iii. An optimised water absorption capacity of RPC made from unrefined MK can be predicted using the equation

$$A'_c = 3 - 0.0708MK + 0.00425MK^2 - 0.0000667MK^3 + 0.8GIW$$

- iv. That the use of 20% unrefined MK in the production of RPC has been found to be optimum.
- v. The use of 0.25% GIW has been found to enhance tensile and flexural strengths of RPC produced using unrefined MK.

References

- Abbas, A.N. (2014). Experimental Study on Reactive Powder and Normal Concrete Rectangular Beams under Different Loading Rate, *International Journal of Engineering and Advance Technology Studies*, 2(2): 1-10, www.ea-journals.org, accessed 05/06/2016 at 02:08PM
- Abbas, S. Soliman, A.M. & Nehdi, M.L. (2015), Exploring Mechanical and Durability Properties of Ultra-High-Performance Concrete Incorporating Various Steel Fiber Length and Dosages, *Construction and Building Materials, Elsevier*
- Abdallah S., Fan M. & Cashell K.A. (2017). Bond-slip behaviour of steel fibres in concrete after exposure to elevated temperatures, *Construction and Building Materials, Elsevier* 140, 542–551
- Abdullahi, A.K., Ibrahim, H.D. & Buga M.L. (2014). *Investment opportunities in industrial raw materials in Nigeria: value addition to selected commodities*, raw materials research and development council, Abuja, Nigeria
- ACI (1993). Guide for Specifying, Proportioning, Mixing, Placing, and Finishing Steel Fiber Reinforced Concrete, American concrete institute ACI544.3R-93, 1998
- ACI Committee 232 Use of Raw or Processed Natural Pozzolans in Concrete, American concrete institute ACI 232.1R-00, 2001
- ACI Committee 363, State of the Art Report on High- Strength Concrete, (ACI 363R-84), American concrete Institute, Detroit, 1997.
- Aitcin, P.C. (2003). The Durability Characteristics of High-Performance Concrete: A Review, *Cement & Concrete Composites*:409–420, www.elsevier.com/locate/cemconcomp, accessed on 31/10/2016 at 06:34PM
- Ahmed, S.A. (2014), Effect of RPC Compositions on: Compressive Strength and Absorption *Journal of Babylon University/Engineering Sciences*
- Aghabaglou, A.M. Sezer, G.I. & Ramyar, K. (2014). Comparison of Fly Ash, Silica Fume and Metakaolin From Mechanical Properties and Durability Performance of Mortar Mixtures View Point, *Construction and Building Materials, Elsevier*: 17-25,
- Agharde, A.D. & Bhalchandra, S.A. (2015). Mechanical Properties of Reactive Powder Concrete by Using Fly Ash, *International Journal of Advanced Technology in Engineering and Science*, www.ijates.com, accessed on 02/04/2016 at 11:06 pm
- Al-hassani, H.M., Khalil, W.I. & Danha, W.I. (2014). Mechanical Properties of Reactive Powder Concrete with Various Steel Fiber and Silica Fume Contents, *Acta Tehnica Corviniensis- Bulletin of Engineering*

- Aiswarya, S. Prince, A. G. & Dilip, C. (2013). A Review on Use of Metakaolin In Concrete *IRACST – Engineering Science and Technology: An International Journal (ESTIJ)*
- Ambika, D. & Shivaraja M. (2015). Study on Fracture Energy of Reactive Powder Concrete Beams, *International Journal of Earth Sciences and Engineering*, 8(2)
- Anjan, K.M.U. Asha, U.R. & Narayana, S. (2013). Reactive Powder Concrete Properties With Cement Replacement Using Waste Material, *International Journal of Scientific & Engineering Research: 203-206*, www.ijser.org, accessed on 22/05/2016 at 07:09PM
- Ashish, K. P. & Rinku, P. (2012), Utility of Wastage Material as Steel Fibre in Concrete Mix M-20, *International Journal of Advancements in Research & Technology*, 3(1)
- Asteray, B. Oyawa, W. & Shitote, S. (2017). Experimental Investigation on Compressive Strength of Recycled Reactive Powder Concrete Containing Glass Powder and Rice Husk Ash, *Journal of Civil Engineering Research*, 7(4): 124-129
- ASTM C618-05. “Standard specification for coal fly ash and raw or calcined natural pozzolan for use in concrete” American society for testing materials, 2005
- ASTM C494/C494M-05. “Standard specification for chemical admixtures for concrete”, ASTM international, West Conshohocken PA, 2005, https://doi.org/10.1520/C0494_0494M-05
- ASTM C128-15. “Standard Test Method for Relative Density (Specific Gravity) and Absorption of Fine Aggregate” American society for testing materials, 2015
- ASTM C33-08. “Standard Specification for Concrete Aggregates” American society for testing materials, 2008
- ASTM C 1585-13. “Test methods for measurement of rate of absorption of water by hydraulic cement concretes” American Society for Testing and Materials, 2013
- Badogiannis E. *et al.* (2005). Metakaolin as a main cement constituent, Exploitation of poor Greek kaolins, *Cement & Concrete Composites*, 27, 197–203
- Badogiannis, E. & Tsvivilis, S. (2009). Exploitation of poor Greek kaolins: Durability of Metakaolin concrete, *Cement & Concrete Composites, Elsevier*: 128–133
- Bae, B. Choi, H.K. Lee, B.S. & Bang, C.H. (2016). Compressive behavior and mechanical characteristics and their application to stress-strain relationship of steel fiber-reinforced reactive powder concrete, *Advances in Materials Science and Engineering*, Hindawi Publishing Corporation, <http://dx.doi.org/10.1155/2016/6465218>

- Baltakys K., Jauberthie R., Siauciunas R. & Kaminskas, R. (2007). Influence of modification of SiO₂ on the formation of calcium silicate hydrate, *Materials Science-Poland*, 25(3): 663-670
- Bashandy A.A., (2013), Influence of Elevated Temperature on the Behavior of Economical Reactive Powder Concrete, *Journal of Civil Engineering Research*, 89-97, <http://journal.sapub.org/jce> accessed on 21/08/2016 at 12:04 PM.
- BS EN 1097-6 (2013). Testing for Mechanical and Physical Properties of Aggregate: Determination of Particle Density and Water Absorption
- BS EN 12390-3 (2009). Testing Hardened Concrete: Determination of Compressive Strength of Test Specimens
- BS EN 1008 (2002). Mixing Water for Concrete: Specification for Sampling, Testing and Assessing the Suitability of Water
- Buitelaar, P. (2004). Ultra-High Performance Concrete: Developments and Applications during 25 years, *Plenary Session International Symposium on UHPC September 13 - 15, Kassel, Germany*, <http://www.ferroplan.com>, accessed on 1/11/2016 at 11:17 AM
- Chana, Y.N. Luo, X. & Sunb, W. (2000). Compressive Strength and Pore Structure of High-Performance Concrete after Exposure to High Temperature Up to 800⁰C, *Cement and Concrete Research*: 247–251,
- Chan, Y.N., Peng G. & Chan J.K.W. (1996), Comparison between high strength concrete and normal strength concrete subjected to high temperature, *Materials and Structures, Springer*, 29: 616-619
- Chen *et al.* (2006). Evaluation of reactive powder concrete used as a retrofitting material for concrete members, 2nd International symposium on advances in concrete through and technology engineering, 11-13 September 2006, Quebec-city, Canada
- Chen, B.C., An M. Huang, Q. Hu, H. Huang, W. & Zhao, Q. (2016). Application of Ultra-High performance concrete in Bridge Engineering in China, *First International Interactive Symposium on UHPC*
- Colangelo, F. & Cioffi, R. (2013), Use of Cement Kiln Dust, Blast Furnace Slag and Marble Sludge in the Manufacture of Sustainable Artificial Aggregates by Means of Cold Bonding Pelletization, *Materials*, 6: 3139-3159
- Cwirzen , A. Penttala, V. & Vornanen, C. (2008). Reactive Powder Based Concretes:

- Mechanical Properties, Durability and Hybrid Use with OPC, *Cement and Concrete Research, Elsevier*: 1217-1226. <http://ees.elsevier.com/CEMCON/default.asp> . Accessed on 23/07/2016 at 09:03AM.
- De Larrard, F. (1989). Ultrafine Particles for the Making of Very High Strength Concrete, *Cement and Concrete Research*: 161-172.
- De Larrard, F. & Sedran, T. (1993). Optimization of Ultra-High Performance Concrete by the Use of a Packing Model, *Cement And Concrete Research, Elsevier*, 24(6): 997-1009.
- Demirel B. & Kelestemur O. (2010). Effect of elevated temperature on the mechanical properties of concrete produced with finely ground pumice and silica fume, *Fire Safety Journal, Elsevier* 45, 385–391
- Demiss, B.A. Oyawa, W.O. & Shitote, S.M. (2018), Mechanical and microstructural properties of recycled Reactive Powder Concrete containing waste glass powder and fly ash at standard curing, *Cogent Engineering* (Civil & Environmental Engineering; Research Article) <https://www.tandfonline.com/doi/full/10.1080/23311916.2018.1464877>, accessed 02/01/19 at 09:07am
- Ding, J.T. & Li Z. (2002). Effects of Metakaolin and Silica Fume on Properties of Concrete, *ACI Materials Journal*, Technical paper: 393-398
- Donatello, S., Tyrer M. & Cheeseman, C.R., (2010), Comparison of test methods to assess pozzolanic activity, *Cement & Concrete Composites, Elsevier*, 32: 121–127
- Faizan, A. Fawad, B. Zahoor, S. & Shams, K. (2015). Optimizing Mix Proportions for Reactive Powder Concrete (RPC) and Investigating the Compressive Strength, *International Journal of Advanced Structures and Geotechnical Engineering*,4(2): 69-75
- Farny, J.A. & Panarese, W.C. (1994). High-strength concrete, Portland cement Association, https://www.cement.org/docs/default-source/th-paving-pdfs/soil_cement/eb114-high-strength-concrete.pdf,
- Faseyemi, V.A. (2012), Investigations on Microsilica (Silica Fume) As Partial Cement Replacement in Concrete, *Global Journal of Researches in Engineering Civil and Structural Engineering*, (12) 1
- Feng, X. & Clark, B. (2011), Evaluation of the Physical and Chemical Properties of Fly Ash Products for Use in Portland Cement Concrete, 2011 World of Coal Ash (WOCA) Conference – May 9-12, 2011 in Denver, CO, USA, <http://www.flyash.info/>
- Foraminifera Market Research (2016). Kaolin Deposits and Mining in Nigeria: The

- Opportunities, Retrieved from <https://foramfera.com/2016/03/02/kaolin-deposits-and-mining-in-nigeria-the-opportunities>
- Foti D. (2013), Use of recycled waste pet bottles fibers for the reinforcement of concrete, *Composite Structures, Elsevier*, 9(6), 396–404
- Gambhir, M.L. (2006). *Concrete Technology*, Tota McGraw-Hill Publishing Company Limited, New Delhi, India
- Gambhir, M.L. & Jamwal, N. (2014). *Lab. Manual building and construction materials testing and quality control*, McGraw Hill education, Chennai, India
- Ganesan, K. Rajagopal K. & Thangavel K. (2008). Rice husk ash blended cement: Assessment of optimal level of replacement for strength and permeability properties of concrete, *Construction and Building Materials, Elsevier*:1675–1683
- Giménez R.G., Frias M., Villa R.V. & Ramírez S.M. (2018). Ca/Si and Si/Al Ratios of Metakaolinite-Based Wastes: Their Influence on Mineralogy and Mechanical Strengths, *Applied Science*, www.mdpi.com/journal/applsci, Accessed on 15/05/2018 at 03:11pm
- Gopika, S.M. Magudeswaran P, & Eswaramoorthi P. (2017), **Reduction in environmental problems using agricultural solid waste in reactive powder concrete- a review**, *International Journal of Engineering Sciences & Emerging Technologies*, 9(6): 235-242
- Guneyisi E., Gesoglu M., Karaoglu S. & Mermerdas K. (2012). Strength, permeability and shrinkage cracking of silica fume and metakaolin concretes, *Construction and Building Materials, Elsevier*, 34: 120–130
- Hadipramana J. *et al.* (2016), Pozzolanic Characterization of Waste Rice Husk Ash (Rha) From Muar, Malaysia, *International Engineering Research and Innovation Symposium (IRIS), IOP Conf. Series: Materials Science and Engineering* 160
- Haghighi, A. Koohkan, M. & Shekachizadeh, M. (2007). Optimizing Mix Proportions of Reactive Powder Concrete Using Group Method of Data Handling and Genetic Programming, *32nd Conference on Our World in Concrete & Structures*: 28-29 August, 2007, Singapore, <http://cipremier.com/100032023> accessed on 09/05/2016 at 03:09 PM.
- Hager, I. (2013). Behaviour of cement concrete at high temperature. *Bulletin of the Polish Academy of sciences*, 61 (1):1-10.
- Haroon R.K., Ashad I., Vikas S. & Alvin H, (2017). Investigation towards Strength Properties of Hardened Concrete by the use of Metakaolin as a Mineral Admixture, *International Journal of Innovative Research in Science, Engineering and Technology*

- Hiremath P.N. & Yaragal S.C. (2018). Performance evaluation of reactive powder concrete with polypropylene fibres at elevated temperatures, *Construction and Building Materials, Elsevier*, 169, 499-512
- Hiremath P.N. & Yaragal S.C. (2017), Influence of mixing method, speed and duration on the fresh and hardened properties of reactive powder concrete, *Construction and Building Materials*, 141: 271-288
- Hou X., Cao S., Rong Q., Zheng W. & Li G. (2018). Effects of steel fiber and strain rate on the dynamic compressive stress-strain relationship in reactive powder concrete, *Construction and Building Materials, Elsevier*: 570-581
- Ibrahim, A.G. Garba, M.M. Usman, J. & Gambo, S. (2018). Experimental study of Mortar containing Steel Fibre from Waste Gear Inner Wire, *Environmental Technology & Science Journal (ET SJ), School of Environmental Technology, Federal University of Technology, Minna, Niger State, Nigeria* 9(2), 87-93
- Ibrahim, A.G. Okoli, O.G. & Dahiru D. (2016). Comparative Study of the Properties of Ordinary Portland Cement Concrete and Binary Concrete Containing Metakaolin Made from Kankara Kaolin in Nigeria, *ATBU Journal of Environmental Technology*, 9(2): 53-59
- Imteyazuddin, M. & Arafath, S. (2014), An Experimental Investigation on Strength Characteristics of Concrete with Partial Replacement of Silica Fume and Metakaolin with Cement on M-30 Grade of Concrete, *International Journal of Modern Engineering Research (IJMER)*
- International Atomic Energy Agency, (IAEA, 2010). Guidebook on non-destructive testing of concrete structures, Vienna, Austria
- Jalal, M. (2012), Compressive Strength Enhancement of Concrete Reinforced by Waste Steel Fibers Utilizing Nano SiO₂, *Middle-East Journal of Scientific Research*, 12 (3): 382-391,
- Kadhun, M.M. (2015), Studying of Some Mechanical Properties of Reactive Powder Concrete Using Local Materials, *Journal of Engineering*, 7(21): 113-137
- Karim, M.R. Hossain, M.M. Khan, M.N.N. Zain, M.F.M. Jamil, M. & Lai F.C. (2014), On the Utilization of Pozzolanic Wastes as an Alternative Resource of Cement, *Materials*, 7: 7809-7827; doi: 10.3390/ma7127809

- Kartini, K. (2011), Rice Husk Ash – Pozzolanic Material for Sustainability, *International Journal of Applied Science and Technology*, Centre for Promoting Ideas, USA 1(6), www.ijastnet.com, accessed on 09/05/18 at 05:22pm
- Khan, H.R. Imam, A. Srivastava, V. & Harison, A. (2017), Investigation towards Strength Properties of Hardened Concrete by the use of Metakaolin as a Mineral Admixture, *International Journal of Innovative Research in Science, Engineering and Technology, IJRSET*
- Khater, H.M.M. (2015), Influence of electric arc furnace slag on characterisation of the produced geopolymer composites, *Epítôanyag, Journal of Silicate Based and Composite Materials*
- Kim, H.S. *et al.* (2011), Activation of Ground Granulated Blast Furnace Slag Cement by Calcined Alunite, *Materials Transactions, Express Regular Article*, Japan Institute of Metals, 52(2)
- Kiran, T & Jayaramappa, N. (2017), Reactive Powder Concrete, *International Journal of Trend in Research and Development*, 4(3) www.ijtrd.com, accessed 22/04/2018 at 02:12pm
- Koehler, E.F. & Fowler, D.W. (2003). Measurement of concrete workability: key principles and current methods: *International Center for Aggregates Research 11th Annual symposium: Aggregates - Asphalt Concrete, Bases and Fines*, Austin, Texas,
- Kumar, K.S. & Baskar, K. (2014). Response Surfaces for Fresh and Hardened Properties of Concrete with E-Waste (HIPS), *Journal of Waste Management*, Hindawi Publishing Corporation
- Kumar, A.M.U., Rao, A.U., & Sabhahit, N. (2013), Reactive Powder Concrete Properties with Cement Replacement Using Waste Material. *International Journal of Scientific & Engineering Research*, 4 (5)
- Kosmatka, S.H. & Wilson, M.L. (2012). *Design and control of concrete mixtures: the guide to applications, methods and materials*, EB001, 15th edition, Portland association, Skokie, Illinois, USA
- Kushartomo, W. Bali, I. & Sulaiman B. (2015). Mechanical behavior of reactive powder concrete with glass powder substitute, The 5th International Conference of Euro Asia Civil Engineering Forum (EACEF-5), *Procedia Engineering* 125: 617 – 622
- Lee, M.G. Wang, Y.C. & Chiu, C.T. (2007). A Preliminary Study of Reactive Powder Concrete as a New Repair Material, *Construction and Building Materials, Elsevier*
- Lee, M.K. Koh, K.T, Kim, M.O. & Ryub, G.S. (2018), Uncovering the role of micro silica

- in hydration of ultra-high performance concrete (UHPC), *Cement and Concrete Research, Elsevier*: 68–79
- Liew, Y.M. *et al.* (2011). Investigating the Possibility of Utilization of Kaolin and the Potential of Metakaolin to Produce Green Cement for Construction Purposes – A Review, *Australian Journal of Basic and Applied Sciences*, 5(9): 441-449
- Liu, C.T. & Huang, J.S. (2009), Fire Performance of Highly Flowable Reactive Powder Concrete, *Construction and Building Materials, Elsevier*
- Mahmuda, G.H. Yang, Z. & Hassan, A.M.T. (2013). Experimental and numerical studies of size effects of Ultra High Performance Steel Fibre Reinforced Concrete (UHPRFC) beams, *Construction and Building Materials, Elsevier*, 48: 1027–1034
- Maroliya, M.K. (2012). Micro Structure Analysis of Reactive Powder Concrete, *International Journal of Engineering Research and Development*, 4(2): 68-77., www.ijerd.com accessed on 23/04/2016 at 09:06Pm
- Maroliya, M.K. & Modhere, C.D. (2010). A Comparative Study of Reactive Powder Concrete Containing Steel Fibers and Recron 3S Fibers, *Journal of Engineering Research and Studies*
- Masgood, Z. & Ibrahim, M. (2015). The significance of P-value in medical research, *Journal of Allied Health Sciences*, 1(1): 74-88
- Meddah, M.S. Ismail, M.A. El-Gamal, S. & Fitriani, H. (2018). Performances evaluation of binary concrete designed with silica fume and metakaolin, *Construction and Building Materials, Elsevier*, 166, 400–412
- Mehrotra, V.K. (2009). *Concrete and concrete materials for practicing engineers*, Standard publishers distributors, 1705-B, Nai Sarak, Delhi, India
- Mehta, P.K. (1999). *Advancements in Concrete Technology*, Concrete International, Farmington Hills,
- Mitchell, D.R.G. Hinczak, I. & Day, R.A. (1998). Interaction of Silica Fume With Calcium Hydroxide Solutions and Hydrated Cement Pastes, *Cement and Concrete Research*, 28(11): 1571–1584,
- Mohd, A.Y. (2005), Investigating the Potential for Incorporating Tin Slag in Road Pavements, *Thesis submitted to the University of Nottingham for the degree of Doctor of Philosophy*, University of Nottingham, UK.
- Momtazi, A.S. Ranjbar, M.M. Balalaei, F. & Nemati, R. (2007). The effect of Iran's metakaolin in enhancing the concrete Compressive strength, *Department of civil engineering, University of guilan*, www.claisse.info/special%/20papers/sadrmomtazi_full_text.pdf, accessed

21/09/2016 by 06:22 am.

- Mujamil K., Vinay D., Sikandar M.A., Shridhar B. M. & Kulkarni K. S. (2015), Mechanical Strength Assessment of Reactive Powder Concrete Containing Silica Fume by Non- Destructive Testing, *International Journal of Advance Research in Engineering, Science & Technology(IJAREST)*, 2(6): 2394-2444.
- Murali, G. *et al.*, (2012), Experimental Investigation on Fibre Reinforced Concrete Using Waste Materials, *International Journal of Engineering Research and Applications (IJERA)*, www.ijera.com, assessed on 12/02/2018 at 06:04pm
- Nayak, N.V. & Jain, A.K. (2012). Handbook on advanced concrete technology, Narosa publishing house PVT limited, India
- Nematollah, B. Saifulnaz, R.M.R. Jaafar, M.S. & Voo Y.L. (2012), A Review on Ultra-High Performance 'Ductile' Concrete (UHPdC) Technology, *International Journal of Civil and Structural Engineering*
- Nguyen, V.T. Guang, Y.Klaas, V.B. & Oguzhan, C. (2011). Hydration and microstructure of ultra high performance concrete incorporating rice husk ash, *Cement and Concrete Research* 41(11):1104-1111
- Nochaiya, T. Wongkeo, W. & Chaipanich, A. (2010), Utilization of fly ash with silica fume and properties of Portland cement–fly ash–silica fume concrete, *Fuel, Elsevier*: 768–774
- Oakdale Engineering (2019). Data fit version 9.0.59.UK. www.curve fitting.com.
- Patil, S. N. Gupta, A. K. & Deshpande, S. S. (2013). Metakaolin Pozzolanic Material for Cement in High Strength Concrete. In *Proceedings of the 2nd International Conference on Emerging Trends in Engineering (SICETE'13)*: 46-49
- Peng, G.F. Kang, Y.R..Huang, Y.Z., Liu, Z.P. & Chen Q. (2015). Experimental Research on Fire Resistance of Reactive Powder Concrete, *Advances In Materials Science and Engineering, Hindawi Publishing Corporation*,
- Peng, Y., Hu, S., & Ding, Q. (2010), Preparation of Reactive Powder Concrete Using Fly Ash and Steel Slag Powder, *Journal of Wuhan University of Technology-Mater. Sci. Ed*: 349-354
- Peng G.F. *et al.* (2006). Explosive spalling and residual mechanical properties of fiber toughened High-performance concrete subjected to high temperatures, *Cement and Concrete Research* 36, 723–727
- Pereira de Oliveira L.A. & Castro-Gomes J.P. (2011) Physical and mechanical behaviour

- of recycled PET fibre reinforced mortar, *Construction and Building Materials, Elsevier*, (25), 1712–1717
- Qureshi, L.A. Tasaddiq, R.M. Ali, B. & Sultan, T. (2017), Effect of Quartz Content on Physical Parameters of Locally Developed Reactive Powder Concrete, *The Nucleus* 54(4) 242-249, www.thenucleuspak.org.pk, Accessed on 06/02/2018 at 08:13pm
- Ramezaniyanpour, A.A., khani, M.M. & Ahmadibeni, G. (2009) The Effect of Rice Husk Ash on Mechanical Properties and Durability of Sustainable Concretes, *International Journal of Civil Engineering. ResearchGate* 7(2),
- Raw Material Research and Development Council (2019). Development and Utilization of Industrial Minerals (Kaolin, Barytes and Lead/Zinc). Retrieved from <https://rmrdc.gov.ng/strategic-projects.php?project=development-and-utilization-of-industrial-minerals-kaolin-barytes-and-lead-zinc-> on 14/11/2019 at 11:45am
- Richard, P. & Cheyrezy, M. (1995). Composition of Reactive Powder Concretes, *Cement and Concrete Research, Elsevier*, 25(7): 1501-1511, <http://www.sciencedirect.com/science/article/pii/0008884695001442>, accessed 20/10/2016 at 03:10PM
- Rougeau, P. & Borys, B. (2004). Ultra-High-Performance Concrete With Ultrafine Particles other than Silica Fume, *Proceedings of the International Symposium on Ultra High-Performance Concrete*, Kassel, Germany: 213-225.
- Roussel, N. (2007). Rheology of fresh concrete: from measurements to predictions of casting processes, *Materials and Structures*, 40, 1001–1012, DOI 10.1617/s11527-007-9313-2
- Shan, C.S. Rijuldas, V. & Aiswarya, S. (2016). Effect of Metakaolin on Various Properties of Concrete- An Overview, *International Journal of Advanced Technology in Engineering and Science*, 4(1), www.ijates.com,
- Shetty, M.S. (2015). *Concrete technology: theory and practice*, S. Chand & Company Ltd, Ran Nagar, New Delhi, India
- Siddique R. & Klaus I. (2009). Influence of metakaolin on the properties of mortar and concrete: A review, *Applied Clay Science, Elsevier*, 43: 392–400
- Silica Fume Association (2005), *Silica Fume Users' Manual*, Federal Highway Administration, USA
- Smith, K.K. Gururaj, A. & Siddesh, R.K.M. (2015). Reactive Powder Concrete with mineral admixtures, *Journal of engineering technologies and Innovative Research (JETIR)*, www.jetir.org accessed on 23/04/2016 at 09:03Pm.

- So, H.S. Yi, J.B. Khulgadai, J. & So, S.Y. (2014). Properties of Strength and Pore Structure of Reactive Powder Concrete Exposed to High Temperature, *ACI Materials Journal*, accessed on 01/07/2014 at 11:09PM.
- Song, J. & Liu, S. (2016). Properties of Reactive Powder Concrete and Its Application In Highway Bridge, *advances in materials science and engineering*, <http://www.hindawi.com/journals/amse/2016/5460241/> on 7/01/2016 at 09:17PM.
- Srinivasu, K. Sai, M.L.N.K. & Kumar, V.S.N. (2014). A Review on Use of Metakaolin in Cement Mortar and Concrete, *International Journal of Innovative Research in Science, Engineering and Technology*,
- Srivastava, V. Agarwal, V.C. & Kumar, R. (2012). Effect of Silica fume on mechanical properties of Concrete, *J. Acad. Indus. Res.* 1(4), 176-179
- Sujatha, T. & Basanthi, D. (2014). Modified Reactive Powder Concrete, *International Journal of Education and Applied Science*, www.ijear.org, accessed 23/06/2016 at 09:09AM
- Suresh D. & Nagaraju K., (2015), Ground Granulated Blast Slag (GGBS) In Concrete—A Review, *IOSR Journal of Mechanical and Civil Engineering (IOSR-JMCE)* 2(4): 76-82
- Tam, C.M. Tam, V.W.Y. & Ng, K.M. (2010). Optimum Conditions For Producing Reactive Powder Concrete, *Magazine of Concrete Research*, 62(10). www.concrete-research.com, accessed 23/08/2016 at 05:4 AM.
- Tai, Y.S. Pan, H.H. & Kung, Y.N. (2011). Mechanical properties of steel fiber reinforced reactive powder concrete following exposure to high temperature reaching 800°C, *Nuclear engineering and design*, 241, Elsevier:2416-2424
- Tian, K. Ju, Y. Liu, H. Liu, J. Wang, L. Liu, P. & Zhao, X. (2012). Effects of Silica Fume Addition on The Spalling Phenomena of Reactive Powder Concrete, *Applied Mechanics and Materials*: 1090-1095. www.scientific.net/AMM, accessed 23/08/2016 at 05:49 AM.
- Uduweriya, R. B.Y. B. Subash, C. M. M. A. Sulfy, M.M.A. & Silva, S.D., (2010), Investigation of Compressive Strength of Concrete Containing Rice-Husk-Ash, International Conference on Sustainable Built Environment (ICSBE-2010) Kandy,
- Usman, J. Sam, A.M. & Hussin, M.W. (2016). Behavior of palm oil fuel ash and metakaolin ternary blend cement at elevated temperatures, *Journal of materials in civil engineering*, DOI: 10.1061/(ASCE)MT: 1943-5533.0001722.
- Varga, G. (2007). The structure of kaolinite and metakaolinite, <http://dx.doi.org/10.14382/epitoanyag-jsbcm.2007>, accessed 15/05/2018 at 02:45pm

- Venkatanarayanan, H.K. & Rangaraju, P.R. (2013), Material Characterization Studies on Low- and High-Carbon Rice Husk Ash and Their Performance in Portland Cement Mixtures, *Advances in Civil Engineering Materials*, 2(1)
- Vipat, A.R. & Kulkarni, P. M. (2016), Performance of Metakaolin Concrete in Bond and Tension, *International Journal of Engineering Sciences & Research Technology*, *IJESRT*
- Wu, D. Sofi, M. & Mendis, P. (2010), High Strength Concrete For Sustainable Construction, *International Conference on Sustainable Built Environment (ICSBE-2010)* Kandy
- Yalcinkaya, C. Sznajder, J. Beglarigale, A. Sancakoglu, O. & Yazici, H.(2014). Abrasion Resistance of Reactive Powder Concrete: The Influence of Water-To-Cement Ratio and Steel Micro-Fibers, *Advance Materials Letters*, www.amlett.com, accessed 19/07/2016 at 09:03AM
- Yazici, H. Yardimci, M.Y. Yigiter, H. Aydin, S. & Turkel, S. (2010). Mechanical Properties of Reactive Powder Concrete Containing High Volumes of Groundgranulated Blast Slag, *Cement & Concrete Composites*, *Elsevier*, www.elsevier.com/locate/cemconcom, accessed 21/08/2016 at 06:464A.M.
- Yazıcı H., Yigiter H., Karabulut A. & Baradan B. (2008), Utilization of fly ash and ground granulated blast furnace slag as an alternative silica source in reactive powder concrete. *Fuel*, *Elsevier*: 2401–2407
- Yazici, H. Yardimci, M.Y. Aydin, S. & Karabulut, A.S. (2009). Mechanical Properties Of Reactive Powder Concrete Containing Mineral Admixtures Under Different Curing Regimes, *Construction and Building Materials*, *Elsevier*: 1223-1231, www.elsevier.com/locate/conbuildmat, accessed 21/08/2016 at 06:34AM.
- Yigiter, H. Aydin, S. Yazici, H. & Yardimci, M.Y. (2012). Mechanical Performance of Low Cement Reactive Powder Concrete (LCRPC), *Composite: Part B*, *Elsevier*: 2907-2914 www.elsevier.com/locate/compositesb, accessed 21/08/2016 at 06:31AM.
- Yoo, D.Y. Banthia, N. Kim, S.W. & Yoon, Y.S. (2015). Response of ultra-high-performance fiber-reinforced concrete beams with continuous steel reinforcement subjected to low-velocity impact loading, *Composite Structures*, *Elsevier*, 126: 233–245
- Zangeneh, N. Azizian, A. Lye, L. & Popescu R. (2002), Application of Response Surface Methodology in Numerical Geotechnical Analysis, *55th Canadian Society for Geotechnical Conference*, *Hamilton, Ontario*
- Zhang Z., Zhang B. & Yan P. (2016), Comparative study of effect of raw and densified

silica fume in the paste, mortar and concrete, *Construction and Building Materials* 105: 82–93

Zheng W., Li H. & Wang Y. (2012). Compressive stress-strain relationship of steel fiber-reinforced reactive powder concrete after exposure to elevated temperatures, *Construction and Building Materials, Elsevier*: 35, 931-940

Zheng W., Li H. & Wang Y. (2012). Compressive behaviour of hybrid fiber-reinforced reactive powder concrete after high temperature, *Materials and Design, Elsevier*, 41, 403–409

Zheng, W. Luo, B. & Wang, Y. (2013). Compressive and Tensile Properties of Reactive Powder Concrete with Steel Fibers at Elevated Temperatures, *Construction and Building Materials, Elsevier*: 844-851
www.elsevier.com/locate/conbuildmat, accessed on 24/08/2016 at 09:12pm

Zheng, W. Luo, B. & Wang, Y. (2014). Stress–strain relationship of steel-fibre reinforced Reactive Powder Concrete at elevated temperatures, *Materials and Structures*, DOI 10.1617/s11527-014-0312-9

APPENDICES

Appendix A: Trials test

Trial Test Results on fibre content @ 7 days

% of Fibre	Compressive strength(N/mm ²)	Tensile strength(N/mm ²)	Flexural strength(N/mm ²)
0	8.9	3.2	7.5
0.25	25.9	3.8	19
0.75	22.8	2.5	10.7
1	21.6	2.5	9.4
2	12.5	2.0	0.2

Source: Experiment (2018)

Trial test Results of RPC (Compressive Strength)

Specimen	Materials					Compressive Strength (N/mm ²)		
	Cement	Metakaolin	Sand	Quartz	W/C	7	14	28
RPC1	2.7	0.27	2.98	0	0.3	51.52	63.26	66.13
RPC2	2.7	0.27	2.98	0.14	0.3	50.24	55.89	58.09

Source: Experiment (2018)

Trial test Results of RPC (Tensile Strength)

Specimen	Materials					Tensile Strength (N/mm ²)		
	Cement	Metakaolin	Sand	Quartz	W/C	7	14	28
RPC1	2.7	0.27	2.98	0	0.3	4.8	4.9	4.1
RPC2	2.7	0.27	2.98	0.14	0.3	4.2	4.8	5.1

Source: Experiment (2018)

Trial test Results of RPC (Flexural Strength)

Specimen	Materials					Flexural Strength (N/mm ²)		
	Cement	Metakaolin	Sand	Quartz	W/C	7	14	28
RPC1	2.7	0.27	2.98	0	0.3	18.5	11.9	13.2
RPC2	2.7	0.27	2.98	0.14	0.3	16.9	7.8	12.3

Source: Experiment (2018)

Appendix B: Hardened properties of RPC

Compressive strength (N/mm²)

Unfibred RPC specimens				
Age (days)	20% SF	10% MK	20% MK	30% MK
7	43.6	39.3	42.4	52.1
14	57.5	55.3	56.3	56.1
28	66.4	59.9	64.5	61.1
90	67.7	65.1	66.6	63.3
180	74.9	69.8	72.5	65.5

Fibred RPC specimens				
Age (days)	20% SF	10% MK	20% MK	30% MK
7	38.9	37.4	38.8	29.9
14	48.9	44.3	47.2	35.4
28	52.8	46.8	50.3	36.2
90	55.6	49.9	54.1	38.5
180	63.7	55	57.6	42.9

Tensile strength (N/mm²)

Unfibred RPC specimens				
Age (days)	20% SF	10% MK	20% MK	30% MK
7	2.7	3.8	3.01	3.2
14	3.8	4.3	3.6	4.1
28	4	4.5	4.1	4.3
90	4.5	5.1	4.8	4.7
180	4.9	5.8	5.5	5

Fibred RPC specimens				
Age (days)	20% SF	10% MK	20% MK	30% MK
7	2.9	4.3	3.5	3.3
14	3.9	4.4	4.2	3.3
28	4	4.8	4.7	3.7
90	4.3	5.1	5.1	4.9
180	5.1	7.1	6.1	5.7

Flexural strength (N/mm²)

Unfibred RPC specimens				
Age (days)	20% SF	10% MK	20% MK	30% MK
7	9.2	11.8	7.6	13.2
14	10.4	12.8	10.4	17.1
28	10.8	13.3	11.2	17.6
90	12.9	18.1	16.3	14.5
180	15.6	18.9	17.6	16.3

Fibred RPC specimens				
7	14.8	11.4	10.44	8.6
14	14.9	12.1	17.35	9.4
28	15.1	18.7	17.9	11.5
90	16.8	18.8	18.8	17.4
180	18.3	22.3	20.9	18.8

Appendix C: Relationships results**Relationship between UPV and Residual compressive strength of unfibred RPC**

Samples	Temperature (°C)	Residual strength	UPV
10%MK	27	59.9	3.8
	200	87.1	4.1
	400	68.6	3.8
	800	21	1.9
20%MK	27	64.5	4
	600	41.6	2.3
	800	26.9	2
30%MK	27	61.1	3.5
	200	77.6	3.8
	600	34.9	2.2
	800	26.7	2

Relationship between UPV and Residual compressive strength of fibred RPC

Samples	Temperature (°C)	Residual strength	UPV
10%MK	27	46.8	4
	200	57.4	4
	400	54.8	3.6
	800	16.7	1.8
20%MK	27	50.3	3.7
	200	58.9	3.9
	400	48.9	3.8
	800	25	1.9
30%MK	200	47.9	3.7
	400	40.1	3.4
	800	16	1.9

Relationship between UPV and absorption of unfibred RPC

Samples	Temperature (°C)	Absorption (%0	UPV (km/sec)
10%MK	27	3.8	3.8
	200	4	4.1
	400	4.5	3.8
	600	12.5	2.2
	800	14.9	1.9
20%MK	27	4	4
	200	4.1	4.2
	400	5.8	3.8
	600	13.5	2.3
	800	16.3	2
30%MK	27	3.5	3.5
	200	4.2	3.8
	400	4.7	3.5
	600	13.4	2.2
	800	16.7	2

Relationship between UPV and absorption of fibred RPC

Samples	Temperature (°C)	Absorption (%0	UPV (km/sec)
10%MK	27	4	4
	200	3.7	4
	400	5.2	3.6
	600	13.2	2.3
	800	14.5	1.8
20%MK	27	3.7	3.7
	200	2.6	3.9
	400	4.3	3.8
	600	12.7	2.3
	800	15.8	1.9
30%MK	27	3.4	3.4
	200	2.9	3.7
	400	4.7	3.4
	600	13.1	2.2
	800	16.6	1.9

Appendix D: Residual strength of RPC specimens

Normalized compressive strength of unfibred RPC exposed to elevated temperature

Temperature	Samples of RPC			
(°C)	20% SF	10%MK	20%MK	30% MK
27 °C	1.00	1.00	1.00	1.00
200 °C	1.28	1.45	0.99	1.27
400 °C	0.69	1.15	0.63	0.57
600 °C	0.59	0.93	0.64	0.57
800 °C	0.38	0.35	0.42	0.44

Normalized compressive strength of fibred RPC exposed to elevated temperature

Temperature	Samples of RPC			
(°C)	20% SF	10%MK	20%MK	30% MK
27 °C	1.00	1.00	1.00	1.00
200 °C	1.10	1.23	1.17	1.32
400 °C	1.07	1.17	0.97	1.11
600 °C	0.59	0.97	0.88	0.90
800 °C	0.31	0.36	0.50	0.44

Residual compressive strength of unfibred RPC exposed to elevated temperature

Temperature (°C)	Samples of RPC			
	20% SF	10%MK	20%MK	30% MK
27 °C	66.4	59.9	64.5	61.1
200 °C	85.2	87.1	63.6	77.6
400 °C	45.7	68.6	40.9	35.1
600 °C	39.3	56.0	41.6	34.9
800 °C	24.9	21.0	26.9	26.7

Residual compressive strength of fibred RPC exposed to elevated temperature

Temperature (°C)	Samples of RPC			
	20% SF	10%MK	20%MK	30% MK
27 °C	52.8	46.8	50.3	36.2
200 °C	58.1	57.4	58.9	47.9
400 °C	56.6	54.8	48.9	40.1
600 °C	31.2	45.3	44.2	33.1
800 °C	16.4	16.7	25.0	16.0

Appendix E: Absorption Capacity of RPC exposed to different elevated temperature

Absorption Capacity of unfibred RPC exposed to different elevated temperature

Sample	Temperature				
	27 °C	200 °C	400 °C	600 °C	800 °C
U20%SF	3.1	4.1	6.7	11.3	15.1
U10%MK	3.8	4.0	4.5	12.5	14.9
U20%MK	4.0	4.1	5.8	13.5	16.3
U30%MK	3.5	4.2	4.7	13.4	16.7

Absorption Capacity of fibred RPC exposed to different elevated temperature

Sample	Temperature				
	27 °C	200 °C	400 °C	600 °C	800 °C
F20%SF	3.0	3.8	6.3	11.0	14.8
F10%MK	4.0	3.7	5.2	13.2	14.5
F20%MK	3.7	2.6	4.3	12.7	15.8
F30%MK	3.4	2.9	4.7	13.1	16.6

Appendix F: Ultrasonic Pulse Velocity of RPC exposed to different elevated temperature

Ultrasonic Pulse Velocity of unfibred RPC exposed to different elevated temperature

Sample	Temperature				
	27 °C	200 °C	400 °C	600 °C	800 °C
20%SF	3.9	4.0	3.6	2.4	2.1
10%MK	3.8	4.1	3.8	2.2	1.9
20%MK	4.0	4.2	3.8	2.3	2.0
30%MK	3.5	3.8	3.5	2.2	2.0

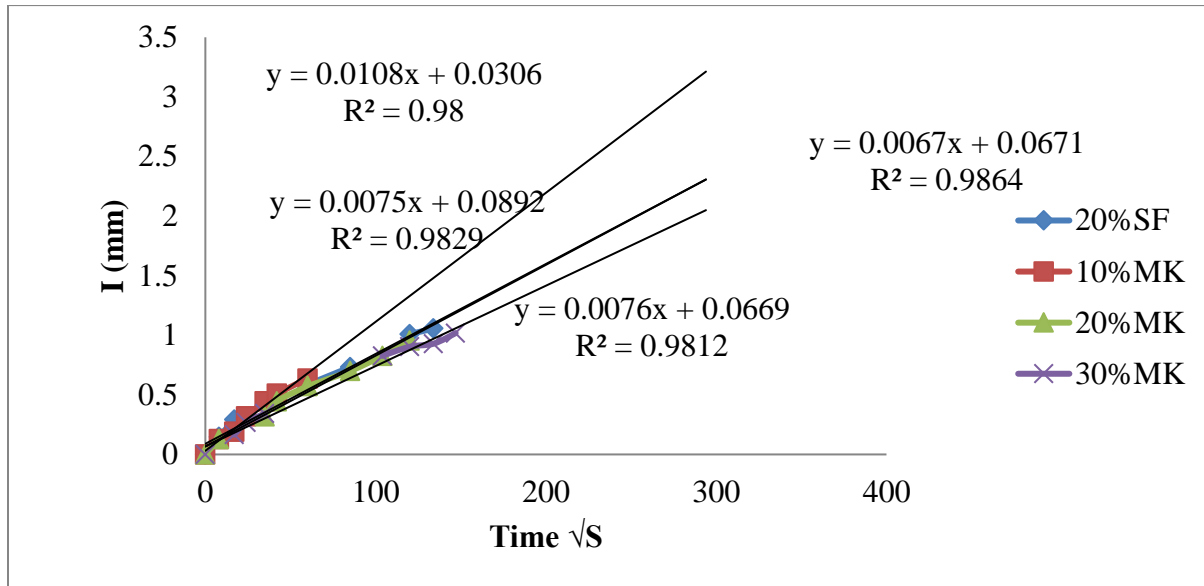
Ultrasonic Pulse Velocity of fibred RPC exposed to different elevated temperature

Sample	Temperature				
	27 °C	200 °C	400 °C	600 °C	800 °C
20%SF	3.9	3.9	3.4	2.2	1.9
10%MK	4.0	4.0	3.6	2.3	1.8
20%MK	3.7	3.9	3.8	2.3	1.9
30%MK	3.4	3.7	3.4	2.2	1.9

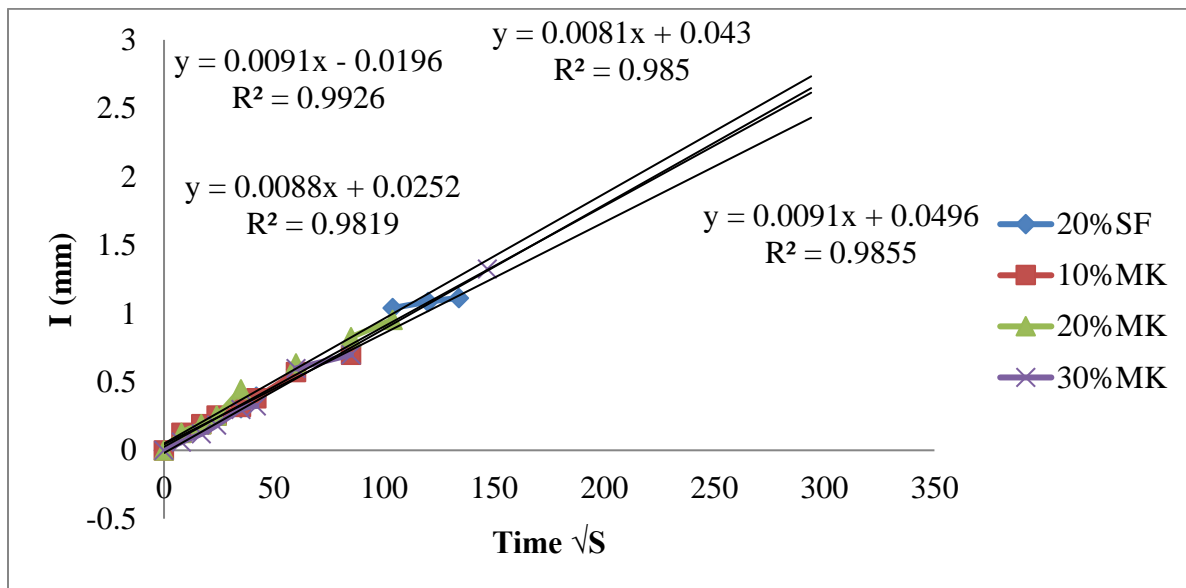
Appendix G: Sorptivity of RPC specimens

RPC specimens at 27°C

Unfibred specimens

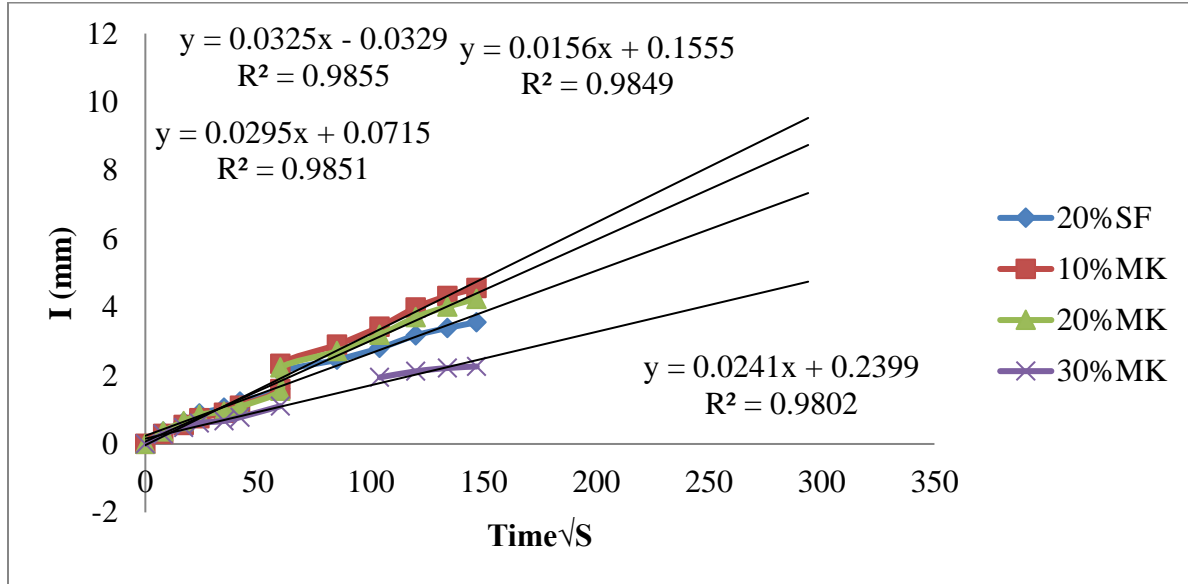


Fibred specimens

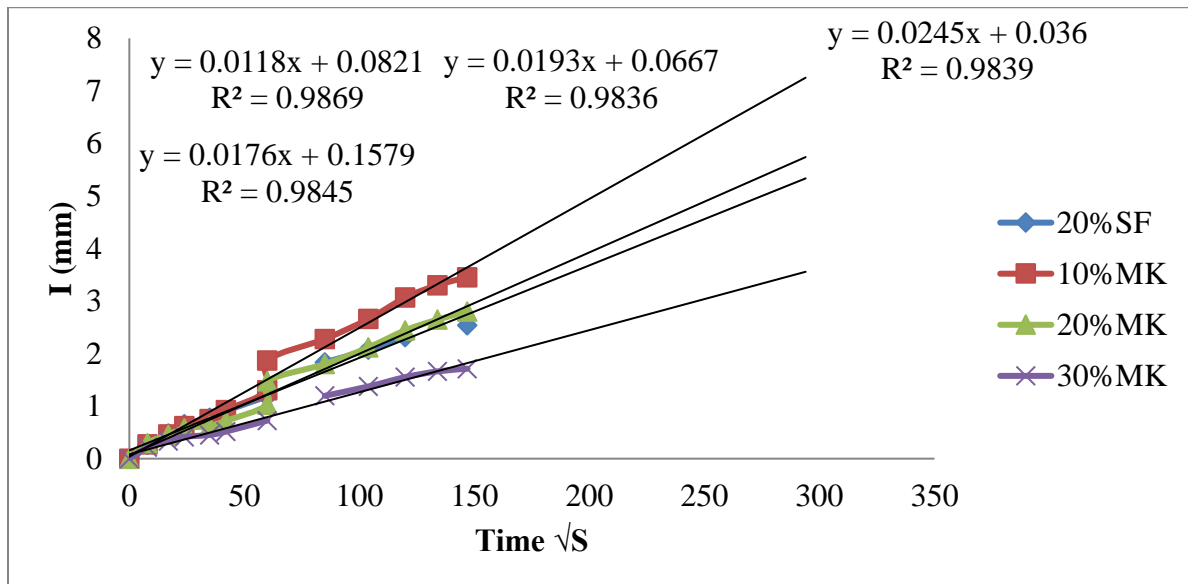


RPC specimens at 200°C

Unfibred specimens

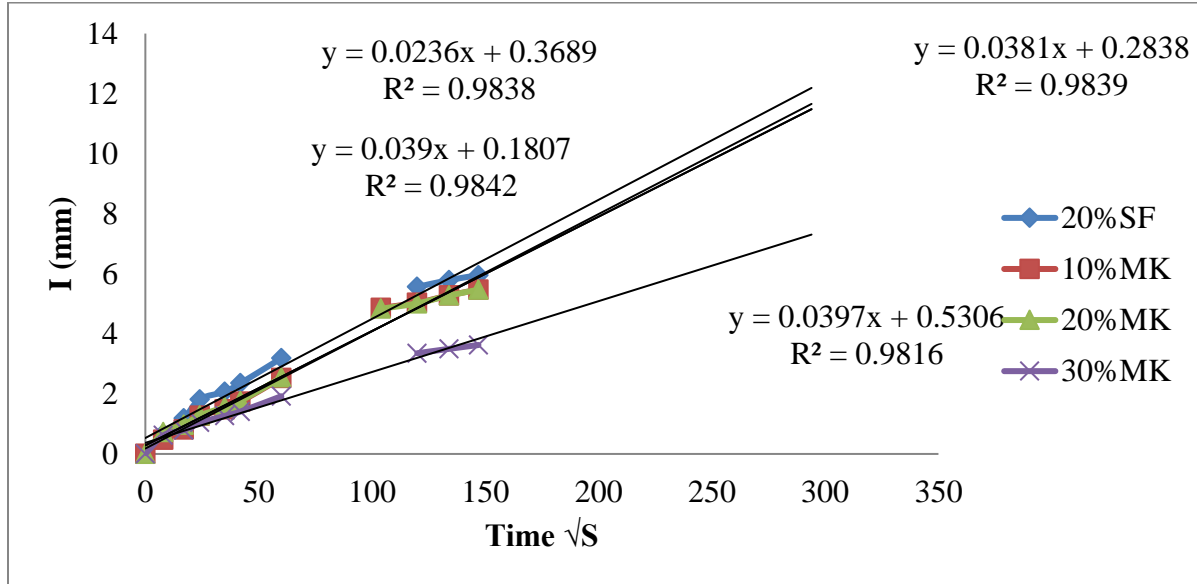


Fibred specimens

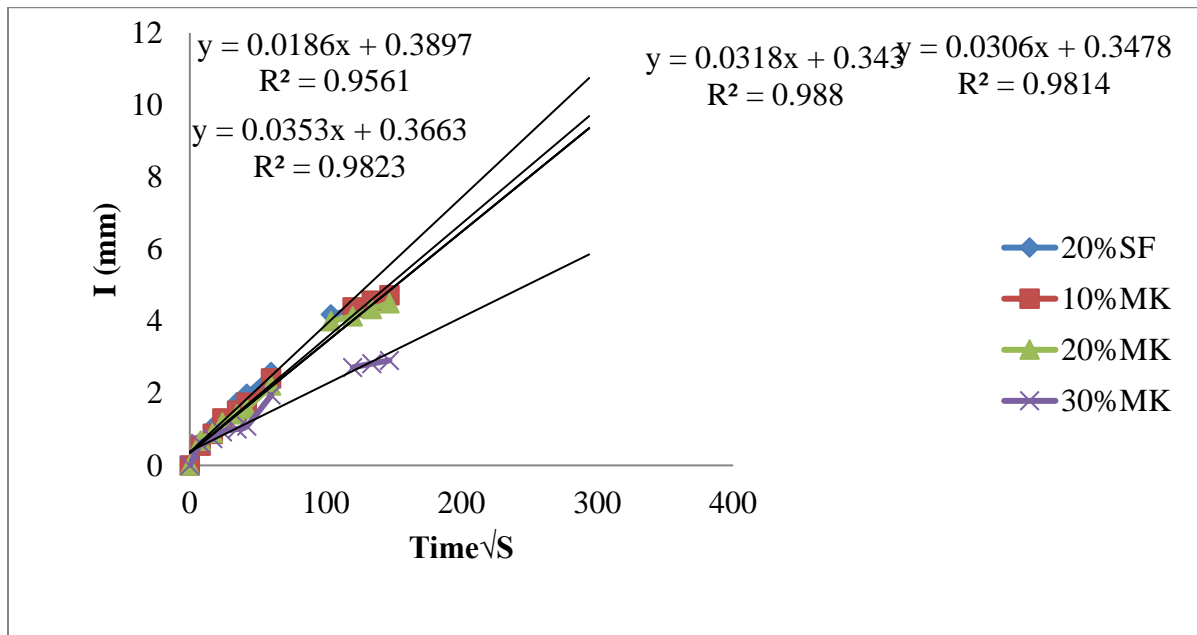


RPC specimens at 400°C

Unfibred specimens

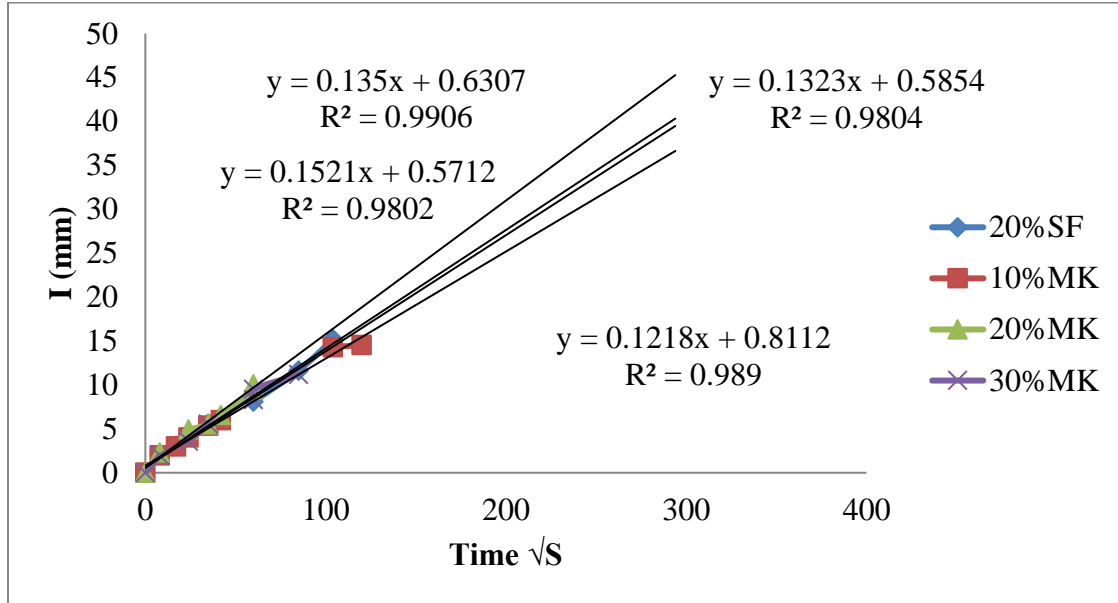


Fibred specimens

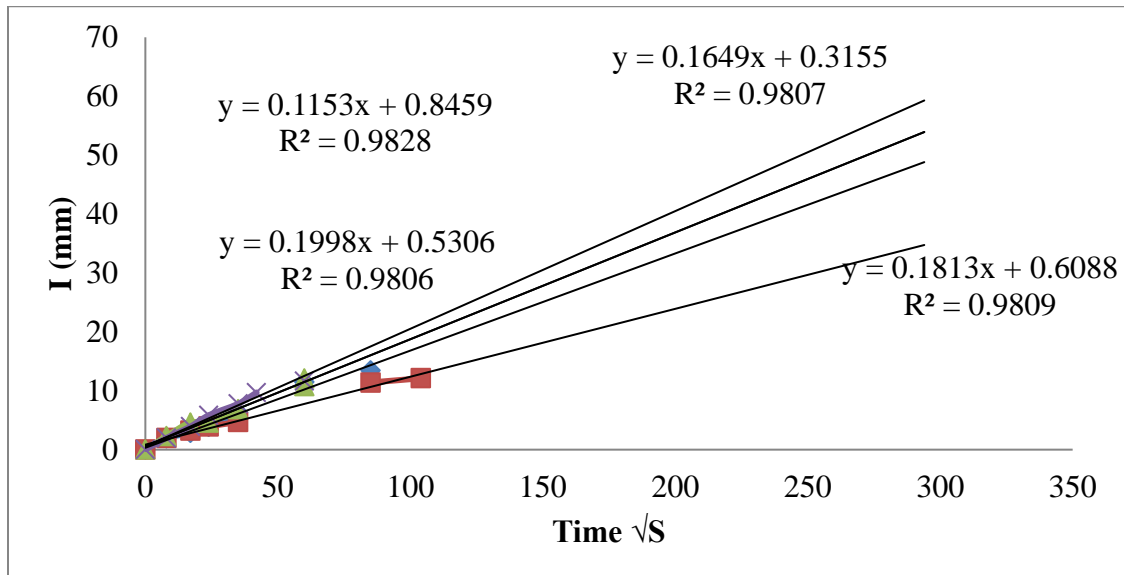


RPC specimens at 600°C

Unfibred specimens

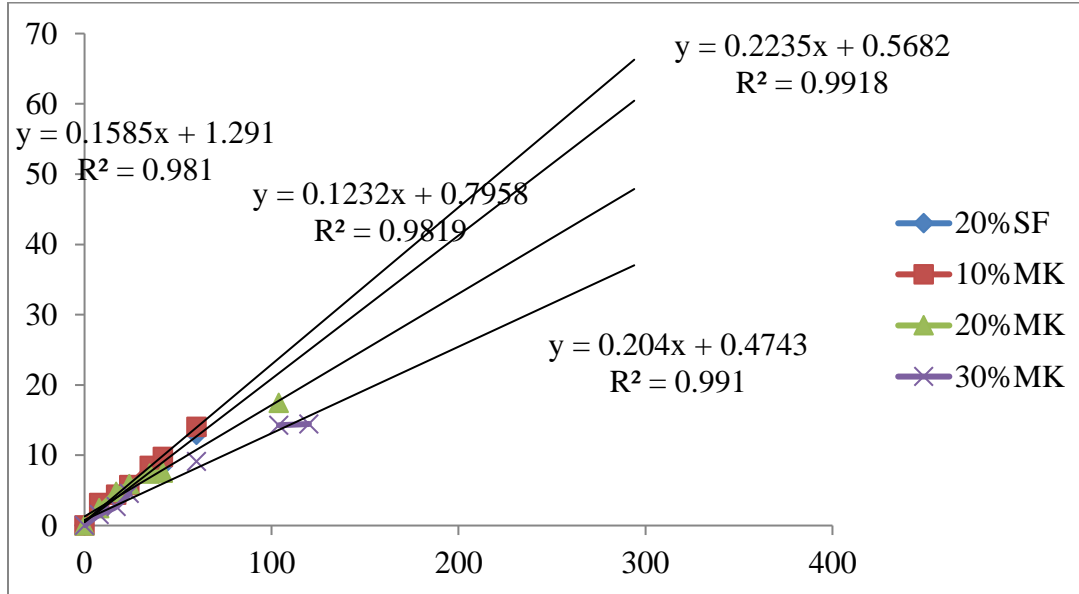


Fibred specimens

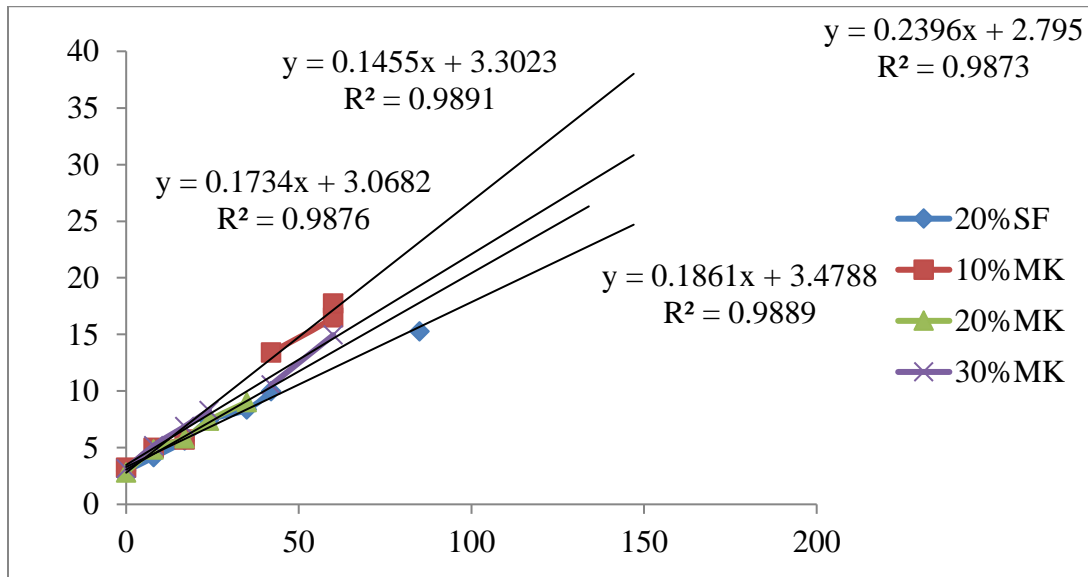


RPC specimens at 800°C

Unfibred specimens



Fibred specimens



Appendix H: Model development

Compressive strength

Equation 1

DataFit version 9.1.32

Results from project "C:\Users\Getso\Desktop\Datafit models\Untitled2 Compressive strength control.dft"

Equation ID: $a+b*x1+c*x1^2+d*x1^3+e*x2$

Model Definition:

$Y = a+b*x1+c*x1^2+d*x1^3+e*x2$

Number of observations = 8

Number of missing observations = 0

Solver type: Nonlinear

Nonlinear iteration limit = 250

Diverging nonlinear iteration limit = 10

Number of nonlinear iterations performed = 1

Residual tolerance = 0.0000000001

Sum of Residuals = -4.2632564145606E-14

Average Residual = -5.32907051820075E-15

Residual Sum of Squares (Absolute) = 47.905

Residual Sum of Squares (Relative) = 47.905

Standard Error of the Estimate = 3.99603970617577

Coefficient of Multiple Determination (R^2) = 0.9342452027

Proportion of Variance Explained = 93.42452027%

Adjusted coefficient of multiple determination (R_a^2) = 0.8465721397

Durbin-Watson statistic = 1.67654733326378

Regression Variable Results

Variable	Value	Standard Error	t-ratio	Prob(t)
a	67.82	3.159147	21.4694	0.00022
b	-1.91	1.08418	-1.7617	0.17633
c	0.167	9.58E-02	1	0.17972
d	3.85E-03	2.11E-03	1.82803	0.16499
e	-65.8	11.30251	5.82172	0.01009

68% Confidence Intervals

Variable	Value	68% (+/-)	Lower Limit	Upper Limit
	67.82		64.0690	71.5809
a	5	3.75591	9	1
			-	-
b	-1.91	1.288982	3.19898	0.62102
			5.31E-	0.28092
c	0.167	0.113922	02	2
	-			
d	3.85E-03	2.50E-03	-6.35E-03	-1.35E-03
e	-65.8	13.43755	79.2376	52.3624

90% Confidence Intervals

Variable	Value	90% (+/-)	Lower Limit	Upper Limit
	67.82		60.3902	75.2597
a	5	7.434736	6	4
			-	-
b	-1.91	2.55151	4.46151	0.64151
			-5.85E-	0.39250
c	0.167	0.225507	02	7
	-			
d	3.85E-03	4.96E-03	-8.81E-03	1.11E-03
e	-65.8	26.59932	92.3993	39.2007

95% Confidence Intervals

Variable	Value	95% (+/-)	Lower Limit	Upper Limit
	67.82		57.7713	77.8786
a	5	10.05367	3	7
				1.54029
b	-1.91	3.450295	-5.3603	5
			-	0.47194
c	0.167	0.304943	0.13794	3
	-			
d	3.85E-03	6.70E-03	-1.06E-02	2.85E-03
e	-65.8	35.9691	101.769	29.8309

99% Confidence Intervals

Variable	Value	99% (+/-)	Lower Limit	Upper Limit
a	67.82	18.45226	49.3727	86.2772
b	-1.91	6.332588	8.24259	4.42258
c	0.167	0.559685	0.39268	0.72668
d	3.85E-03	1.23E-02	-1.62E-02	8.45E-03
e	-65.8	66.01681	131.817	0.21681

Variance Analysis

Source	DF	Sum of Squares	Mean Square	F Ratio	Prob(F)
Regression	4	680.635	170.158	10.6560	0.04049
Error	3	47.905	15.9683		
Total	7	728.54			

x1 value	x2 value	Y value	Calc Y	Residual	% Error	Abs Residual	Min Residual	Max Residual
10	0	59.9	61.575	-1.675	2.79633	1.675	-4.225	4.225
20	0	64.5	65.625	-1.125	1.74419	1.125		
30	0	61.1	56.875	4.225	6.91489	4.225		
10	0.25	46.8	45.125	1.675	3.57906	1.675		
20	0.25	50.3	49.175	1.125	2.23658	1.125		
30	0.25	36.2	40.425	-4.225	11.6713	4.225		
0	0	66.4	67.825	-1.425	2.14608	1.425		
0	0.25	52.8	51.375	1.425	2.69886	1.425		

Flexural strength

Equation 3

DataFit version 9.1.32

Results from project "C:\Users\Getso\Desktop\Datafit models\Untitled2 flexural strength.dft"

Equation ID: $a+b*x1+c*x1^2+d*x2$

Model Definition:

$Y = a+b*x1+c*x1^2+d*x2$

Number of observations = 8

Number of missing observations = 0

Solver type: Nonlinear

Nonlinear iteration limit = 250

Diverging nonlinear iteration limit = 10

Number of nonlinear iterations performed = 11

Residual tolerance = 0.0000000001

Sum of Residuals = -1.35891298214119E-13

Average Residual = -1.69864122767649E-14

Residual Sum of Squares (Absolute) = 1.46

Residual Sum of Squares (Relative) = 1.46

Standard Error of the Estimate = 0.604152298679728

Coefficient of Multiple Determination (R^2) = 0.9875753933

Proportion of Variance Explained = 98.75753933%

Adjusted coefficient of multiple determination (R_a^2) = 0.9782569383

Durbin-Watson statistic = 2.37628424657541

Regression Variable Results

Variable	Value	Standard Error	t-ratio	Prob(t)
a	10.25	0.467974358	21.90290946	0.00003
b	0.51875	6.69E-02	7.757890281	0.00149
c	-2.19E-02	2.14E-03	-10.24110038	0.00051
d	21.7	1.708800749	12.69896447	0.00022

68% Confidence Intervals

Variable	Value	68% (+/-)	Lower Limit	Upper Limit
a	10.25	0.530870112	9.719129888	10.78087011
b	0.51875	7.59E-02	0.442895615	0.594604385
c	-2.19E-02	2.42E-03	-2.43E-02	-1.95E-02

	02			
d	21.7	1.93846357	19.76153643	23.63846357

90% Confidence Intervals

Variable	Value	90% (+/-)	Lower Limit	Upper Limit
a	10.25	0.997627737	9.252372263	11.24762774
b	0.51875	0.142547936	0.376202064	0.661297936
	-2.19E-			
c	02	4.55E-03	-2.64E-02	-1.73E-02
d	21.7	3.642821437	18.05717856	25.34282144

95% Confidence Intervals

Variable	Value	95% (+/-)	Lower Limit	Upper Limit
a	10.25	1.299284008	8.950715992	11.54928401
b	0.51875	0.185650666	0.333099334	0.704400666
	-2.19E-			
c	02	5.93E-03	-2.78E-02	-1.59E-02
d	21.7	4.7443144	16.9556856	26.4443144

99% Confidence Intervals

Variable	Value	99% (+/-)	Lower Limit	Upper Limit
a	10.25	2.154600743	8.095399257	12.40460074
b	0.51875	0.307864224	0.210885776	0.826614224
	-2.19E-			
c	02	9.83E-03	-3.17E-02	-1.20E-02
d	21.7	7.867489529	13.83251047	29.56748953

Variance Analysis

Source	DF	Sum of Squares	Mean Square	F Ratio	Prob(F)
Regression	3	116.04875	38.68291667	105.9805936	0.00029
Error	4	1.46	0.365		
Total	7	117.50875			

x1 value	x2 value	Y value	Calc Y	Residual	% Error	Abs Residual	Min Residual	Ma
10	0	13.3	13.25	0.05	0.37594	0.05	-0.675	
20	0	11.2	11.875	-0.675	-6.0268	0.675		
30	0	6.2	6.125	0.075	1.20968	0.075		
10	0.25	18.7	18.675	0.025	0.13369	0.025		
20	0.25	17.9	17.3	0.6	3.35196	0.6		
30	0.25	11.5	11.55	-0.05	-0.4348	0.05		
0	0	10.8	10.25	0.55	5.09259	0.55		

0 0.25 15.1 15.675 -0.575 -3.8079 0.575

Water absorption capacity

Equation 1

DataFit version 9.1.32

Results from project "C:\Users\Getso\Desktop\Datafit models\Untitled2 absorption.dft"

Equation ID: a+b*x1+c*x1^2+d*x1^3+e*x2

Model Definition:

Y = a+b*x1+c*x1^2+d*x1^3+e*x2

Number of observations = 8

Number of missing observations = 0

Solver type: Nonlinear

Nonlinear iteration limit = 250

Diverging nonlinear iteration limit =10

Number of nonlinear iterations performed = 11

Residual tolerance = 0.0000000001

Sum of Residuals = -1.14575016141316E-13

Average Residual = -1.43218770176645E-14

Residual Sum of Squares (Absolute) = 0.01

Residual Sum of Squares (Relative) = 0.01

Standard Error of the Estimate = 5.77350269189626E-02

Coefficient of Multiple Determination (R^2) = 0.9574468085

Proportion of Variance Explained = 95.74468085%

Adjusted coefficient of multiple determination (Ra^2) = 0.9007092199

Durbin-Watson statistic = 2.74999999999939

Regression Variable Results

Variable	Value	Standard Error	t-ratio	Prob(t)
a	3	4.56E-02	65.72671	0.00001
b	-7.08E-02	1.57E-02	-4.52196	0.02022
c	4.25E-03	1.38E-03	3.069839	0.05457
d	-6.67E-05	3.04E-05	-2.19089	0.11616
e	0.8	0.163299	4.898979	0.01628

68% Confidence Intervals

Variable	Value	68% (+/-)	Lower Limit	Upper Limit
a	3	5.43E-02	2.945734	3.054266
b	7.08E-02	1.86E-02	-8.95E-02	-5.22E-02
c	4.25E-03	1.65E-03	2.60E-03	5.90E-03
d	6.67E-05	3.62E-05	-1.03E-04	-3.05E-05
e	0.8	0.194147	0.605853	0.994147

90% Confidence Intervals

Variable	Value	90% (+/-)	Lower Limit	Upper Limit
a	3	0.107418	2.892582	3.107418
b	7.08E-02	3.69E-02	-0.1077	-3.40E-02
c	4.25E-03	3.26E-03	9.92E-04	7.51E-03
d	6.67E-05	7.16E-05	-1.38E-04	4.95E-06
e	0.8	0.384309	0.415691	1.184309

95% Confidence Intervals

Variable	Value	95% (+/-)	Lower Limit	Upper Limit
a	3	0.145256	2.854744	3.145256
b	7.08E-02	4.99E-02	-0.12068	-2.10E-02
c	4.25E-03	4.41E-03	-1.56E-04	8.66E-03
d	6.67E-05	9.68E-05	-1.64E-04	3.02E-05
e	0.8	0.519684	0.280316	1.319684

99% Confidence Intervals

Variable	Value	99% (+/-)	Lower Limit	Upper Limit
a	3	0.266599	2.733401	3.266599
b	7.08E-02	9.15E-02	-0.16233	2.07E-02
c	4.25E-03	8.09E-03	-3.84E-03	1.23E-02
d	6.67E-05	1.78E-04	-2.44E-04	1.11E-04
e	0.8	0.953815	-0.15381	1.753815

Variance Analysis

Source	DF	Sum of Squares	Mean Square	F Ratio	Prob(F)
Regression	4	0.225	0.05625	16.875	0.02138
Error	3	0.01	3.33E-03		
Total	7	0.235			

x1 value	x2 value	Y value	Calc Y	Residual	% Error	Abs Residual	Min Residual	Max Residual
10	0	2.7	2.65	0.05	1.851852	0.05	-0.05	0.05
20	0	2.7	2.75	-0.05	-1.85185	0.05		
30	0	2.9	2.9	0	0	0		
10	0.25	2.8	2.85	-0.05	-1.78571	0.05		
20	0.25	3	2.95	0.05	1.666667	0.05		
30	0.25	3.1	3.1	0	0	0		
0	0	3	3	0	0	0		
0	0.25	3.2	3.2	0	0	0		

